NANOCRYSTALLINE HYDROXYAPATITE REINFORCED GLUTEN PLASTICS

Muhammad Razeen Ahmad

Registration No. 02272113011

Supervised by

Dr. Faiza Rasheed

Department of Biotechnology

Faculty of Biological Sciences

Quaid-i-Azam University

Islamabad, Pakistan 2024

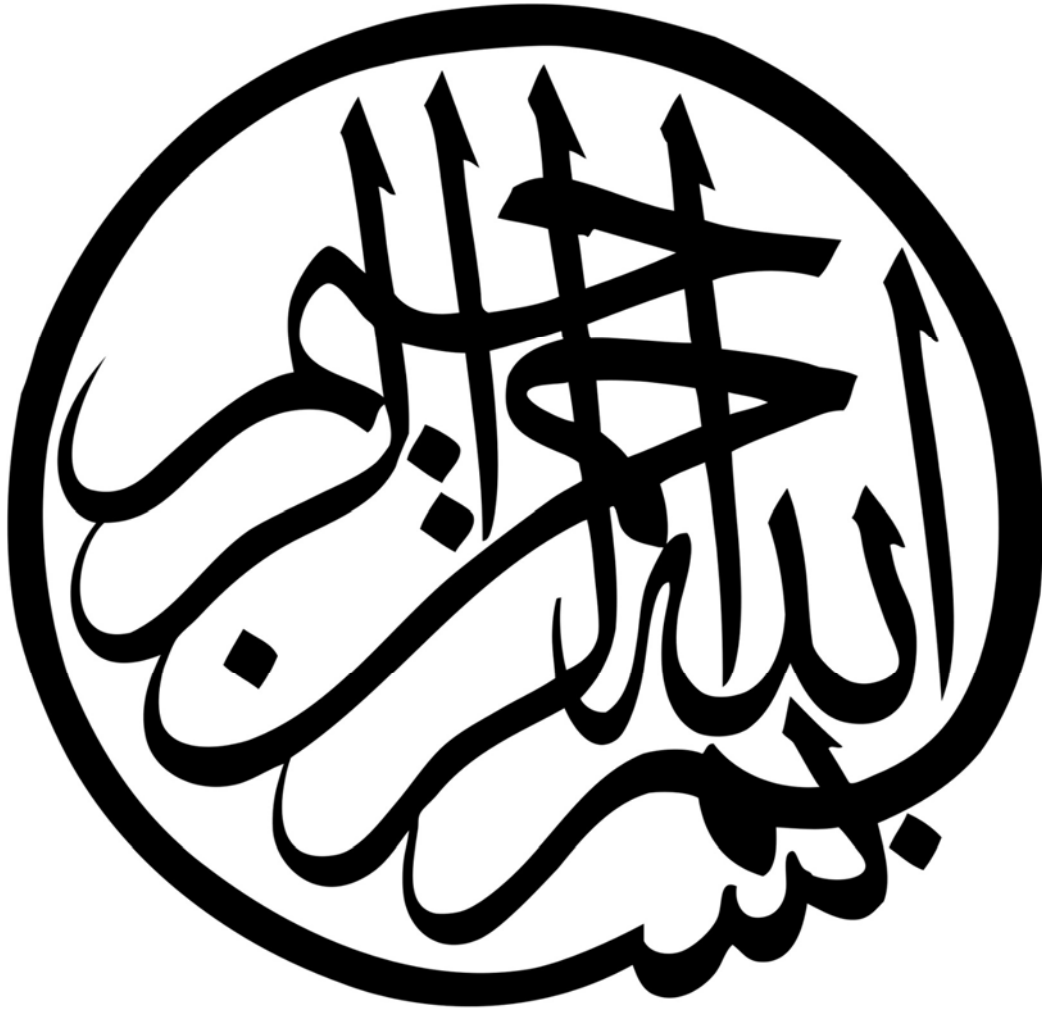# Nanocrystalline Hydroxyapatite Reinforced Gluten Plastics

A thesis submitted in the partial fulfillment of the requirements for the degree of **Master of Philosophy in biotechnology.**

By

Muhammad Razeen Ahmad

Department of Biotechnology

Faculty of Biological Sciences

Quaid-i-Azam University

Islamabad, Pakistan 2024

In the name of Allah, the most Beneficent and the most Merciful!

DECLARATION

I hereby affirm that the work provided in this thesis is entirely my own creation, except for any places where it has been acknowledged. Nothing from this thesis has ever been published or submitted for consideration for another degree or certificate.

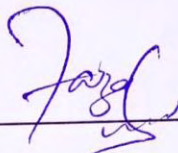Signature of student

Muhammad Razeen Ahmad

Reg.# **02272113011**

CERTIFICATE OF APPROVAL

This is to certify that the research work presented in this thesis, entitled **"Nanocrystalline Hydroxyapatite Reinforced Gluten Plastics"** was conducted by **Mr. Muhammad Razeen Ahmad** under the supervision of **Dr. Faiza Rasheed.**
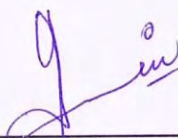
No part of this thesis has been submitted anywhere else for any degree. This thesis is submitted to the Department of Biotechnology, Faculty of Biological Sciences, Quaid-i-Azam University, Islamabad, Pakistan, in partial fulfillment of the requirements for the Degree of Master of Philosophy (MPhil) in the field of Biotechnology.

Supervisor
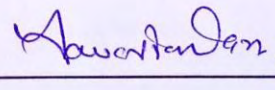
Dr. Faiza Rasheed

External Examiner

Dr. Yamin Bebi

Chairperson

Dr. Javeria Qazi

Dated: --/--/2024

DEDICATION

*I dedicate this thesis to my beloved Prophet Hazrat Muhammad (صَلَّى ٱللّٰهُ عَلَيْهِ وَسَلَّم),
whose teachings have always pushed me towards science and discovering new
things. I also dedicate this to my parents who have supported me unyieldingly.*

Muhammad Razeen Ahmad

ACKNOWLEDGEMENT

Table of Contents

List of Tables

List of Figures

List of Abbreviations

Physical/ chemical quantities and units (not including chemical symbols):

δ	deformation as a result of force
σ	stress
σ_y	specific strength
σ_{UT}	ultimate tensile stress/ stress at break/ tensile strength
ε	strain
ρ	density
θ or Th.	angle in degrees
k	stiffness
K_{sp}	solubility product constant
pK_{sp}	-log of K_{sp}
E	Young's modulus/ elastic modulus
F	force
T_s	tensile strength
T_g	glass transition temperature
hP	hexagonal Bravais lattice
$P6_3/m$	Laue space group no. 176 in hP
k_ / M_ / G_	kilo/ mega/ giga
Pa	Pascal
s	second(s)
min	minute(s)
h	hour(s)
m	meter(s)
°C	degree Celsius
Hz	Hertz (s^{-1})
Mg/m³	mega grams per cubic meter (density)
λ	Wavelength in nanometers

Å	Angstroms (0.1 nm)
M	Molar (mol.dm^{-3})
α/ β/ δ/ γ/ ω	Greek alphabets (alpha/ beta/ delta/ gamma/ omega)

Abbreviations in thesis:

AA	Acrylic Acid
ACP	Amorphous Calcium Phosphate
ATR	Attenuated Total Reflectance
BSP	Bone Sialoprotein
β-TCP	Beta-Tricalcium Phosphate
Ca	Calcium
CD	Celiac Disease
cHAP	Carbonated Hydroxyapatite
cdHAP	Calcium Deficient Hydroxyapatite
CMC	Carboxymethyl Cellulose
CNC	Cellulose Nanocrystal
CNF	Cellulose Nanofiber
COD	Crystallography Open Database
CTD	C-terminal Domain
Cys/ C	Cysteine
Da	Dalton(s)
DAP	Diammonium hydrogen Phosphate
DGP	Dentin Glycoprotein
DMP1	Dentin Matrix Protein-1
DPP	Dentin Phosphoprotein
DSP	Dentin Sialoprotein
DSPP	Dentin Sialophosphoprotein
E	Glutamic acid/ glutamate
ECM	Extracellular Matrix
EDTA	Ethylene-diamine-tetra-acetic acid
eHap	hydroxyapatite synthesized from eggshell
EHAP	hydroxyapatite synthesized from eggshell using titrations

ES	Eggshell
ESM	Eggshell Membrane
ESP	Eggshell Powder
EU	European Union
F	Phenylalanine
FOM	Frequency of Match
FTIR	Fourier Transform Infrared Spectroscopy
FWHM	Full Width at Half Maximum
G/ Gly	Glycine
Gb	Gigabases
GEL	Gelatin
GLI/ Gli	Gliadin
GLT	Glutenin
GLY	Glycerol
HAP/Ca-HAP/ Hap	Hydroxyapatite/ Calcium Hydroxyapatite
H-bond	Hydrogen bond
HLA	Human Leukocyte Antigen
HMW-GS	High Molecular Weight Glutenin Subunit
Hyp	Hydroxyproline
ICDD	International Center for Diffraction Data
IgE	Immunoglobulin E
IWGSC	International Wheat Genome Sequencing Consortium
LMW-GS	Low Molecular Weight Glutenin Subunit
M$_w$	Molecular Weight
MEPE	Matrix Extracellular Phospoglycoprotein
MGP	Matrix Gla Protein
MSC	Mesenchymal Stem Cell(s)
nano-EHAP	Nano-HAP synthesized from eggshell, with titrations
nHAP/ nHap	Nano-Hydroxyapatite
NTD	N-terminal Domain
OCN	Osteocalcin

OPN	Osteopontin
P/ Pro	Proline
P$_i$	Inorganic phosphate
PAA	Poly(acrylic acid)
PAMPS	Poly(2-Acrylamido-2-Methylpropane Sulfonic acid)
PCL	Poly-ε-caprolactone
PDL	Periodontal Ligament
PEG	Polyethylene Glycol
PLA	Poly (Lactic Acid)
PLGA	Poly (Lactic-co-Glycolic Acid)
PLLA	Poly (L-Lactic Acid)
PMMAAm	Poly-*N,N'*-Dimethyl Acrylamide
PolyP$_i$	Polypyrophosphate
PP$_i$	Pyrophosphate
PPF	Poly (Propylene Fumarate)
Q/ Gln	Glutamine
rhBMP-7	Recombinant Human Bone Morphogenic Protein-7
S/ Ser	Serine
SBF	Simulated Body Fluid
SDS-PAGE	Sodium Dodecyl Sulfate-Polyacrylamide Gel Electrophoresis
SIBLING	Small-Integrin-Binding Ligand N-linked Glycoprotein
T/ Thr	Threonine
TG2	Transglutaminase 2
TNAP	Tissue Non-specific Alkaline Phosphatase
W/ Trp	Tryptophan
WDEIA	Wheat-Dependent Exercise-Induced Anaphylaxis
WG	Wheat Gluten
X	Amino acid residue (any)
XRD	X-ray Diffraction
Y/ Tyr	Tyrosine

Abstract

Nature has intelligent solutions for designing and building materials. Many of such important materials go to waste. Eggshells are a neglected waste and contain high-purity calcium. Wheat gluten is also an industrial byproduct with interesting plastic-forming properties. This study focused on utilizing eggshells biowaste for synthesizing high-value mineral hydroxyapatite (HAP), used in bone tissue engineering. Nano-hydroxyapatite was formed by less-energy intensive EDTA/ microwave-irradiation method, and the process was optimized. The synthesized hydroxyapatite was used in different combinations with wheat gluten, gelatin, and glycerol, to form novel composite materials, through thermo-compression molding and temperature-controlled extrusion. The composite formation was optimized for temperature, materials concentrations, and pressure of molding and extrusion. The products were analyzed by FTIR, XRD, and tested for moisture content, water vapor permeance, biodegradability, and tensile strength.

Equal amounts of gluten and gelatin with less amount of HAP resulted in excellent quality and uniform strength composite materials. The synthesized materials showed good water-barrier properties and strength. These studies provide a new way of creating, modulating, and testing novel/ multifunctional materials for a wide variety of applications.

Chapter-1

INTRODUCTION

Nature has evolved clever ways to build structure and function inside living organisms and their products. Our civilization is built on some principles directly mimicked from the biological realm. Such nature-inspired solutions are all around us and form the basis of structural and functional materials in our daily lives. Major structural materials include wood and wood products, plant fiber, leather, silk, cotton, nails, horns and bones. These materials are formed by only the simplest building blocks of life, i.e., wood and fiber from cellulose, leather/ hair and silk from structural proteins; keratin and silk proteins[1] (Figure-1.1). Bone is another highly resilient structural material formed by mineralization of collagen networks with calcium phosphate. If we see from a macroscopic materials perspective, all these materials are lightweight, highly durable, tough, strong and fracture resistant. Furthermore, these are manufactured by cells, tissues, or organisms at ordinary ambient conditions such as room temperature and ordinary pressure levels. Meanwhile, our engineered materials like steel rebar and iron structures are made at extreme conditions of high temperature, pressure, and often controlled atmosphere. Additionally, nature weaves, into these materials, special abilities so that these materials can often be healed when fractured. This is seen clearly in bone remodeling.

There is a huge global demand of structural and functional materials that are:

- Strong
- Tough
- Lightweight
- Fracture-resistant, crack-resistant
- Flexible, and
- Self-healing

1.1. Materials Properties

Some durable and strong materials are classified by toughness, strength and fracture-toughness or fracture-resistance. Toughness or stiffness is defined as the amount of resistance to elastic deformation in a material to an applied force.

$$k = \frac{F}{\delta}$$

Where k is the stiffness, F is the applied force, and δ is the displacement or deformation as the result of the force. The unit of stiffness is N.m^{-1}. A complementary property is the flexibility or pliability of a material. For example, elastic or pliable materials have less stiffness because they get deformed due to an applied force but return to their original condition, as long as their elastic limit is not crossed. Stiff materials, on the other hand, resist deformation and crack as the applied force is increased. This is why diamond, touted as the strongest material, cracks but does not deform as a huge force is applied. High-carbon steels are also brittle because they do not deform but crack under the influence of a large stress.

Strength of a material is measured as the amount of force or stress (force per unit area) required to produce a permanent deformation in its structure. In mechanics, Young's modulus E describes the ratio of stress σ to the strain ε resulting from that stress:

$$E = \frac{\sigma}{\varepsilon}$$

Stiff materials have very high amounts of Young's moduli, typically measured in gigapascals (GPa). Densities of materials are commonly shown in g/cm^3 or kg/dm^3 or Mg/m^3 units [see supplementary table 1.1 for details]. **Specific strength σ_y,** of a material can be calculated from its tensile strength (**T_s**)**,** measured in megapascals MPa, and density ρ, as follows:

$$\sigma_y = \frac{T_s / \rho}{\vec{g}} \qquad \text{(Unit: MPa/Mg.m}^3\text{)}$$

As opposed to specific strength**, specific stiffness K_s** of a material is the modulus of a material divided by mass density ρ**,** as follows:

$$K_s = \frac{E}{\rho} \qquad \text{(Unit: GPa/Mg.m}^3\text{)}$$

Figure-1.2 shows the material properties [strength vs density and elastic/compressive moduli][2] of some natural and synthetic materials and their composites.

Fracture-resistance of a material is the ability of a material to resist propagation of a fracture/ crack inside its structure. It is the energy required to propagate a crack inside the material. We see in the hierarchical structure of biomaterials such as bone and wood, alternatively aligned layering of fibrillar structures to resist breaking and propagation of fractures[3].

1.2. Bone--a versatile composite of mineral and collagen

If we look at the hierarchical structure of bone, it consists of a peripheral compact bone structure with a spongy core (Figure-1.3). The structures of spongy bone are called trabeculae. If we zoom in to the compact bone, long cylindrical structures can be found running along the length of the bone, bundled together, which are called osteons. Each osteon contains bone cells embedded in an extracellular matrix (ECM) of collagen fibers and mineral crystals of calcium hydroxyapatite. The collagen fibers bundle together to form cross-aligned layers held together by extra-collagenous proteins and hydroxyapatite mineral composite phase. Approximately, 60% of bone by weight is hydroxyapatite and ~10-20% part is protein, of which 90% is type-I collagen. Type-I collagen (Figure-1.4a) has three chains that form the nanofibril of collagen; its ends have complex interactions with hydroxyapatite and the neighboring nanofibrils. Overall, the collagen fibers provide tensile strength and elasticity of bone. Stiffness is provided by reinforcement via hydroxyapatite crystals.
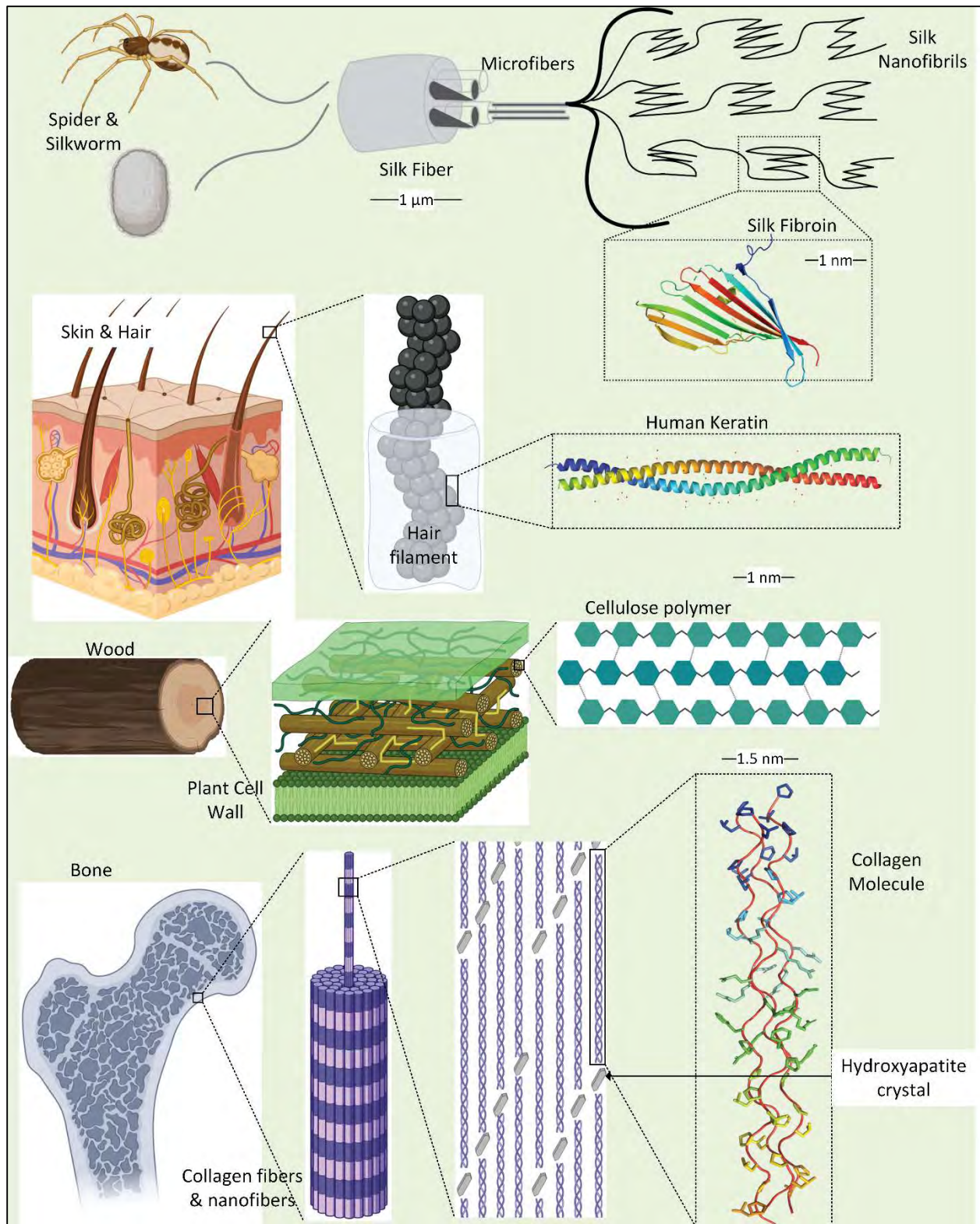
Figure-1.1: Hierarchical Structure of Biomaterials; (starting from top) **Silk:** spider and silkworm silk is a single fiber made up of bundles of micro and nano fibrils. Each nanofibril is

made of long running polymers of silk fibroin protein **[PDB: 3ua0]**. **Leather (skin)/ hair:** hair strands are made up of long keratin polymers (nanofibrils) running parallel in bundles. Here the structure of human keratin **[PDB: 6ec0]** is shown. **Wood:** all plant cell walls contain fibers of cellulose. Each fiber is made up of microfibrils that are made up of bundles of cellulose nanofibers. Each nanofiber is a polysaccharide chain of β-D (1→4) Glucose units. **Bone:** bone has complex hierarchical structure. Bundles of mineralized collagen run in the haversian canals of bone extracellular matrix. In each bundle, there are bundles of nanofibers of mineralized collagen. Each collagen nanofiber has tropocollagen molecules **[PDB: 7cwk]** running in parallel, with each molecule joined by a hydroxyapatite (HAP) crystal. The arrangement of crystals and collagen molecules is staggered such that the plies of each mineralized collagen fiber accumulate huge amounts of strength and fracture resistance.
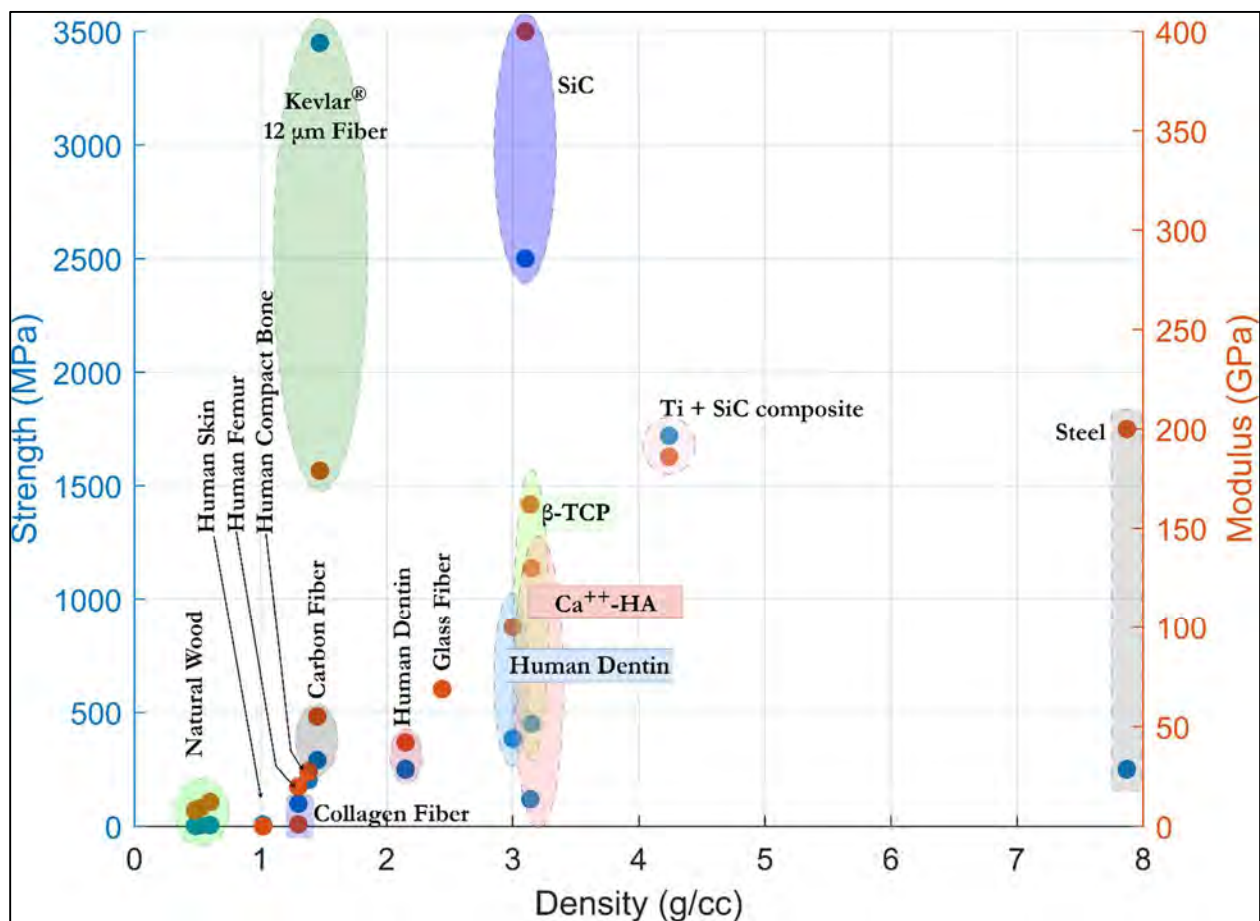
Figure-1.2: A materials properties chart, showing *Strengths* [Tensile/Compressive] in megapascals (MPa)—blue dots, and *Moduli* [Young's modulus/compressive modulus] in gigapascals (GPa)—red dots, versus *Densities* in (g/cm^3) of natural and synthetic materials. For more details, see **Supplementary Table-1.** [**SiC:** Silicon Carbide; **Ti:** Titanium; **β-TCP:** Tricalcium phosphate; **Kevlar®:** used in bulletproof jackets; **HA:** Hydroxyapatite].

Collagen nanofibrils are about 300 nm long and ~1.5 nm wide, while nano-hydroxyapatite crystals have dimensions of about [a= 25 nm x b= 1.5 nm x c= 50 nm][1,3-6]. The c-axes of crystals are aligned to be parallel to collagen fibrils (Figure-1.3). The N- and C-termini of tropocollagen electrostatically interact with calcium ions and phosphate ions of hydroxyapatite. Figures 1.4b and 1.4c represent collagen-HAP interactions of N-termini and C-termini, respectively. Extracollagenous proteins intrude the staggered stacks of mineralized collagen and HAP[7]. Each collagen nanofiber is not only attached to HAP on its ends, but also attached with the neighboring mineral crystals. The prolines and hydroxyprolines interact with the PO_4^{3-} and Ca^{++} ions respectively, along the entire length of the tropocollagen molecule. These additional sites of interaction form resistance points against sliding of mineral-collagen nanofibers. Further reinforcement from extracollagenous proteins like osteocalcin and osteopontin happens at the interfaces of fibrils. Osteocalcin and osteopontin interact with HAP to stabilize the Ca^{++} ions, as well as form sacrificial bonds that break at high shear stress. These sacrificial bonds are reversible and provide the bone with fracture resistance and resistance to crack propagation.

Human
Femur

Haversian
Canals

Osteons

Cross-
plies

Trabecular
Bone

Cancellous
Bone

200-500 µm

1.5 nm

300 nm

Fiber

Fibril
(10-300 nm)

Hydroxyapatite crystals
(50 nm x 25 nm x 1.5 nm)

Collagen molecule
1.5 nm x 67 nm

Extracollagenous proteins
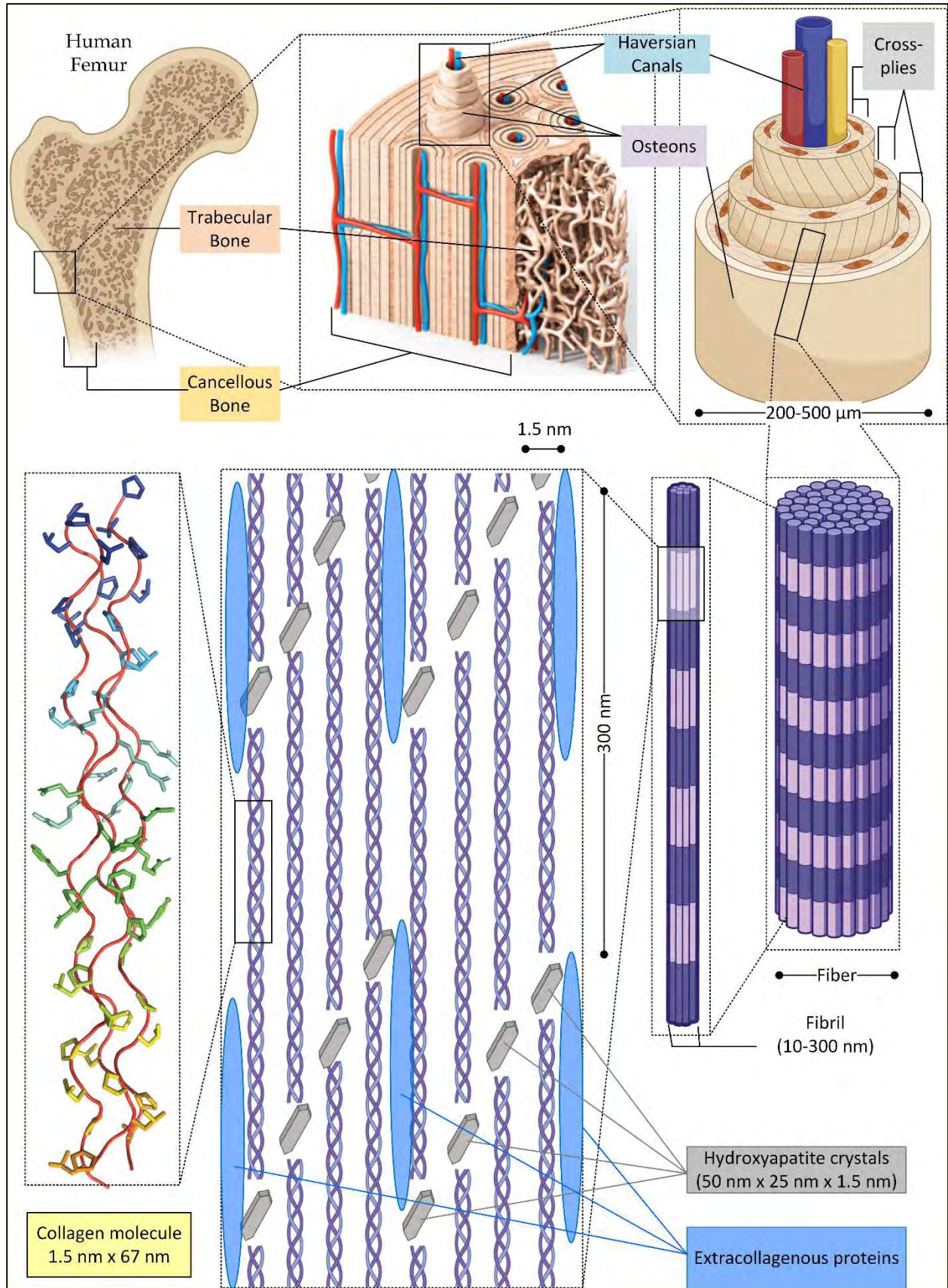
Figure-1.3: Hierarchical Structure of Human Bone: Bone consists of outer compact part (**cancellous bone**) and inner spongy part (**trabecular bone**). In compact bone, **osteons** run parallel with holes in their centers, called **haversian canals**, which contain blood vessels and lymph vessels. Each osteon has concentric lamellae; each lamella has osteocytes embedded in extracellular matrix, of parallel running mineralized collagen fibers. Each lamella has orientation of fibers perpendicular to that of adjacent lamella. Cross-plies of mineralized **collagen fibers** typically span 3-7 µm. Each collagen fiber contains **fibrils** bundled together with extracollagenous proteins. Each fibril is about 10-300 nm in diameter; having parallel **tropocollagen [PDB: 7cwk]** fibers of 300 nm –each fiber attached to **hydroxyapatite (HAP)** crystals on its ends. The HAP crystals are staggered in arrangement such that they provide additional attachment to the surrounding collagen molecules and provide sites of friction between the stacked molecules. Therefore, the multiple bonds multiply to cause an enormous increase in strength and toughness.
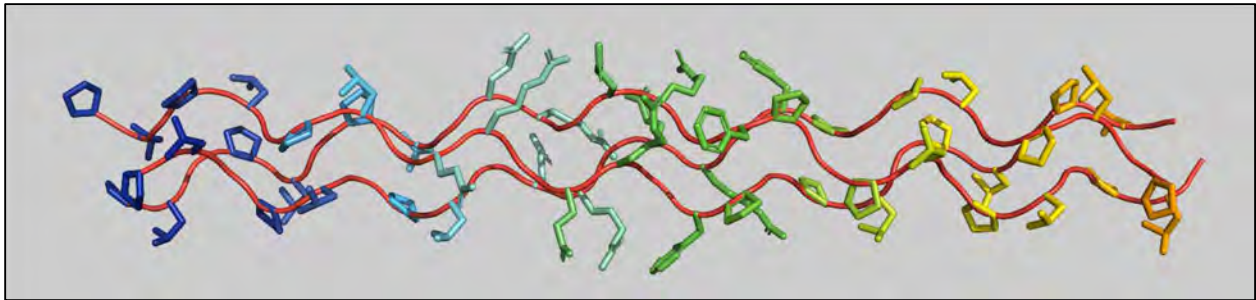
Figure-1.4a: *3D Structure of Human Collagen Type-I* [left: N-terminus; right: C-terminus]. Notice the characteristic prolines abundant in all chains, PDB: 7CWK.
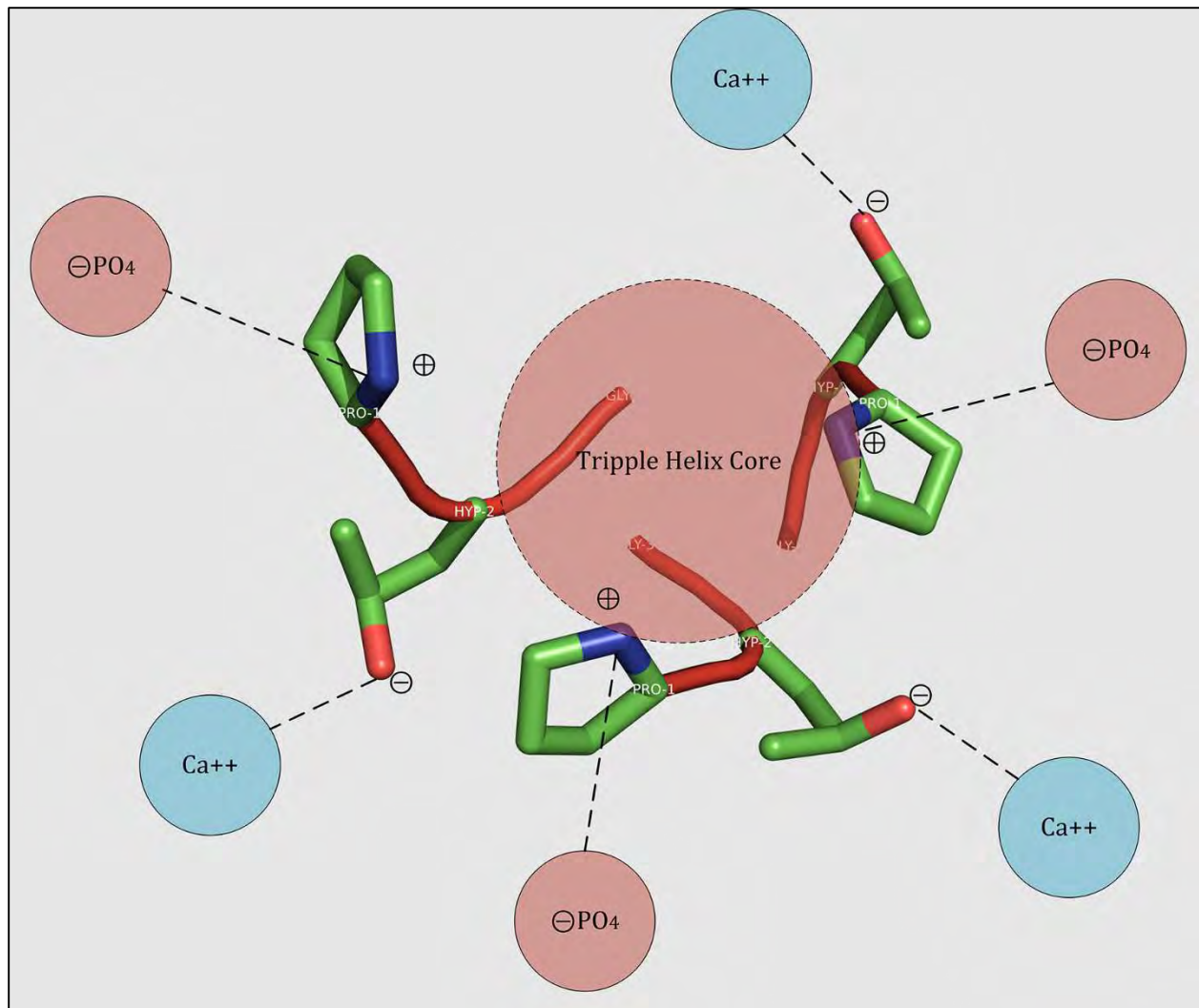
Figure-1.4b: Electrostatic interactions of collagen N-terminus with calcium phosphate.
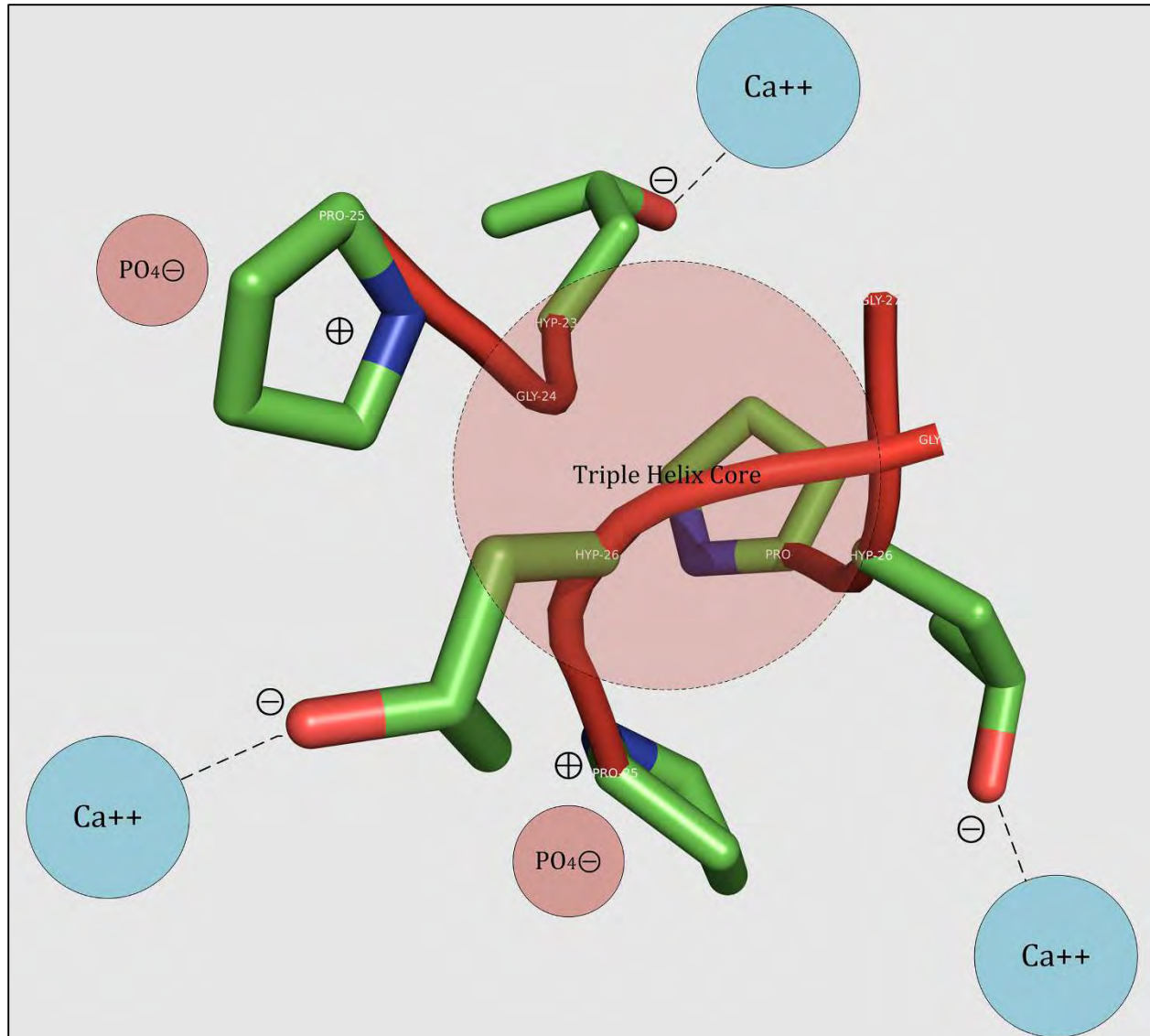
Figure-1.4c: Electrostatic interactions of collagen C-terminus with calcium phosphate.

1.3. The Bone Mineral—Calcium Hydroxyapatite

HYDROXYAPATITE or HAP is the apatite mineral form of calcium phosphate. Minerals of phosphate that typically have hexagonal symmetry are called apatite. Of mineral origin, apatite usually refers to the calcium phosphate form $Ca_5.(PO_4)_3.(OH)$, in contrast to commonly used lab chemical tricalcium phosphate $Ca_3(PO_4)_2$ [also referred to as TCP or β-TCP]. Here, I shall refer to the inorganic phosphate group as P_i. The Ca^{++} to P_i ratio or Ca^{++}/P_i is important in recognizing

the mineral. The Ca^{++}/P_i of TCP is 3:2 or 1.5. Two entities of apatite form the crystal structure and unit cell of Ca^{++} -hydroxyapatite, hydroxyapatite, or HAP; these terms shall be used alternatively, and these refer to the same thing (Figure-1.5).
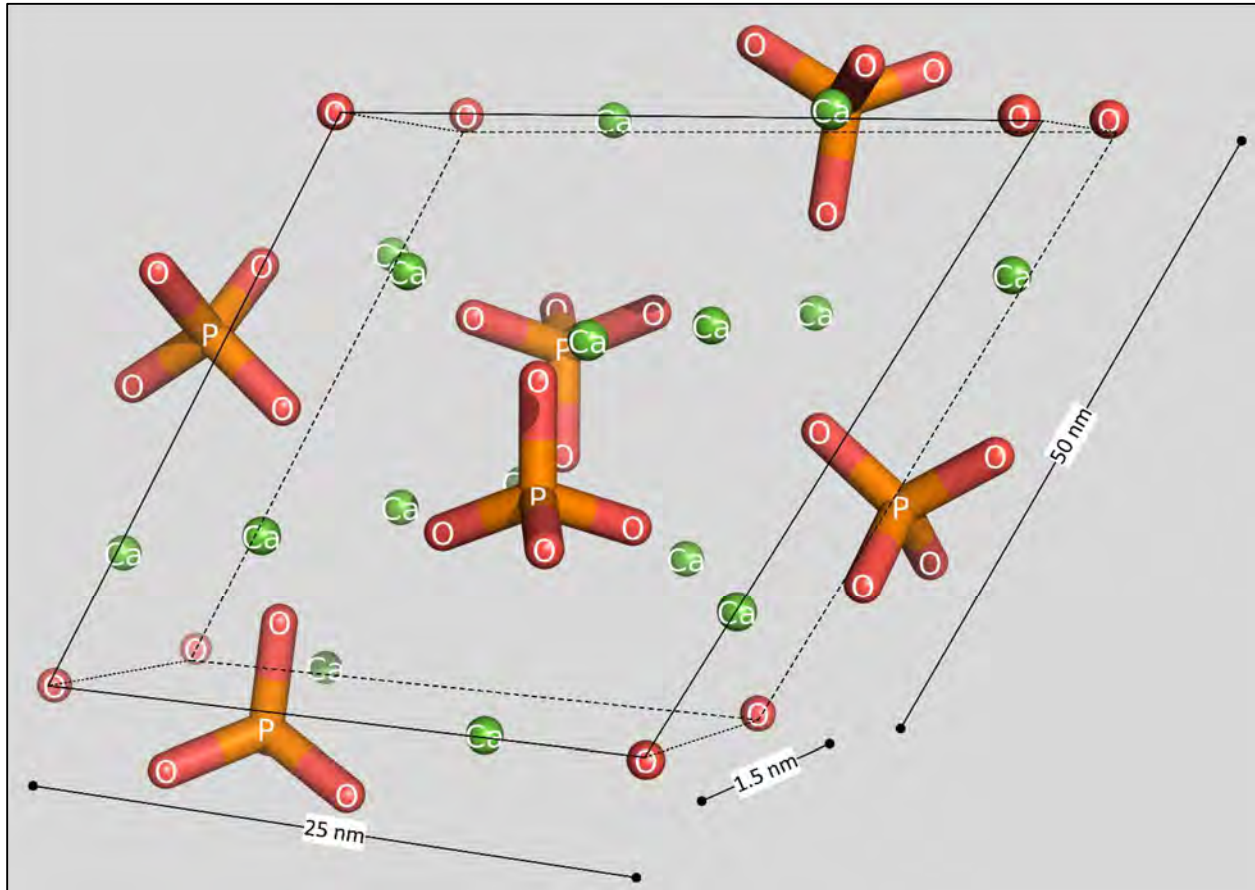
Figure-1.5: 3D structure of HAP unit cell. the HAP nanocrystal has hexagonal symmetry, dipyramidal crystal with space group $P6_3/m$ [5].

HAP typically has the formula $Ca_{10}.(PO_4)_6.(OH)_2$ and a Ca^{++}/P_i ratio of 10:6 or 1.67. This is the stoichiometric HAP. The OH⁻ of stoichiometric HAP may be substituted by a carbonate (CO_3^{2-}), or a halogen like fluoride F⁻ or chloride Cl⁻, rendering the stoichiometric HAP carbonated, fluorine substituted, chlorine substituted; making the products carbonated HAP (cHAP), fluorapatite and chlorapatite, respectively. The carbonated HAP is also called "Ca^{++} -deficient" in the sense that CO_3^{2-} -substituted HAP has a Ca^{++}/P_i ratio <1.67. A Ca^{++}/P_i ratio in the range of 1.5-1.67 is typically found in ion-substituted HAP species[8]. Stoichiometric HAP can be prepared in the lab by

reacting calcium hydroxide $Ca(OH)_2$ with orthophosphoric acid H_3PO_4. This reaction gives a suspension of HAP nanocrystals (nHAP) (Figure-1.6).

$10.Ca(OH)_2 + 6.H_3PO_4 \rightarrow Ca_{10}(PO_4)_6(OH)_2 + 18.H_2O$
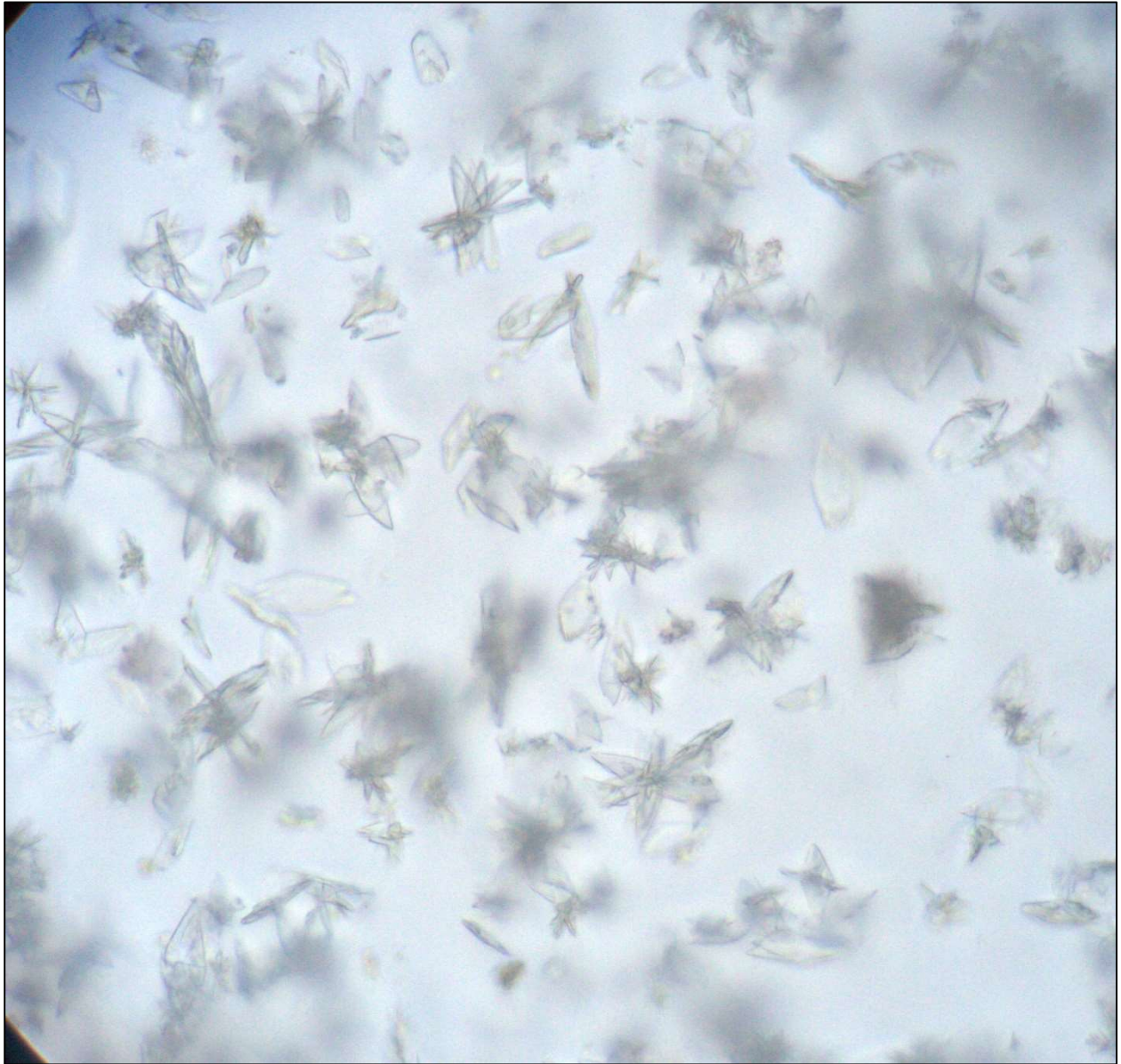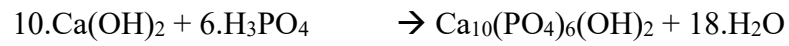
Figure-1.6a: nHAP crystals chemically synthesized in the lab (optical, 400x), courtesy of author.
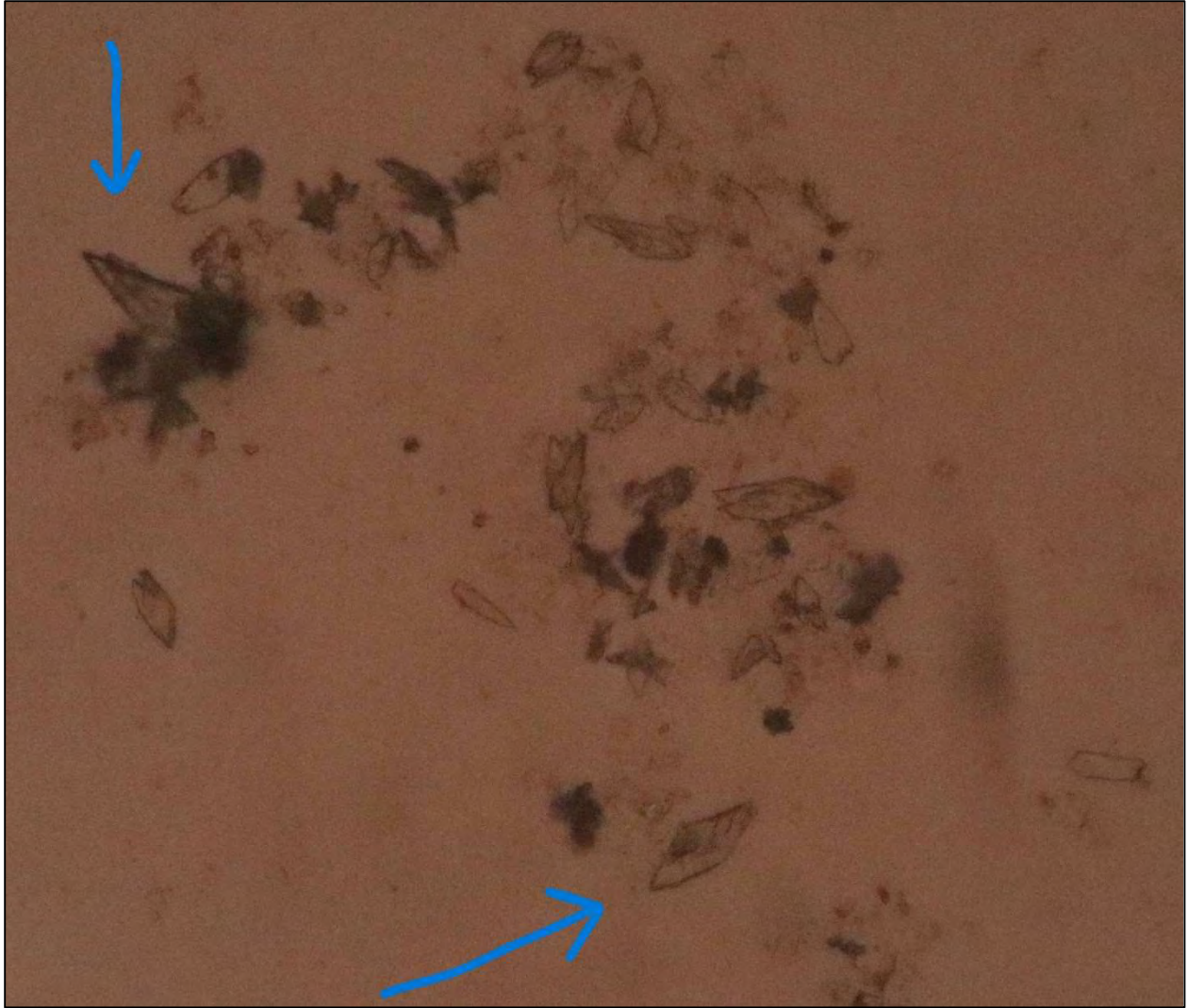
Figure-1.6b: nHAP crystals chemically synthesized in the lab (optical, 1000x). Notice the beautiful, demarcated crystals with definite symmetry, courtesy of author.

True calcium deficient HAP or cdHAP is a non-stoichiometric HAP that contains a Ca^{++}/P_i ratio in the range of 1.5-1.67. cdHAP can be synthesized in the lab precipitation reaction of calcium nitrate and diammonium phosphate. This creates precipitates of cdHAP as follows:

9.6 $Ca(NO_3)_2$ + 6 $(NH_4)_2.HPO_4$ → $Ca_{9.6}.(PO_4)_{5.6}.(HPO_4)_{0.4}.(OH)_{1.6}$ [cdHAP; Ca^{++}/P_i : 1.6]
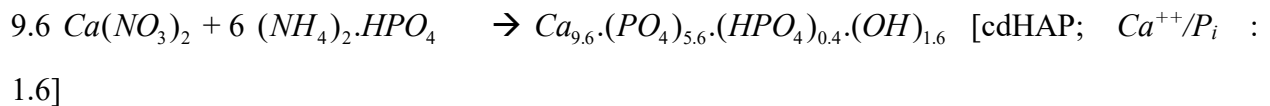
From this we can draw a general formula for cdHAP as:

$Ca_{10-x}.(PO_4)_{6-x}.(HPO_4)_x.(OH)_{2-x}$ where $0 < x < 1$.
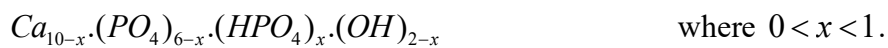
1.4. Hydroxyapatite Mineralization in Human Body

In humans, carbonated calcium hydroxyapatite is present in bones, whereas calcium hydroxyapatite is present in dentin (the hard tissue of tooth). The calcium concentration in human serum is 2.2-2.7 mmol/L, which is regulated by the endocrine system[9]. The intracellular calcium concentration is four orders of magnitude lower than that of blood.

The solubility product constant $= K_{sp} = \dfrac{ionic - concentraion}{undissolved - solid}$

Since blood and intracellular concentrations of calcium are very small, we take $-\log K_{sp} = pK_{sp}$.

The pK_{sp} of carbonated Ca-HAP is *-58* to *-59*, and the pK_{sp} of simple calcium phosphate is *-29*[10,11]. This means that the bone HAP is 30 orders of magnitude less soluble than the calcium phosphate in physiologic solutions. Our body knows how to molecularly determine which collagen fibrils to mineralize (bone and dentin) and which not to mineralize (of ligaments, tendons, extracellular matrix, etc.). The physiologic phosphate PO_4^{3-} (*P_i*) in blood (pH= 7.35) is present in two forms: pyrophosphate (*PP_i*) and poly-pyrophosphate (*polyP_i*). *PolyP_i* – packed granules are present in both blood plasma and the interstitial fluid in haversian canals of osteons. These granules can chelate Ca^{++} ions to form "calciprotein particles"[12]. An inhibitor of mineralization, **Fetuin A**, is a circulating protein that inhibits systemic mineralization of HAP[13].

PolyPi's contain alkaline phosphatases and other proteins; if alkaline phosphatases are activated, they increase the free P_i in the plasma or tissue microenvironment[14]. The ratio of *polyP_i/P_i* determines the mineralization of phosphate in a tissue.

$\uparrow \dfrac{polyP_i}{P_i} \Rightarrow$ inhibits mineralization.

$\downarrow \dfrac{polyP_i}{P_i} \Rightarrow$ promotes mineralization.

Osteoblasts in bone express **TNAP**—tissue-nonspecific alkaline phosphatase[14] that degrades *PP_i* and *polyP_i* to promote mineralization in bone. If alkaline phosphatases are activated within the calciprotein particles, hydroxyapatite crystallizes in the core of the particles, whereas the proteins

acting on Ca^{++}/P_i are displaced to periphery of the particle[15]. The crystalline core and amorphous shell form just like hydroxyapatite nucleation within amorphous calcium phosphate (ACP) particles in vitro[16].

DMP1: Dentin Matrix acidic Phosphoprotein 1 is expressed in dentin and promotes Hap mineralization in dentin extracellular matrix[17].

DSPP: Dentin Sialophosphoprotein is a precursor to extracollagenous proteins in teeth, which are dentin sialoprotein (DSP), dentin glycoprotein (DGP) and dentin phosphoprotein (DPP). These are involved in dentin mineralization. DMP1 and DSPP proteins are not limited to teeth and are also found in bone[18].

BSP: Bone Sialoprotein promotes mineralization[18]. It is a Ca^{++}-binding, small-integrin-binding ligand N-linked glycoprotein (SIBLING). BSP is present in the ECM of bone and teeth but absent in the rest of the body. It causes mineral nucleation in the ECM of mineralized tissues. The mineralization cannot occur without the stabilization of cations and anions by negatively charged ($C\!=\!\!=\!O^{\ominus}$) and positively charged ($H\!-\!\!-\!N^{\oplus}$) groups on the surrounding proteins. In case of HAP mineralization, the glycines and prolines on tropocollagen termini stabilize Ca^{++}/P_i, respectively (Figures 1.4b and 1.4c); they are also stabilized by non-collagen proteins in the bone ECM.

HAP mineralization inhibition is required at the interfaces of mineralized—non-mineralized tissues where a sharp mineralization stop is needed. For example, the periodontal ligament (PDL) that attaches tooth to alveolar bone, or the sites of tendon attachment to bone. In ECM mineralization, inhibitor proteins regulate mineralization in the skeleton by inhibition of crystal growth.

Osteopontin [OPN] is a protein, abundant in bones, which inhibits Hap crystal growth at interfaces with abrupt stop to mineralization, such as the above mentioned PDL[7].

MGP: Matrix Gla Protein is important in native inhibition of mineralization in chondrocytes and vascular smooth muscles. It is expressed in high collagenous tissue that does not need mineralization, i.e., walls of arteries and cartilage[19].

MEPE: Matrix Extracellular Phospoglycoprotein is also a SIBLING and is commonly found in both mineralized and non-mineralized tissue. Like OPN, MEPE is also an inhibitor of mineralization [18]. To put all of this in perspective, Table-1.1 outlines the promoters and inhibitors of calcium phosphate/HAP mineralization in humans.

Table-1.1. Promoters and Inhibitors of HAP mineralization in Humans

Protein	Major site of action	Mineralization	Action
Tissue Non-specific Alkaline Phosphatase (TNAP)	bone	promoter	degrades $polyP_i$ and PP_i to form free P_i
Bone Sialoprotein (BSP)	bone	promoter	causes nucleation of calcium phosphate for HAP formation
Dentin Matrix Protein 1 (DMP1)	teeth	promoter	HAP mineralization in teeth
DSPP proteins	dentin	promoter	HAP mineralization in teeth
Fetuin A	systemic (blood vessels)	inhibitor	inhibits systemic HAP mineralization
Osteopontin (OPN)	bone/interfaces	inhibitor	inhibits HAP crystal growth at interfaces
MGP	artery walls/ cartilage	inhibitor	inhibits/ fine-tunes HAP mineralization
MEPE	mineralized and non-mineralized tissue	inhibitor	inhibits/ fine-tunes HAP mineralization

1.5. Wheat Gluten

Wheat Gluten (WG) is a rubbery mass obtained when raw dough is washed under water, and is responsible for elastic and viscous properties of dough and bread. WG is a group of storage proteins present in the wheat seed endosperm, responsible for viscoelastic properties of bread and baked goods[20]. Seed storage proteins in plants, called prolamins, are vast amino acid reserves for the germination of embryo. In cereal crops, prolamins have similar properties to gluten proteins. Common bread wheat (***Triticum aestivum***) is the staple food of over 30% of global population[21]. *T. aestivum* genome is hexaploid, seven chromosome genome of A, B and D subgenome types; a total of 21 chromosomes. Its genome is about 17 gigabases (Gb) with over 100,000 genes[22] [check IWGSC RefSeq v2.1]. Out of these, approximately 650 proteins of gluten family can be identified in *T. aestivum*[23]. Most of these are isoforms and can be classified into groups of similar proteins. If wheat gluten proteins are separated on a denaturing polyacrylamide gel (SDS-PAGE) more than 100 proteins can be separated on a 2-dimensional (2D) gel. There are polymeric gluten proteins in the seed storage, called "glutenins" (GLT), and some in monomeric form, called "gliadins" (GLI). The hierarchy of gluten protein groups is illustrated in Figure-1.7. Gliadins are natively monomeric in the wheat seed and polymerize only when treated with water, some plasticizer, or when kneading dough. On the other hand, polymeric glutenins form one of the largest biopolymers in nature, with molecular weights (M_w) in excess of tens of millions of Daltons (10x MDa). Gliadins are soluble in aqueous alcohols (~70% ethanol) while the polymeric glutenins are virtually insoluble and can only be dissolved in reducing solvents. This is because glutenins have cysteine residues that form intra-chain and inter-chain disulfide bonds. On the other hand, gliadins have few or no cysteine residues and only form intra-chain disulfide bonds. Glutenins are responsible for the elasticity of dough/bread, while gliadins are responsible for the viscosity of the dough/bread[20,24-26].

GLTs are high molecular weight as compared to GLIs (Figure-1.7). GLTs can be subdivided into two groups based on their M_w, high-molecular weight glutenin subunits or **HMW-GS** and low-molecular weight glutenin subunits or **LMW-GS**. There are a total of 6 types of HMW-GS and 17 types of LMW-GS. For a detailed description of gluten proteins names and chromosomal locations, see Supplementary Tables 2 and 3. GLIs can be divided into 4 groups based off their homologies: (1) Alpha/beta-Gliadins [**α/β-GLI**], (2) Delta-Gliadins [**δ-GLI**], (3) Gamma-Gliadins [**γ-GLI**], and (4) Omega-Gliadins [**ω-GLI**]. There are other gliadin-like proteins that include in the gluten

matrix when dough is formed, but they are only in small amounts and are out of the scope of this work. The M_w of HMW-GS is 67-88 kDa, while that of LMW-GS is 32-39 kDa. The molecular weights of α/β-GLI and γ-GLI are in the range of 28-35 kDa, and those of ω-GLI are in range of 39-55 kDa[27,28]. There are only two proteins in δ-gliadin and they are usually not classified as a separate group. The names α-/ β-/ γ-/ ω- are given on the basis of electrophoretic mobility on a low-pH gel, in decreasing order of mobility, respectively.

In HMW-GS, there are two protein types, *x-type* and *y-type*. The HMW-GS has similar N-terminal domains (NTDs) and C-terminal domains (CTDs), with central region having repetitive domains in the center. The repetitive domains have tandem and interspersed repeats of short peptides usually hexapeptides (6 residues) or nonapeptides (9 residues). Because of the highly repetitive nature of sequence, the structure of HMW-GS has been hard to elucidate. The repetitive sequences (consensus) in x-type are PGQGQQ followed by GQQ; in y-type are PGQGQQ followed by GYYPTSLQQ. Predicted structure includes multiple β-reverse turns in the repetitive region, as well as no significant secondary structure. While the NTD/CTD regions usually have some secondary structure, they are rich in glutamine (Q) and proline (P) residues [Supplementary Figures S1 & S2]. This is important in the viscoelastic and dough-forming properties of gluten. When heated to around 125 °C in the presence of a plasticizer (e.g., H_2O, glycerol), these free regions form tandem mass of randomly organized chains intermolecularly bonded with hydrogen bonds, intermolecular disulfide bonds and Van der Waals interactions. The plasticizer acts as a hydrogen bond (H-bond) bridge between amino acid residues on the same protein chains or different chains. This agglomeration of proteins at this temperature turns gluten into plastic and this temperature is called **glass transition temperature (T_g)** of gluten. In the presence of starch in the wheat flour, the concentration of gluten in less and the HMW-GS and LMW-GS unstructured regions render elastic properties of the dough. Gluten elasticity is majorly attributable to the HMW-GS and the hydrogen bonding in their structure, which is attributable to the high concentration of Q residues, forming H-bonds both within and between different subunits[24,27-30].

1.6. Gluten Intolerance and Wheat Allergies

Wheat gluten, along with other prolamins, are a potential cause of human conditions Celiac Disease (CD), and wheat allergies including immunoglobulin E (IgE)-mediated wheat allergy, baker's asthma, contact urticaria (dermal allergy) and WDEIA (wheat-dependent exercise-induced

anaphylaxis). Approximately 1% of global population suffers from CD and much more from wheat allergies[31]. Gluten sensitivity is another condition, having little symptoms-based evidence, which is sometimes correlated with gut problems and associated with irritable bowel syndrome. Regardless of wheat allergies and sensitivity, celiac disease is the chronic and slow atrophy of small intestine villi. The disease is associated with but not caused by gluten proteins. CD is an autoimmune inflammatory response to the partially digested α-gliadin peptides. WG proteins are rich in proline and glutamine residues, which are poorly digested by intestinal proteases. An enzyme transglutaminase 2 (TG2) carries out a deamidation reaction and converts glutamine residues to glutamate (E). The resulting E residues bind the human leukocyte antigen (HLA) on $CD4^+$ T-cells more strongly. Thus, the partially digested oligopeptides do not come off the HLA and antibodies form against gluten peptides, which now attack the T-cells. Individuals with risk of developing CD almost always express either or both HLA-DQ2.5/ HLA-DQ8 antigens. Table-1.2 outlines the gliadin epitope modifications by TG2 and their affinity for HLA-DQ2.5/ HLA-DQ8[32-34]. People with CD show outstanding improvement with using gluten-free flour and gluten-free products, as there is no formal cure of the disease available. Especially in the European Union (EU), wheat gluten is an industrial byproduct available in large quantities[31].
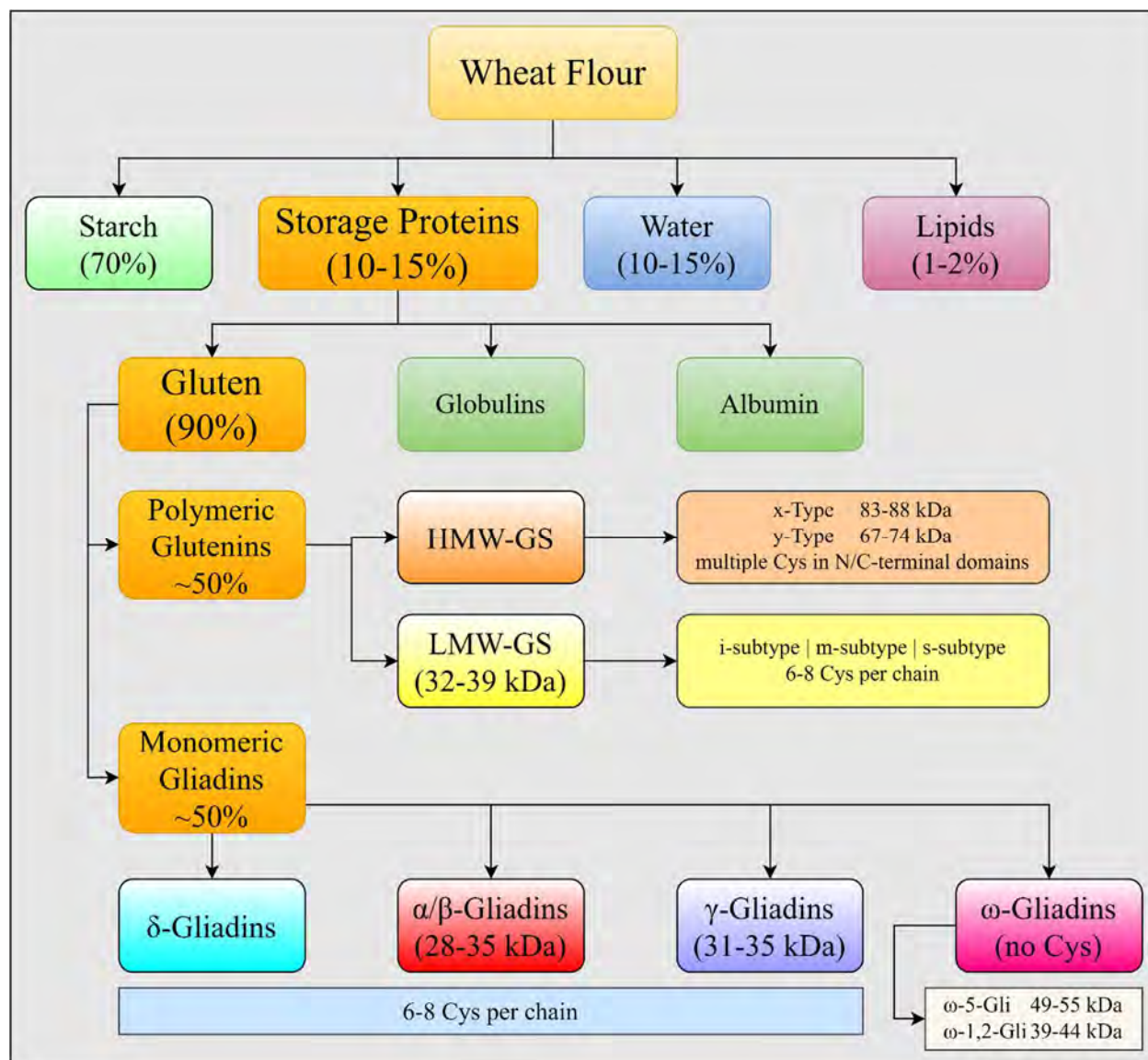
Figure-1.7: Classification of Gluten Proteins

Table-1.2: Modification of gluten peptides by tissue transglutaminase[32].

HLA–modified gluten complex	Original peptide sequence	HLA-DQ2-binding modified sequence (XXXEXEEXX)*	HLA-DQ8-binding modified sequence (EXXXXXXXE)*
DQ2.5–α1-gliadin	PFPQPQFPY	PFPQPELPY	–
DQ2.5–α2-gliadin	PQPQLPYPQ	PQPELPYPQ	–
DQ2.5–ω1-gliadin	PFPQPQQPF	PFPQPEQPF	–

DQ2.5–ω1-gliadin	PQPQQPFPW	PQPEQPFPW	–
DQ2.5–α3-gliadin	FRPQQPYPQ	FRPEQPYPQ	–
DQ2.5–γ1-gliadin	PQQSFPQQQ	PQQSFPEQQ	PQQSFPEQE
DQ8–α1-gliadin	QGSFQPSQQ	–	EGSFQPSQE
DQ8–γ1a-gliadin	QQPQQPFPQ	–	EQPQQPFPQ

*HLA-DQ2.5 requires E at positions 4, 6/7 and HLA-DQ8 requires E at 1 or 9 positions. This gives strong binding of gluten peptide to the HLA antigen.

Wheat allergies like baker's asthma, contact urticaria, and food allergy are usually IgE mediated, and depend on the route of the antigen exposure. Food wheat allergy is present in 0.5% children, and it vanishes over time. However, some reactions to wheat exposure may be life threatening. In any case, wheat exposure is minimized for the person's safety. Some people are hypersensitive to wheat, but those cases are rare. WDEIA is also quite a rare condition that involves wheat intake while performing physical activity. ω-5-GLI and HMW-GS are associated with such type of interactions[26]. Supplementary Table-3 lists wheat gluten proteins associated with risks of wheat allergies and CD.

Chapter-2

LITERATURE REVIEW

In literature review, I shall address hydroxyapatite synthesis and HAP composites separately and WG composites separately.

2.1. Synthesis of Hydroxyapatite from Biogenic and Chemical Sources

Hydroxyapatite is a calcium phosphate mineral, and it can be formed by direct nucleation of HAP inside a Ca/P_i solution or nucleation of HAP inside amorphous calcium phosphate (ACP)[16].

The simplest chemical synthesis method is **direct reaction** of calcium carbonate ($CaCO_3$) and orthophosphoric acid (H_3PO_4). *Pham Minh et al.* (2014)[35] showed one-step Ca-HAP synthesis with $CaCO_3$ as calcium source and H_3PO_4 as phosphate source, for a reaction time of 24 h at 80 °C. They created a suspension of $CaCO_3$ in water at 80 °C, under constant stirring of 400 rpm, using a mechanical, vertical stirrer. The H_3PO_4 was into the suspension at a small rate of 2 mL/min. The product was separated by filtration on a filter paper and dried overnight. The reaction was as follows:

$$10.CaCO_3 + 6.H_3PO_4 \rightarrow Ca_{10}(PO_4)_6(OH)_2 + 10.CO_2 + 8.H_2O$$
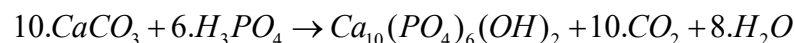
The Xray Diffraction (XRD) Analysis showed a highly crystalline product. Elemental analysis confirmed a Ca/P_i ratio of 1.67. Furthermore, they demonstrated that the obtained Ca-HAP could be carbonated by incubation of HAP gel with CO_2 at a pressure of ~13 bar for 48 h. The carbonated HAP could be decarbonized at temperatures of 740-1250 °C. Overall, the study showed the potential ease of HAP synthesis from relatively cheap starting materials, with only CO_2 as a byproduct. *Verwilghen et al.* (2007)[36] showed simple one-step synthesis of HAP by **direct reaction** of $Ca(OH)_2$ and H_3PO_4.

$$10.Ca(OH)_2 + 6.H_3PO_4 \rightarrow Ca_{10}(PO_4)_6(OH)_2 + 18.H_2O$$
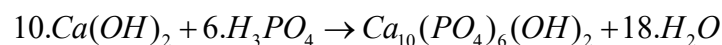
They added H_3PO_4 slowly to a lime suspension at room temperature, under continuous stirring. The resulting solution was aged for 12 h at 75 °C, filtered and air dried at 105 °C. After air drying, the solids were ball milled to obtain a particle size of 80 μm. The powders were then sintered at

1000 °C. XRD and SEM showed crystalline product with small particle size and specific surface area (SSA) analysis showed 120-160 m^2/g for solutions aged for 48 h. This demonstrated the effect of **aging** of suspension of ACP in good nucleation and formation of HAP. They also synthesized HAP using a **double decomposition method,** in which monoammonium dihydrogen phosphate ($NH_4H_2PO_4$) and calcium nitrate solution ($Ca(NO_3)_2$) were mixed and the pH was adjusted to 10.7 using ammonium hydroxide (NH_4OH). Under basic conditions, HAP precipitates formed. They used the same above-described scheme for aging of 48 h, drying, milling followed by sintering at 1000 °C. The double decomposition reaction involved decomposition of both the calcium source and the phosphate source. One big drawback of the process was formation of byproduct ammonium nitrate. The synthesis reaction was as follows:

$$10.Ca(NO_3)_2.4H_2O + 6.NH_4H_2PO_4 + 14.NH_4OH$$
$$\rightarrow Ca_{10}(PO_4)_6(OH)_2 + 20.NH_4NO_3 + 52.H_2O$$
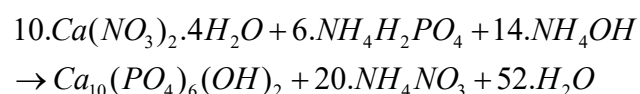
Similarly, double decomposition method has been used for HAP synthesis using calcium nitrate and a variety of ammonium phosphates [$NH_4H_2PO_4$; $(NH_4)_2HPO_4$; $(NH_4)_3PO_4$] in the presence of NH_4OH. However, they all have the drawbacks of high initial materials costs and a byproduct (NH_4NO_3) in the end[35]. Reactions between solid $CaCO_3$ and solutions of different phosphorus sources [H_3PO_4, Na_2HPO_4, K_2HPO_4, KH_2PO_4] result in surface reactions on solid $CaCO_3$; resulting in production of HAP. However, the reaction occurs on the surface of solid $CaCO_3$ particles, not all the way through to the core of the particles[37].

Sol-gel method is widely used in the synthesis of nano hydroxyapatite (nHAP). In this method, solutions ("sol") containing calcium and phosphate source separately are prepared and mixed under lab conditions. The resulting reaction creates a suspension of calcium phosphate and/or HAP ("gel"), which is then processed to obtain dry powders of HAP. Typically, calcium nitrate, calcium chloride, calcium hydroxide, or an organic calcium salt (e.g., Ca-acetate) are used as calcium source; mono-/di-sodium phosphates [NaH_2PO_4/ Na_2HPO_4], mono-/di-potassium phosphates [KH_2PO_4/ K_2HPO_4], mono-/di-ammonium phosphates [$NH_4H_2PO_4$/ $(NH_4)_2HPO_4$], or phosphoric acid are used as phosphate sources[35,38,39]. Many methods described here are based on the sol-gel method.

Saha et al. (2009)[40] used **reverse microemulsion method** for HAP synthesis; **micoemulsion** involves using an organic phase and a non-ionic surfactant to create nano-sized micelles in aqueous

solution of calcium and phosphate source. The micelles can immobilize Ca^{++} on their surfaces, which can create nucleation sites for HAP. So, in essence, they created a reverse microemulsion by adding aqueous solutions to organic phases. They used $Ca(NO_3)_2$ and H_3PO_4 in aqueous solution. They created different microemulsions using various [organic solvent: surfactant] systems as hexane: dodecyl phosphate; isooctane: dioctyl sulfosuccinate; cyclohexane: poly(oxyethylene) nonylphenol ether. pH was adjusted to 9 and the emulsion was dried at 150 °C. This method created nano-sized HAP with high crystallinity. In a similar method, microemulsion was used to create HAP nanocrystals on the surface of micelles. *Lim et al.* (1999)[41] used $CaCl_2$ solution as aqueous phase; petroleum ether as organic phase and a non-ionic surfactant KB6ZA. They added organic: surfactant to the $CaCl_2$, created emulsion and then added di-ammonium phosphate. The $(NH_4)_2HPO_4$ solution was slowly titrated and then aged for 24 h at 34.5 °C. The resulting solids were ethanol washed and calcinated at 650 °C for 6 h. The procedure resulted in nanosized HAP particles. *Gopi et al.* (2012)[42] used glycine (Gly) and acrylic acid (AA) as organic phase and solution of $Ca(NO_3)_2$ and $(NH_4)_2HPO_4$ as aqueous phase. They mixed solutions of $Ca(NO_3)_2$ and $(NH_4)_2HPO_4$ slowly and aged the mixture for 5 h under constant stirring. Then Gly and AA were added slowly and aged under constant stirring at pH 9. Afterwards, the emulsion was vigorously shaken for 3 h and treated with ultrasonicator at 150 W/ 28 kHz for 3 h. The precipitate was washed, calcinated and sintered at >600 °C. The results showed nano size, and the crystallinity of HAP decreased with increasing the ultrasonication time. These studies show that microemulsion can be used to obtain HAP of controlled size, however, the multitude of steps and chemicals involved and the calcination/ sintering at temperatures >600 °C, make these methods less reliable and quite expensive. *Jillavenkatesa et al.* (1998)[43] demonstrated sol-gel synthesis of HAP using organic calcium and phosphate sources. They used Ca-acetate and triethylphosphate, using alcohols—methanol, ethanol, and propanol—in solutions. The reaction was conducted in a controlled nitrogen environment and the gel product was calcinated at 1000 °C. It was found that alcohols were useful in the gelation process, however, the end product took longer time and had alcohol impurities in the final product.

To avoid application of high temperatures in post processing of HAP, **microwave-irradiation method** has been devised to trigger the nucleation of HAP in a solution/ mixture containing amorphous form of calcium and phosphate. *Parhi et al.* (2004)[44] demonstrated the ability to synthesize HAP from a solid phase mixture of $CaCl_2$ and Na_3PO_4 through a microwave-mediated

metathesis reaction. The solid $CaCl_2$ and Na_3PO_4 were ground and mixed well. The mixture was irradiated with microwaves for 30 min, washed with water to remove resulting NaCl and dried at 80 °C. Analyses showed nano-sized crystals. Although they did not mention the exact microwave power and specifications. They proposed the following reaction.

$$10.CaCl_2 + 6.Na_3PO_4 \xrightarrow{H_2O \ from \ air} Ca_{10}(PO_4)_6(OH)_2 + 18.NaCl + 2.HCl$$
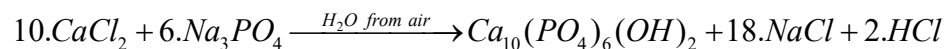
They also demonstrated that by addition of Na_2CO_3 to the same procedure, carbonated HAP could be obtained. *Karishna et al.* (2007)[45] demonstrated a sol-gel method coupled with microwave irradiation. They sourced their Ca from eggshells; washed hen's raw eggshells, heated at 900 °C for 2 h to convert $CaCO_3$ to CaO.

$$CaCO_3 \xrightarrow{900 \ ^\circ C} CaO + CO_2$$
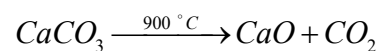
This process is also used for commercial production of lime from limestone. After the eggshell calcination, the lime (CaO) was finely ground and made into an aqueous suspension ($Ca(OH)_2$), and mixed with $(NH_4)_2HPO_4$ solution. The mixture was microwave-treated at 800 W/ 2.5 GHz. The precipitate was washed and dried at 100 °C overnight. The results showed good quality nano-HAP.

Using **eggshells** as calcium source, *Kumar et al.* (2012, 2013) showed that eggshell calcination at high temperatures could be avoided by chelating eggshell Ca^{++} with EDTA[46,47]. In both studies, they treated eggshells with sodium hypochlorite (NaClO; liquid bleach) to remove organic components in the eggshell. After washing and drying, the eggshells were ground and treated with EDTA. The Ca-EDTA complex in solution form was slowly mixed with Na_2HPO_4 solution under constant stirring. The pH was adjusted to 13 and the solution was microwave-treated [600 W/ 2.45 GHz] for 10 min. The resulting precipitates were washed and oven dried. Both studies showed promising results in HAP microcrystal formation.

Turk et al. (2017)[48] showed microwave-treated HAP nucleation in conditions similar to physiologic conditions. They prepared simulated body fluid (SBF) with an ionic concentration 1.5 times that of the human blood. They added $Ca(NO_3)_2$, $CaCl_2$ and $Ca(OH)_2$ to the SBF 1.5 separately to make different solutions. Then they mixed $(NH_4)_2HPO_4$ solution to each solution and set pH to 7.4. Each mixture was microwave treated at 800 W for 15 min. The precipitates were

washed and dried at 37 °C overnight, followed by heat treatment at 900 °C for 1 h. Analyses showed highly crystalline HAP microcrystals.

Ibrahim et al. (2013)[49] used waste eggshells and reacted them with HNO_3 to create $Ca(NO_3)_2$. They added dilute phosphoric acid with a syringe pump at slow rates of 200 mL/h. The reaction resulted in pure HAP phase, which was calcinated at 700 °C and 950 °C. XRD analysis showed that the HAP product had very low crystallinity, and good crystallinity was observed with the post-preparation heat treatment at 700 °C. Another study showed HAP synthesized from eggshells using EDTA/microwave method and showed pure HAP, without any calcium-deficient HAP (cdHAP). The use of EDTA to chelate Ca^{++} away from the $CaCO_3$ worked better than involving whole eggshell powder in the reaction[50]. *Umesh et al.* (2021)[51] showed a similar approach of EDTA/microwave method, but with addition of leaf extract of Piper betel plant in the reaction mix. The resulting HAP had antimicrobial properties and had medium crystallinity. The particle size was also in the range of bone HAP.

Rhee et al. (2002)[52] demonstrated a solid-phase reaction via **mechanochemical method**. They used calcium pyrophosphate and calcium carbonate, and ball-milled them in the presence of acetone or water. The formed slurry was dried and heat-treated at 1100 °C for 1 h. The analyses showed that HAP formed only in the presence of water; the product was highly crystalline, and the surface area of HAP formed increased with increasing the ball milling time. *Silva et al.* (2003)[53] also showed HAP synthesis from ball milling. However, their product showed good formation over a milling period of 60 h. The HAP product was pure and nanocrystalline. The long time of milling indicates that such solid-phase milling reactions may be incomplete. Table-2.1 summarizes the methods and the raw materials for HAP synthesis.

Table-2.1: Summary of HAP production studies.

Calcium Source	Phosphate Source	Addition al chemical (s)	Method of production	Pros	Cons	Ref.

$Ca(OH)_2$; $Ca(NO_3)_2$; $CaCO_3$	H_3PO_4		sol-gel	true nanocrystals; one-step synthesis	high cost of raw materials	[35,36,54]
$Ca(NO_3)_2$; $Ca(OH)$; $CaCO_3$; $CaCl_2$	NaH_2PO_4; Na_2HPO_4; KH_2PO_4; K_2HPO_4; $NH_4H_2PO_4$; $(NH_4)_2HPO_4$		sol-gel	one-step synthesis	high cost of materials	[5,35,36,38,39]
$Ca(NO_3)_2$; $CaCl_2$	H_3PO_4; $(NH_4)_2HPO_4$	surfactants/ organic solvents; ether/ KB6ZA	sol-gel; reverse microemulsion; microemulsion	high-crystallinity of HAP	impurities and expensive materials	[40,41]
Ca-acetate	triethyl phosphate	methanol, ethanol, propanol	sol-gel	increased gelation of HAP in sol	very long reaction times; impurities	[43]
$Ca(NO_3)_2$	$(NH_4)_2HPO_4$	glycine, acrylic acid	ultrasonic treatment	high-purity product, nanocrystals	low-crystallinity, high-temperature use	[42]
$Ca_3(PO_4)_2.2H_2O$; $Ca(OH)_2$; $CaHPO_4$	$NH_4H_2PO_4$	P_2O_5	mechanical; ball milling	true nanocrystals formed	very long reaction (60 h); reaction may be	[53]

					incomplete	
Eggshells (CaCO$_3$)	Ca$_3$(PO$_4$)$_2$.2H$_2$O		mechanical; ball milling	highly crystalline product	high temperature; large crystal size	[55]
CaCO$_3$	Ca$_2$P$_2$O$_7$ (Ca-pyrophosphate)	acetone	ball milling	high crystallinity, high surface area of HAP	large crystals	[52]
CaCl$_2$; Ca(NO$_3$)$_2$; Ca(OH)$_2$	Na$_3$PO$_4$; (NH$_4$)$_2$HPO$_4$		microwave-irradiation	low to high crystallinity of HAP	microcrystals	[44,45,48]
Eggshells	(NH$_4$)$_2$HPO$_4$; H$_3$PO$_4$	EDTA; HNO$_3$	microwave-irradiation	nanocrystalline HAP	low crystallinity	[46,47,49,51,56]

2.2. Composites of HAP with other materials

HAP is bone mineral, and is widely used in skeletal and dental implants, either alone or in combination with some other material[57]. Highest use of HAP composites is in the fields of tissue regeneration and materials for filling up bone defects. Here I shall describe some of the work in the field, with a focus on materials perspective.

Reichert et al. (2012)[58] created a bone regeneration composite scaffold made with medical grade poly-ε-caprolactone (mPCL) and β-TCP, which is a precursor for HAP nucleation in solutions. They created the scaffolds mPCL with 20% TCP via fused deposition. The scaffolds were seeded with mesenchymal stem cells (MSCs) of sheep. The composite scaffolds were grafted in defects created in long bones of sheep models. They also included recombinant human bone morphogenic protein 7 (rhBMP-7) in the scaffold. After 3 months, the long defects were completely healed. In the past 50 years, a lot of research has been put into plasma coating of medical and dental implants with HAP[57]. Similarly, *Ebrahimi et al.* (2022)[59] demonstrated improved differentiation of

osteocytes onto synthesized composite scaffolds made of PCL, HAP and collagen. 3D-printed PCL scaffolds were immersed in 1% HAP suspension overnight, followed by immersion in collagen solution. The HAP/collagen coated scaffolds showed highest osteogenic and osteoconductive properties, as compared with PCL/HAP and PCL/collagen composites alone. This feat is understandable, because in the native bone environment, HAP crystals interact with collagen at multiple sites per collagen molecule. Osteocytes require this kind of assembly to adhere on.

Wada et al. (2016)[60] created a double-network hydrogel using PAMPS (poly-2-acrylamido-2-methylpropane sulfonic acid) and PDMAAm (poly-*N,N'*-dimethyl acrylamide). This double-network hydrogel scaffold was soaked in K_2HPO_4 and $CaCl_2$ solutions, sequentially to produce HAP on the scaffold surface. The scaffold was implanted in bone defects and after 12 weeks, the implant had directly bonded to the bone, with enhanced regeneration. It is apparent from so many studies, that nano-hydroxyapatite is nontoxic in medical implants and grafts, and bonds directly to the bone/ teeth in skeletal/ dental defects[61]. PCL, poly(propylene fumarate) (PPF), poly-L-lactic acid (PLLA), poly-lactic-co-glycolic acid (PLGA), and poly-ethylene glycol (PEG) are attractive synthetic polymers that can be used for composite formation with HAP, for bone tissue engineering[62,63]. A detailed account of these is beyond the scope of this thesis.

Novel composite materials involving HAP also involve materials with cellulose nanocrystals (CNCs) and cellulose nanofibers (CNFs). The rationale behind this is the alignment of cellulose fibers/ crystals with controlled HAP crystallization can mimic bone. One such study used eggshells to produce HAP via sol-gel route and extracted CNFs from waste biomass by alkali treatment/ bleaching, followed by acid hydrolysis[64]. The CNFs and HAP were mixed and sonicated at 20 kHz/ 750 W for 15 minutes. The resulting hybrid material showed enhanced cytocompatibility and osteoblast differentiation in vitro. In another study, CNFs and HAP were used to mix with poly-acrylic acid (PAA) acting as a gel scaffold. The result was a cellulose hydrogel with aligned CNFs, mineralized with HAP[65]. *Syed et al.* (2018)[66] used eggshells to make HAP and complexed it with carboxymethyl cellulose (CMC) to make porous, sponge-like scaffolds. Together these studies show the potential of complexing HAP with other materials to derive novel and biocompatible composites with unique properties.

This study focuses on creating nHAP from waste eggshells through a low-temperature method. The HAP synthesis via one-step sol-gel synthesis and microwave-irradiation methods needs to be

explored. The industrial byproduct gluten and gelatin can provide a unique combination of properties in gluten plastics, meanwhile gelatin can also bind to HAP nanocrystals. The composites synthesis in this study needs to be explored for synthesis method and optimization of the method.

Aims and Objectives

The aims and objectives of this study were:

1. Valorization of eggshell waste by production of hydroxyapatite.

- Collecting and processing waste eggshells for calcium sourcing.
- Production and optimization of hydroxyapatite via sol-gel synthesis (direct reaction).
- Production and optimization of hydroxyapatite from eggshells via direct reaction.
- Production and optimization of hydroxyapatite from eggshells, using microwave-irradiation method.

2. Synthesis of novel hydroxyapatite and wheat gluten composites by compression molding and extrusion.

- Production and optimization of wheat gluten-glycerol composites via compression molding.
- Production and optimization of hydroxyapatite-wheat gluten composites via compression molding.
- Production and optimization of hydroxyapatite-wheat gluten-gelatin composites via different techniques.

Chapter-3

MATERIALS AND METHODS

3.1. Chemicals and Reagents

Waste Eggshells were obtained raw from local restaurants in Quaid-i-Azam University, (QAU) Islamabad. **Sodium Hypochlorite** [NaClO; 10% w/v; M_w=76.44 g/mol], **ortho-Phosphoric Acid** [H_3PO_4; 85% ; M_w=98.00 g/mol], **Sodium Hydroxide** [NaOH; pure; M_w=40], **Calcium Hydroxide** [$Ca(OH)_2$; >95%; M_w=74.09 g/mol], **Ethylene-diamine-tetra-acetic acid—EDTA** [pure; M_w=372.24 g/mol], Synthetic **Hydroxyapatite**[$(Ca_5(PO_4)_3OH)_x$; pure; M_w=502.31 g/mol], and **Silica Gel** [mesh size=5-8; coarse, with moisture indicator (blue)] were purchased from Sigma-Aldrich, Merck KGaA, Darmstadt, Germany. **Glycerol** [pure; M_w=92.09 g/mol] and **Gelatin** were purchased from Avantor, VWR International. **di-Sodium hydrogen-Phosphate—DSP** [$Na_2HPO_4.2H_2O$; 98%; M_w=177.99] was purchased from Duksan Reagents, Korea. **Industrial Wheat Gluten** was graciously provided by Lantmännen AB, Sweden.

Solutions:

0.1 M EDTA solution was prepared by dissolving 14.6 g of EDTA in distilled water (dH_2O) to make a final solution volume of 500 mL. **1.25 M EDTA** solution was prepared by taking 0.5 moles EDTA [185.12 g] and dissolving it in dH_2O to make final volume of solution 400 mL. **0.06 M Na_2HPO_4** solution was prepared by dissolving 4.26 g of DSP in dH_2O to make a final volume of solution up to 500 mL. **3 M Na_2HPO_4** solution was prepared by dissolving 0.3 mol DSP [53.4 g] in dH_2O to make a final volume of solution to be 100 mL. **1 N NaOH** solution was prepared by dissolving 20 g of NaOH in distilled water to make a final volume of 500 mL. **1 M H_3PO_4** solution was prepared by dissolving 49 g (28.65 mL stock solution) phosphoric acid in dH_2O to make a final solution of 500 mL. **1 M $Ca(OH)_2$** solution (suspension) was prepared by taking 37 g of dry $Ca(OH)_2$ powder and adding water to make a final volume of 500 mL. Since $Ca(OH)_2$ is sparingly soluble in water, the suspension was treated at 80 °C on a hot plate with magnetic stirrer at 400 rpm for 30 min. **6% NaClO** (bleach) solution was prepared from 10% stock solution by taking 300 mL of stock and adding dH_2O in it to make a final volume of 500 mL.

(The details of instruments used in this study are available in Supplementary Table-4).

3.2. Eggshell Pretreatment

Waste eggshells were obtained raw from local restaurants in QAU area. Waste contained eggshells contaminated with other food wastes, municipal solid waste, and hen's feces. First, the eggshells were segregated from big waste chunks and washed thoroughly under water. After thorough washing, the raw eggshells were boiled in water for 3 h in a water bath. Boiled eggshells were drained and dried in a drying oven at 110 °C for 5 h. Dried eggshells were coarsely crushed with hand and milled in a laboratory pulse grinder (Silver Crest® SC-150) at 28,000 rpm for up to 5 min total, ground in 10 s to 30 s intervals.

The ground eggshell powder (ESP) was taken in a 500 mL beaker, and 6% bleach solution (NaClO) was added in enough volume to completely submerge the ESP. The mixture was stirred with a magnetic stirrer at 800 rpm for 15 min. Afterwards, the mixture was allowed to rest for 30 min, then the supernatant was discarded, and the white precipitate was taken. Ample amount of distilled water was added, stirred on a magnetic hot plate for 10 min at 800 rpm. The mixture was allowed to settle; the supernatant was discarded, and the white precipitate taken. The washing step was performed 3 times to remove any organic matter. The precipitate was dried in a drying oven at 110 °C for 5 h and alternatively dried at 80 °C for 12 h. In both cases, the dry solid obtained was ground in the pulse grinder again for 5 min and the powder was stored at room temperature in airtight containers. This was the "**pretreated ESP**".

3.3. One-step sol-gel synthesis of nano-hydroxyapatite

Procedure-1: One step synthesis of nano-HAP was chemically performed by mixing $Ca(OH)_2$ solution with H_3PO_4 solution. Exactly, 500 mL of 1 M $Ca(OH)_2$ [0.5 mol of $Ca(OH)_2$] was taken in a 1000 mL beaker and put on a hot plate with magnetic stirrer at 800 rpm/ 70 °C for 15 min. Then 300 mL of 1 M phosphoric acid solution [0.3 mol of H_3PO_4] was gradually added in small batches, while under constant stirring 800 rpm at 70 °C. The reaction formed a gel-like suspension of fine particles. This gel was oven dried at 80 °C for 24 h to obtain fine powder.

Procedure-2: Alternatively, the same reaction was conducted in a titration setting. 1 mol of $Ca(OH)_2$ (74 g) was taken and 400 mL dH_2O was added, and the suspension was set at 80 °C under

constant stirring 400 rpm on a magnetic stirrer. After 30 min, a milky white suspension was obtained. At that point, 0.6 mol of H_3PO_4 stock solution (85%; 34.4 mL) was taken in a burette and titration was performed at a slow rate of ~2 mL/ 5min at 80 °C/ 400 rpm. The reaction was allowed to occur on the same conditions for 2 h. Then the suspension of fine particles was subjected to slow drying at 80 °C overnight, followed by drying at 110 °C for 2 h in a drying oven. Direct reaction HAP without titration was called ***nHap***, and that with titration (procedure-2) was called ***nHAP***.

3.4. One-step chemical synthesis of HAP from eggshells

Procedure-3: The pretreated and dried ESP was ≥98% $CaCO_3$. 102 g of ESP (1 mol $CaCO_3$; accounting for 98% purity) was taken in a 500 mL beaker and 200 mL dH_2O was added. The beaker was set on magnetic stirring at 400 rpm on a hot plate at 80 °C. Exactly 0.6 mol of H_3PO_4 stock solution (58.8 g or 34.9 mL/ accounting for 85% purity) was taken in a burette and titration was carried out at a rate of 2 mL/ 5min at 400 rpm/ 80 °C. After a total reaction time of 2 h, the suspension was slow-dried in hot air oven at 80 °C overnight, followed by drying at 110 °C for 2 h.

3.5. Nano-HAP synthesis from eggshells using microwave method

Two approaches for synthesis of nano-HAP from eggshells were adopted.

Procedure-4: In the first scheme, 20 g of pretreated ESP was taken in a beaker and 25 mL of 0.1 EDTA was added. After some manual shaking and 10 min, 25 mL of 0.06 M Na_2HPO_4 solution was added. The pH of the mixture was set at 13 with 1 N NaOH. The solution was stirred at 100 rpm for 30 min on a magnetic stirrer. Then the solution was subjected to microwave irradiation at 800 W power in short intervals, for a total of 10 min treatment time. After microwave treatment, the suspension was allowed to precipitate for 1 h; the supernatant was discarded the white precipitate was washed with distilled water, 3 times. The washed precipitate was oven-dried at 80 °C overnight. This eggshell-derived hydroxyapatite was named EHap.

Procedure-5: In the second scheme, 75 g of pretreated ESP (~0.75 mol $CaCO_3$) was taken in a beaker. It was titrated against 400 mL of 1.25 M EDTA solution (0.5 mol EDTA) at a slow rate of 2 mL/min, at 80 °C under constant stirring of 400 rpm, on a hot plate with magnetic stirrer. The

pH of the solution was 8.0. After the EDTA titration, the solution was filtered through a Whatman filter paper no. 42. The solids were discarded after filtration and the solution was kept. The remaining solution was titrated against 300 mL of 1 M Na_2HPO_4 solution (0.3 mol of DSP) at similar conditions to the EDTA titration [2 mL/min; 400 rpm; 80 °C]. Afterwards, the pH of the solution was adjusted to 13 by adding solid NaOH pellets. The solution was taken in small portions of 50 mL, put in a beaker of 500 mL. The solution was irradiated in a microwave oven of 700 W power/ 2450 MHz at high temperature setting, in small intervals, for a total of 15 min irradiation time per portion. After the irradiation, all portions were combined and set for aging at 80 °C for 6 h. The aged solution contained precipitates that were kept, and the supernatant solution was discarded. The precipitates were washed with dH_2O three times and dried in a hot air oven at 110 °C for 5 h. This was labeled as **nano-EHAP** (nano-HAP derived from eggshells).

After each synthesis procedure, the product was checked under optical microscope (1000x optical) for a rough estimation of micro or nano size of the particles. Table 4.1 outlines the naming convention followed for each procedure.

Table-3.1: Procedures of HAP synthesis followed in this study; names of product are given in all caps for procedures involving titrations.

Name	Method	Ca^{++} source	PO_4^{-3} source	Distinguishing factor	Hydroxyapatite name given
Procedure-1	direct reaction	$Ca(OH)_2$	H_3PO_4	direct reaction w/o titration	nHap
Procedure-2	direct reaction	$Ca(OH)_2$	H_3PO_4	titration reaction	nHAP
Procedure-3	direct reaction	Eggshell $(CaCO_3)$	H_3PO_4	titration reaction	EHAP
Procedure-4	microwave-irradiation	Eggshell	Na_2HPO_4	EDTA-mediated reaction	eHap
Procedure-5	microwave-irradiation	Eggshell	Na_2HPO_4	EDTA titration/ Na_2HPO_4 titration	nano-EHAP

3.6. Nano-EHAP composites with wheat gluten

Hydroxyapatite composites with wheat gluten (WG) were prepared by mixing HAP powder with WG powder and adding glycerol (GLY) as plasticizer. After thorough mixing of the materials, the samples were compression molded to melt gluten and forming a plastic composite. Several configurations of HAP-WG-GLY concentrations and compression molding conditions were tried to optimize uniform composite formation. The HAP samples used were chemically synthesized HAP from $Ca(OH)_2$ and H_3PO_4 titration, hereby referred to as **nHAP**. The HAP synthesized from ESP and phosphoric acid titration is referred to as **EHAP**. Later, it was confirmed in analyses that the EHAP was not in nano-sized crystals. The **nano-EHAP** synthesized from eggshells and EDTA/DSP titrations was in nano-crystal form. The HAP composites with WG were tried for all three types nHAP, EHAP and nano-EHAP.

In the first batch, a total of 10 g material was prepared with [WG:GLY:HAP] in the ratio [60:30:10] making the composite 10% hydroxyapatite, 60% gluten and 30% glycerol. Similarly, for other proportions of the composites, the effect of amount of glycerol was checked by 20%, 25%, 30%, 35% and 40% GLY composites. In all other batches of composites, the GLY amount was set as 30%. In second and third batches, HAP concentration was increased from 10% to 20% and 30%, respectively. While keeping GLY at 30%, the concentration of WG was reduced to 50% and 40%, respectively. The composite recipe is given in Table-3.2.

Table-3.2: Nano-EHAP composites with wheat gluten—total mass 10 g; nHAP: chemically synthesized nano-hydroxyapatite, nano-EHAP: HAP synthesized from eggshell/microwave conversion, WG: wheat gluten, and GLY: glycerol.

Composite Name	HAP type	HAP amount (g)	WG amount (g)	GLY amount (g)	Final ratio: HAP-WG-GLY
C-10	nano-EHAP	1	6	3	10: 60: 30
Cn-10	nHAP	1	6	3	10: 60: 30
C-20	nano-EHAP	2	5	3	20: 50: 30
Cn-20	nHAP	2	5	3	20: 50: 30

C-30	nano-EHAP	3	4	3	30: 40: 30
Cn-30	nHAP	3	4	3	30: 40: 30
Control [A]	---	---	7	3	---: 70: 30

For each composite mixture, the material was prepared by manual mixing in mortar (with pestle). When the material reached a dough-like consistency, the material was placed in a manual compression mold where top and bottom plates of the mold were set at 125 °C. The manual pressure applied was ≥100 kPa. The temperature in compression was optimized by changing the temperature value between 125 °C and 135 °C. In a similar fashion, conditions were optimized for compression molding of composites based on the total amount of material. The total mass of composite material for compression molding was varied between 2 g and 10 g to find optimal composite formation.

3.7. Nano-EHAP composites with wheat gluten and gelatin

After optimization of compression molding conditions of composite materials, nano-EHAP composites with wheat gluten and gelatin (GEL) were made. The composites of nano-EHAP-WG-GEL were prepared by two different methods. In both methods, no water was added to the composite and only glycerol was added as plasticizer. The exact recipes are given in Table-3.3.

Table-3.3: Nano-EHAP composites with gluten and gelatin; nano-EHAP: HAP synthesized from eggshell/microwave conversion (procedure-5), WG: wheat gluten, GEL: gelatin, and GLY: glycerol.

Composite Name	Formation Method	nano-EHAP amount (g)	WG amount (g)	GEL amount (g)	GLY amount (g)	Total mass (g)	Composite ratio: [nano-EHAP: WG: GEL: GLY]
M-5-GEL10	compression molding	0.15	1.65	0.3	0.9	3	5:55:10:30

M-10-GEL10	compression molding	0.3	1.5	0.3	0.9	3	10:50:10:30
M-10-GEL20	compression molding	0.3	1.2	0.6	0.9	3	10:40:20:30
M-10-GEL30	compression molding	0.3	0.9	0.9	0.9	3	10:30:30:30
M-15-GEL10	compression molding	0.45	1.35	0.3	0.9	3	15:45:10:30
E1	extrusion	5	15	15	15	50	10:30:30:30
E2	extrusion	10	12.5	12.5	15	50	20:25:25:30
E3	extrusion	15	10	10	15	50	30:20:20:30

First, WG, GEL and nano-EHAP were mixed in varying ratios, with 30% GLY in all the composite types. The concentration of nano-EHAP was kept at 5%, 10% and 15%. The concentration of GEL was changed from 10%, 20% to 30% to find optimal amount. In each case, WG concentration was respectively decreased to accommodate GEL in the matrix. The WG-GEL-nano-EHAP-GLY composites were compression molded at 135 °C with a pressure of ~ 100 kPa.

Second, WG-GEL-nano-EHAP-GLY composites were prepared in ratios of *1.* [E1= 30:30:10:30], *2.* [E2= 25:25:20:30], and *3.* [E3= 20:20:30:30]. The composites E1, E2 and E3 were extruded through a single-screw food-grade extruder with a die size of 10.0 mm, at two controlled temperature zones T1 and T2, with a screw speed of 20-30 rpm [as shown in Figure 3.1]. T1 was set at 130 °C and T2 was set at 140 °C.
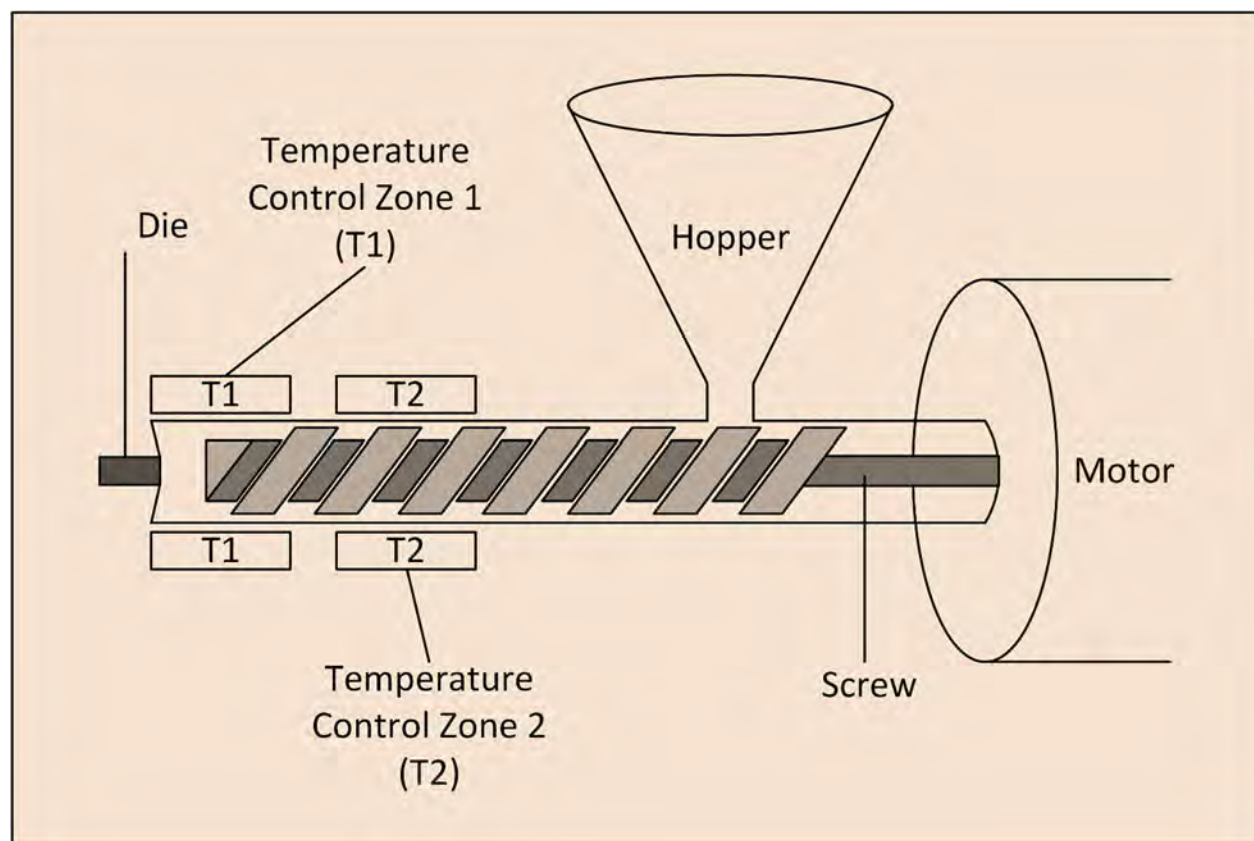
Figure-3.1: Single-screw extruder assembly and temperature control zones.

3.8. FTIR Analysis of HAP and its composites

The samples have been sent for ATR-FTIR analysis and the experiment is underway. Once the data are available, the experimental conditions shall be written here.

3.9. XRD Analysis of ESP and HAP

The X-ray Diffraction (XRD) analysis of control HAP (analytical grade, purchased from Sigma), pretreated eggshell powder and nano-EHAP was performed on a Malvern Panalytical EMPYREAN diffractometer system, fitted with [Empyrean Cu LFF HR] x-ray tube, with copper (Cu) as target material, and nickel (Ni) with a thickness of 0.020 mm as beta filter. X-rays were produced with a 40 kV/ 35 mA current beam. Cu Kα1 radiation of wavelength λ = 1.5405980 nm, Kα2 radiation of λ = 1.5444260 nm, and Kβ radiation of λ = 1.3922500 nm were produced. The ratio of Kα2 to Kα1 was 0.5000. The diffracted beam had a radius of 240 mm, with 2θ positions starting from 20.0050° up to 79.9950°, and a counting time of 0.20 s. The scattered beam was

detected by a point type detector "Proportional detector Xe". The data were collected and exported by EMPYREAN control software version 7.3A and Data Collector version 4.1.

3.10. Water Permeability Analysis of nano-EHAP-WG-GEL-GLY composites

Water vapor transfer rate (WVT) of extruded composites, E1, E2 and E3 was determined according to the desiccant method of ASTM E96—95 standard with slight modifications. Eppendorf Tubes® 2 mL were used with a 6.0 mm hole carved in the centers of their lids. The sample material was cut into small discs that could fit inside the lid. The sample discs were fitted, and their edges sealed with wax, such that only the 6.0 mm hole across the disc would allow water vapor transfer. The tubes were filled with silica gel beads. The closed tubes were then weighed and put inside a desiccator, the bottom of which was filled with distilled water. The tubes were weighed at the time intervals of 0, 3, 9, 21, 33, 44, 68, 92 and 116 hours. The weight gained indicated the moisture absorbed by silica gel, which permeated via the composite material. All samples were treated in duplicates.

The WVT, permeance and permeability were calculated according to the following formulas.

1. **Water Vapor Transmission Rate (WVT):**

$$WVT = \frac{G}{tA} = \frac{(G/t)}{A}, \text{ where:}$$

G = weight change (g; plotted in straight line); t = time (h);

G/t = slope of the weight change line (g.h^{-1}); A = test area (cup mouth area; m^2);

WVT = water vapor transmission rate (g.h^{-1}.m^{-2}).

2. **Permeance:**

$$Permeance = WVT / \Delta p = \frac{WVT}{S(R_1 - R_2)}, \text{ where:}$$

Δp = vapor pressure difference (mmHg; $1.333 \times 10^2 \, Pa$);

S = saturation vapor pressure at test temperature (mmHg; $1.333 \times 10^2 \, Pa$);

R_1 = relative humidity at the source, expressed as a fraction;

$R_2 =$ relative humidity at the vapor sink, expressed as a fraction.

3. Permeability:

Average permeability = permeance × thickness   Unit: $g.Pa^{-1}.s^{-1}.m^{-2}$

3.11. Moisture content of nano-EHAP-WG-GEL-GLY composites

The experiment is underway. Once it is complete, the experimental details shall be written here.

3.12. Biodegradability test of nano-EHAP-WG-GEL-GLY composites

The biodegradability of composites E1, E2 and E3 was tested according to the ASTM D5988-19 standard with slight modifications. The soil used for the experiment was obtained from a local garden in QAU premises. The soil was sieved through a 2 mm mesh and stored at 5 °C for 1 week before conducting the experiment. Prior to the experiment, pH value, moisture content and ash content of the soil were measured. 50 g of soil was placed in a clear plastic cup and 2.5 mL of 1 M diammonium hydrogen phosphate [$(NH_4)_2HPO_4$; DAP] was added in the soil, as a nitrogen source for soil microbes. Cups were prepared in duplicates for each composite sample, with one positive control and one negative control. Composite samples of approximately 0.5 g were placed inside the soil, completely covered with soil. Cups were placed in clear, airtight plastic boxes, and each box had 3 cups; one cup containing soil, one cup containing 50 mL dH_2O and one cup with 20 mL of 0.5 M KOH. The KOH absorbed the CO_2 produced by the microbes. The plastic boxes were placed in dark at ~20 °C. The KOH in each sample box was tested after 3-4 days for first few weeks, and then after every 3-4 weeks for a total of 90 days. In each testing, the box was kept open for 30-60 min for fresh air to circulate through soil. During this time, the KOH undergone incubation was titrated against 0.25 M HCl. The experiment was performed regardless of early biodegradation, as per ASTM standard.

3.13. Tensile testing of compression molded composites

Tensile testing of compression molded samples C-10, C-20 and C-30 was performed according to the ASTM standard D638-22, on an extensometer [Testometric]. ASTM D638-22 was not applicable to E1, E2 and E3, which is why they were not tested by this method. Furthermore, the compression molded composites with gelatin did not show complete mixing and uniformity in

texture, which is why they were not tested by this method. Briefly, compression molded films were cut into dumbbell-shaped strips according to ASTM D638-22—Specimen Type V, with 60 mm overall length, 10 mm overall width and 1.4 mm thickness, and the central area of 14 mm^2. The extension test was performed at a rate of 2.000 mm/min at a data collection rate of 20-25 Hz. The data were collected using winTest™ Analysis software. The elongation (mm) with increasing force (N), was recorded and the force, stress σ, strain ε, and energy at break were recorded. Young's modulus E was calculated for each sample, according to the following formula.

$$E = \frac{\sigma}{\varepsilon}$$

Chapter-4

RESULTS AND DISCUSSION

4.1. Eggshell Processing

Eggshells (ES) were (1) washed, (2) boiled, (3) dried, (4) milled and (5) bleached. For a proof of concept, raw eggshells and boiled eggshells were obtained from local market in Quaid-i-Azam University, Islamabad. After washing, both the raw and boiled eggshells were checked to separate eggshell membranes (ESM) prior to the pretreatment. The ESM is the major organic part of the eggshell, and the ceramic part is 95-99% $CaCO_3$. Manual separation of ESM from the shell was easily done with boiled ES. In both cases, the ESM was removed and the ES subjected to drying. The ES without ESM took almost 50% less time to completely dry, as compared with that of the ES with ESM. The ESM of both raw and boiled ES was observed under optical microscope. The collagen network could be clearly seen in both raw and boiled ESM (Figure-4.1). The dried eggshells starting from raw and boiled eggshells was virtually indistinguishable after drying at 110 °C for 2 h.
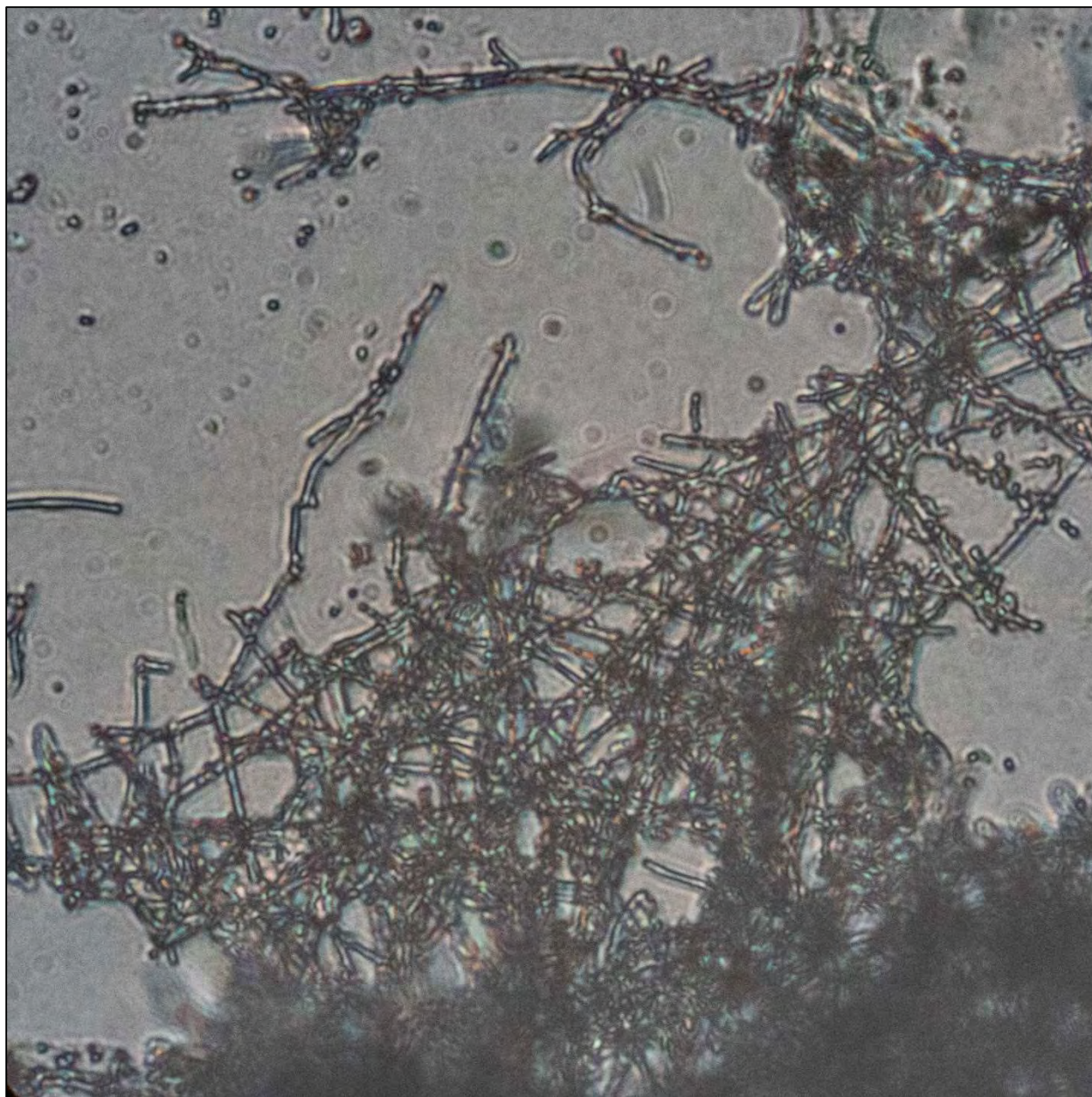
Figure-4.1: Collagen network in raw ESM; optical 1000x, digital zoom 10x.

4.2. Hydroxyapatite from chemical synthesis (direct reaction method)

The HAP synthesized from procedures 1, 2, and 3 was immediately observed under microscope for the approximate size of crystals. The direct reaction of $Ca(OH)_2$ and H_3PO_4 resulted in small nHap crystals [Figure-4.2a]. However, the titration of $Ca(OH)_2$ and H_3PO_4 resulted in very small crystal size (nHAP), as confirmed by optical microscope [Figure-4.2b]. The titration of eggshell

powder and H_3PO_4 resulted in similar crystal morphology but greater size (EHAP) [Figure-4.2c].

In the following formulations, nHAP was used for its smaller crystal size.

Figure-4.2a: nHap crystals formed by procedure-1; 1000x optical, 15x digital zoom.
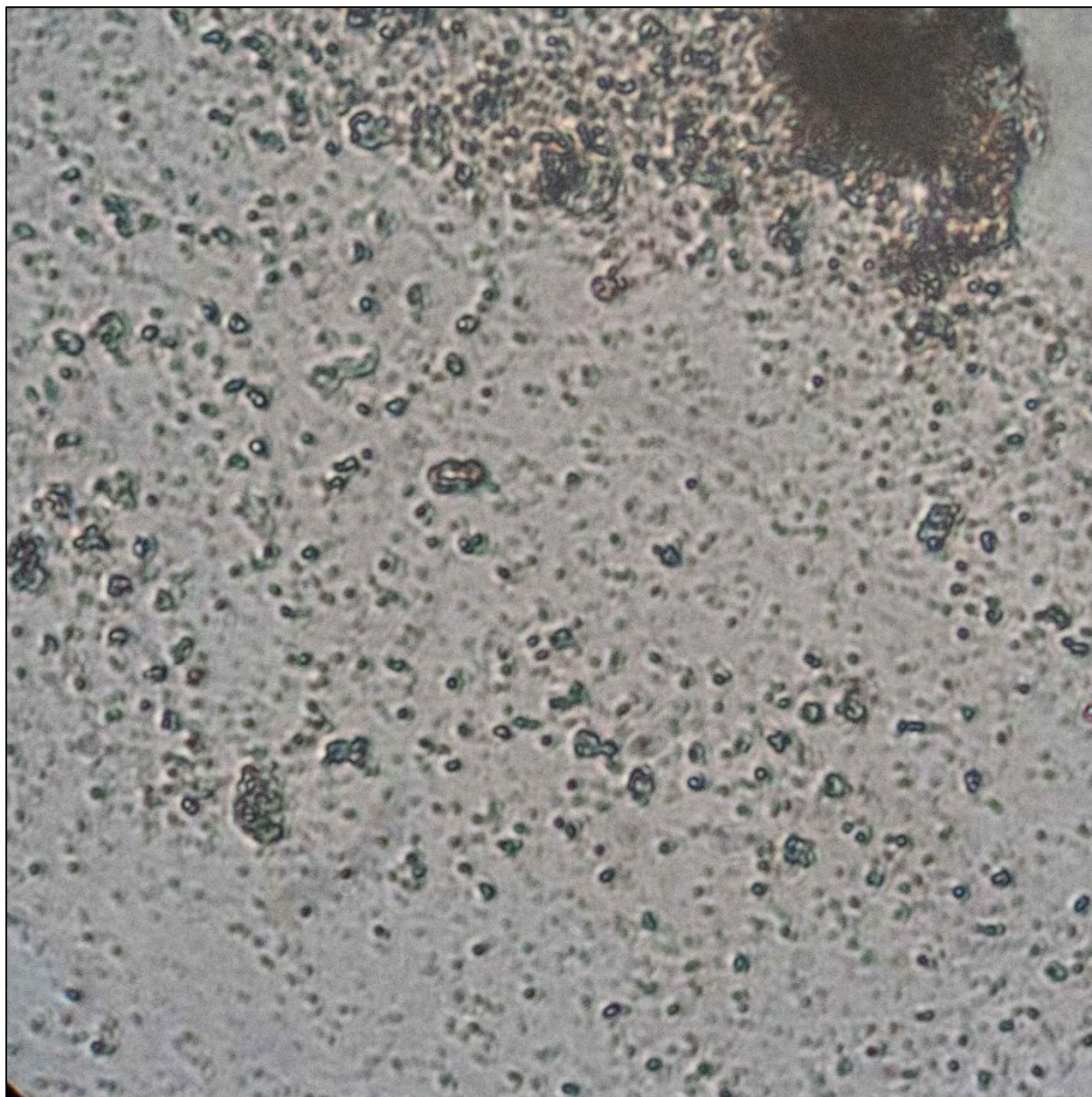
Figure-4.2b: nHAP formed by titration of Ca(OH)$_2$ and H$_3$PO$_4$ (procedure-2); 1000x optical, 15x digital zoom.
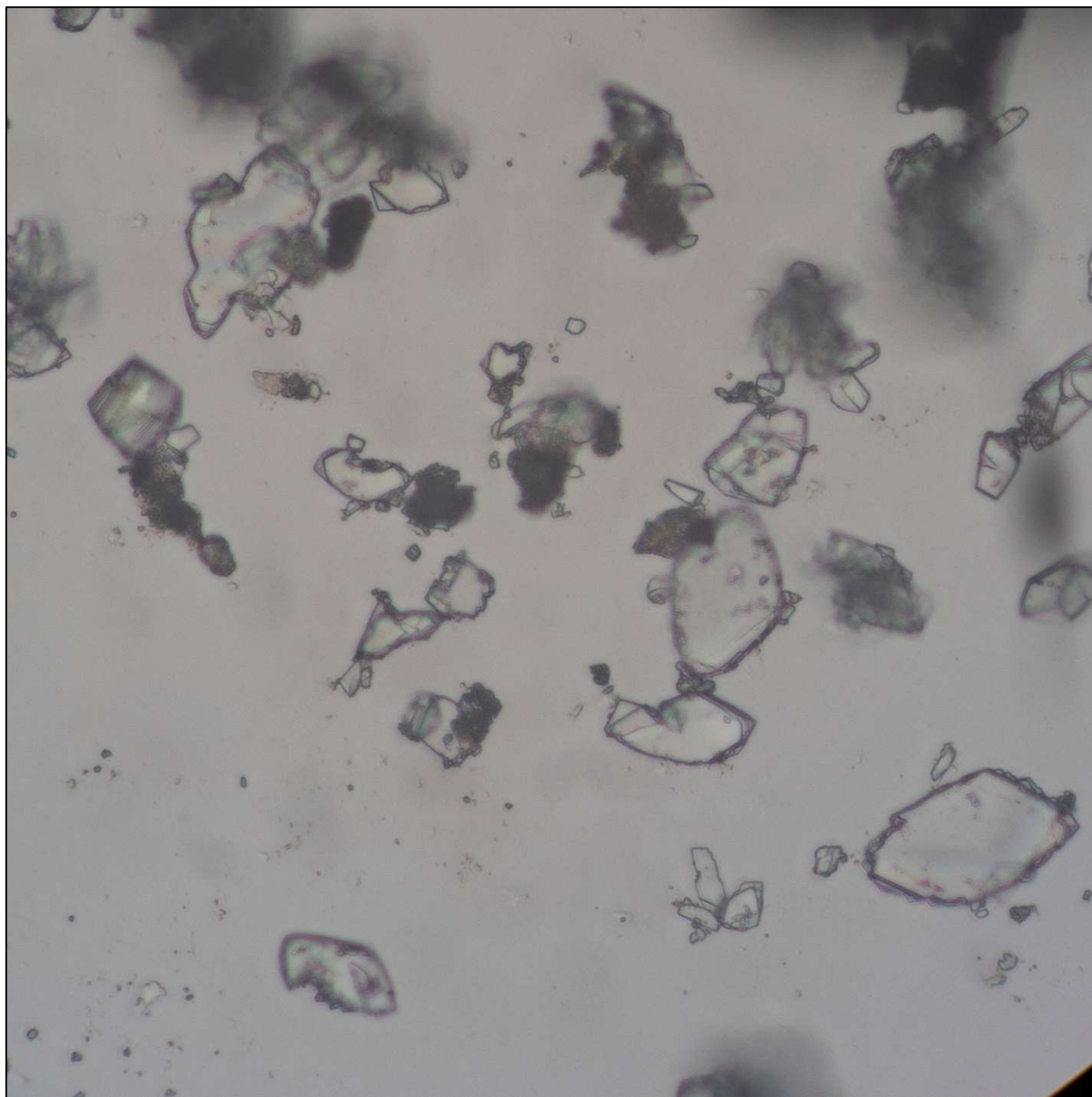
Figure-4.2c: eHAP crystals formed by procedure-3; 1000x optical, 15x digital zoom.

4.3. Hydroxyapatite from microwave-irradiation method

Following procedure-4, without titration, the product (eHap) formed was more amorphous and less crystalline. Furthermore, the FTIR analysis showed that it had more carbonate in it and less phosphate, as compared to the control synthetic hydroxyapatite. It was not used to make composites with gluten and gelatin. Procedure-5, with titrations, resulted in very small particle size, as confirmed by optical microscopy (Figure-4.3).
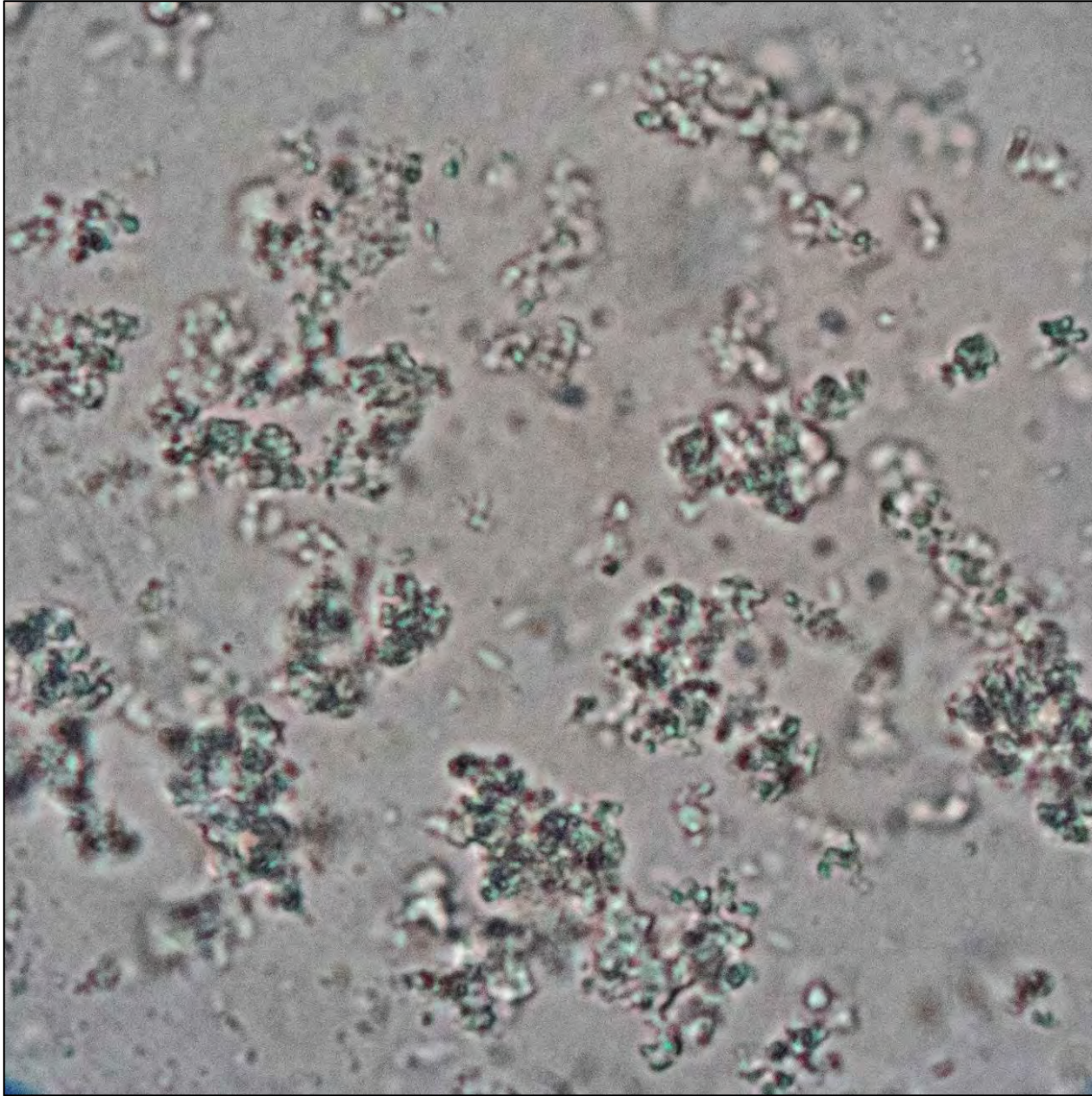
Figure-4.3: nano-EHAP synthesized from procedure-5; 1000x optical, 15x digital zoom.

4.4. Optimization of compression molding conditions for HAP/WG/GLY composites

Starting from hydroxyapatite synthesized from eggshells, compression molded composites were formed according to the recipe given in Table 4.2. For preparation of composites, it was found that continuous mixing of HAP, gluten, and glycerol for 5-8 min resulted in better mixing and uniform consistency of the material. For all compression molded samples, the maximum nHAP concentration of 20% of total material mass was found to be workable. It was found that high concentration of nano-hydroxyapatite resulted in material hardness. The composites containing

nHAP concentration >20% were extremely hard to mix, and even harder to compression mold. The same was not true for the composites of eHap. Probably owing to high amorphous nature and bigger size of particles, the eHap from procedure-4 showed opposite characteristics. The eHap composites with WG and GLY resulted in greater pliability, reduced strength, and greater flow of material from higher concentration of eHap.

Optimum molding conditions: The **time** of compression molding was found to be optimal at 10 min. At a time <9 min, the gluten plastic did not form in the center; for time >12 min, the material started to burn. **Pressure** was found to be the best around 95-105 kPa. Any lower pressure resulted in patches of unformed plastic. Higher pressure resulted in tearing/ shredding of the composite material. **Temperature** was changed from 125 °C to 135 °C, with 130 °C as optimal. Temperatures less than 127 °C did not form the gluten plastic in the periphery of the films. Temperature greater than 132 °C burned the material in the center and caused browning of the composite. The control composite of WG and GLY only, and the composites of HAP with WG/GLY are shown in Figure-4.4.
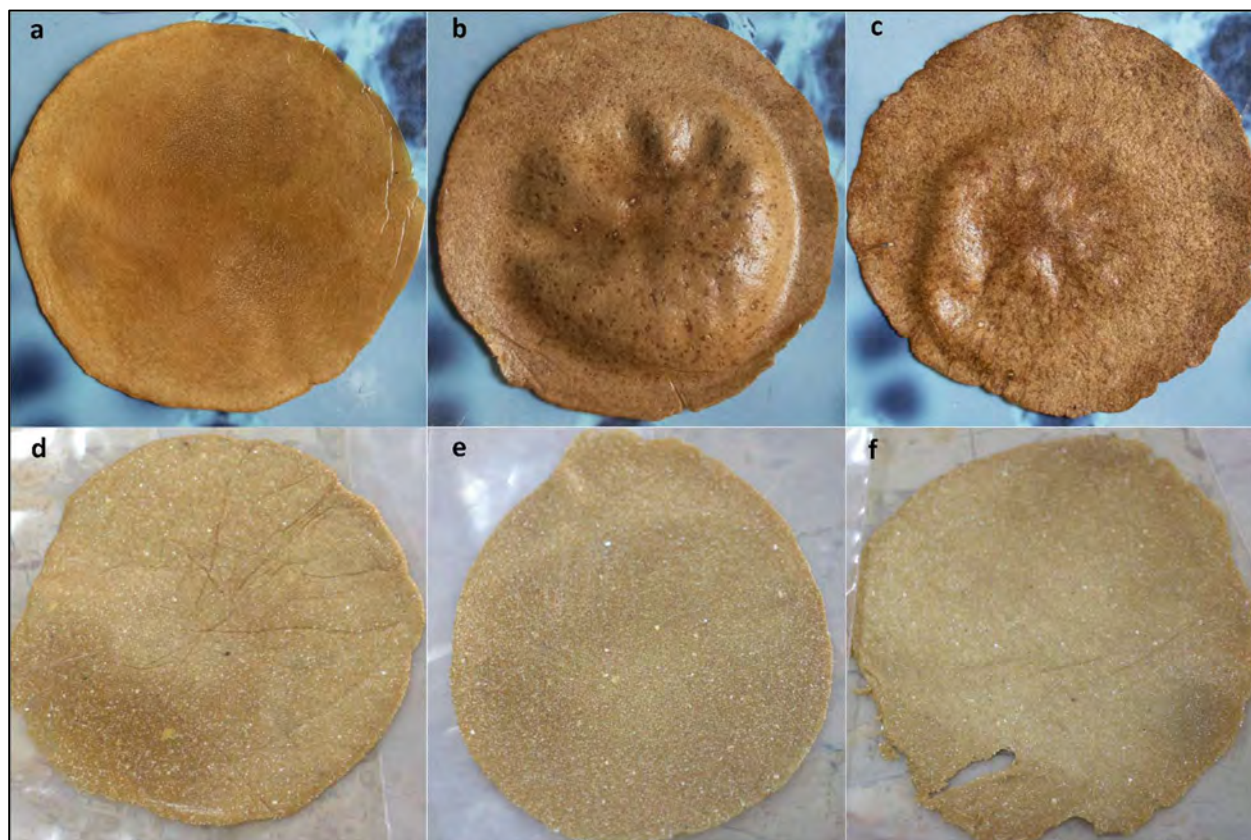
Figure-4.4: nano-EHAP composites with WG and GLY; starting from **(a)** control film of WG:GLY—70:30 with no hydroxyapatite, **(b)** 5% nano-EHAP, **(c)** 10% nano-EHAP, **(d)** 20% nano-EHAP, **(e)** 30% nano-EHAP, and **(f)** shows the shredding/ tearing of material under pressure higher than optimal.

4.5. Optimization of composites of hydroxyapatite with gluten and gelatin

Different concentrations of gluten (WG) and gelatin (GEL) were used with different nano-EHAP concentrations for compression molding of composites. Gelatin did not mix well with gluten and glycerol. Forming compression molded composites revealed localization of GEL in small globules while nano-EHAP and WG mixed thoroughly. This was because GEL was in the form of small coarse grains, and it needed melting to be able to unfold and bond with WG. For that reason, WG and GEL needed to be mixed while being heated. Therefore, extrusion was adopted for nano-EHAP:WG:GEL:GLY composites. The rough mixture was prepared according to the recipe given in table-4.3. The composites formed well with equal concentrations of WG and GEL. The composites E1-3 were formed using equal amounts of WG and GEL. The composites with 10% and 20% nano-EHAP showed uniform structure with less pliability. The E3 composite with 30% nano-EHAP showed increased pliability and less rigidity. These composites are shown in Figure-4.5.

Temperature: The temperature was varied from 120 °C to 170 °C for extruded composites. The temperature of T1 zone in extruder was optimum for 130 °C; lesser temperatures resulted in hindered material flow, while higher temperatures resulted in burning of the sample. For temperature control zone T2 in the extruder, 140 °C allowed proper melting and flow of the material. At 130 °C on T2, the material did not flow properly and added a backpressure in the hopper mouth of the barrel. At T2 temperatures >140 °C, high-pressure bubbles of gas formed in the material, which burst upon exit from the die head.

Screw-speed: At screw speeds of around 60 rpm, the material did not flow consistently, and the edges of material broke into flakes. At a speed of 30 rpm, the material flowed consistently, with occasional breaks in the filament. At 20 rpm, the material showed least breakage of the extrudate.
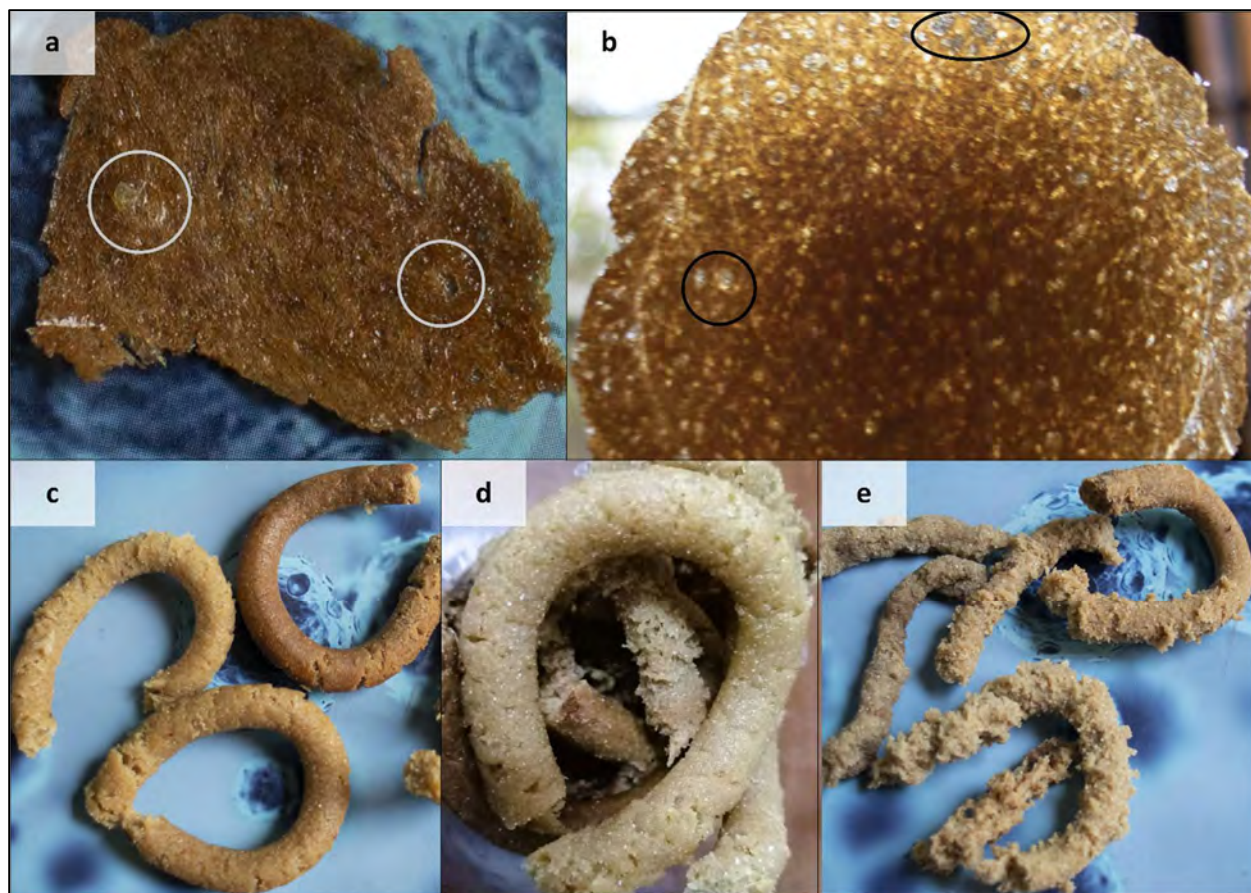
Figure-4.5: nano-EHAP/WG/GEL/GLY composites; starting from compression molded samples **(a)** *M-5-Gel10* [5% nano-EHAP; 10% GEL], **(b)** *M10-Gel20* [10% nano-EHAP; 20% GEL], circles indicate the gelatin globules in the final composite; extruded composites from **(c)** *E1*, smooth part extruded at 20 rpm, **(d)** *E2*, 20 rpm, and **(e)** *E3*, the flaky part extruded at 60 rpm.

4.6. FTIR Analysis of hydroxyapatite and its composites

The FTIR analysis is underway. The details shall be put here once the data are available.

4.7. XRD Analysis of ESP and HAP

The XRD of pretreated eggshell powder (ESP) and hydroxyapatite—analytical grade HAP and nano-EHAP—was carried out for compound identification. The XRD data were analyzed by Panalytical X'Pert Highscore Plus v2.1 and Crystal Impact Match! v3.15 software. The data were analyzed against Crytallography Open Database (COD)—an open-access repository of powder

diffraction data of chemicals, minerals, inorganic and organic materials, excluding biopolymers. The XRD results of ESP, reference-HAP and nano-EHAP are given in Figure-4.6.

In XRD patterns of a sample, the peaks at angle-2θ correspond to the definite spaces between atoms/molecules of a crystal. The 2θ value tells about the d-spacing in angstroms [Å; 0.1 nm], which can be calculated according to Bragg's law:

$$n\lambda = 2d \sin\theta$$

where n is an integer, λ is the wavelength of X-rays, d is the spacing between reflecting planes of the crystal, and θ is the angle (given in 2x multiple in XRD data). The intensity of XRD peaks indicates the amount of particles with that particular d-spacing in the sample material. The width of the peak shows the crystallinity of the samples material; wide peaks show less crystalline phase and more amorphous phase in the sample material. The degree of crystallinity or percent crystallinity can be calculated from the following formula:

$$\%Crystallinity = \frac{area\ under\ crystalline\ peaks}{area\ under\ all\ peaks} \times 100$$

From the XRD data, it is clear that the ESP contains highest crystallinity of the calcium carbonate. The eggshell powder was matched to the calcite mineral form of $CaCO_3$ [COD card# 96-900-7690], with the highest frequency of match (FOM). These patterns of ESP match the data already available in the literature[67]. The details of peaks list and corresponding d-spacings are available in the Supplementary Table-5.

The reference HAP and nano-EHAP both showed striking similarity in peaks (figures 5.8 and 5.9). These peaks were matched with the reference hydroxyapatite peaks in COD [COD# 96-900-2215 and 96-900-2220 (dental HAP)]. The peaks were manually checked against the data available in the literature and matched the ICDD card no. 00-009-0432 in peaks[47,49,51,67-69]. The details of peaks list and the corresponding d-spacings are given in Supplementary table-5. HAP has a hexagonal symmetry (hP) in Bravais lattice system, with $P6_3/m$ space group [no. 176] in Laue classes of space groups. The miller indices for Laue class 176 are four: *h, k, i, l,* and *hki* are permutable for hP. Furthermore, there are no specific reflection conditions for *l* index in the Laue selection rules[70]. This is why the miller indices for reflection planes in HAP were not calculated here.

The degree of crystallinity was calculated in Match! software; crystallinity was 51.72% for ESP, 48.01% for reference HAP, and 29.96% for nano-EHAP synthesized. The reduction in crystallinity is attributable to the presence of water in the nano-EHAP and amorphous calcium phosphate phases present in it. It is notable, however, that my treatment throughout the production process did not involve any temperature higher than 110 °C. Meanwhile, many studies reporting highly crystalline HAP products as well as the reference HAP (analytical grade), involve calcination at >600 °C and sintering at ≥900 °C. The fact that my optimized process can create ~62% crystalline product as compared with the reference HAP is considerable.
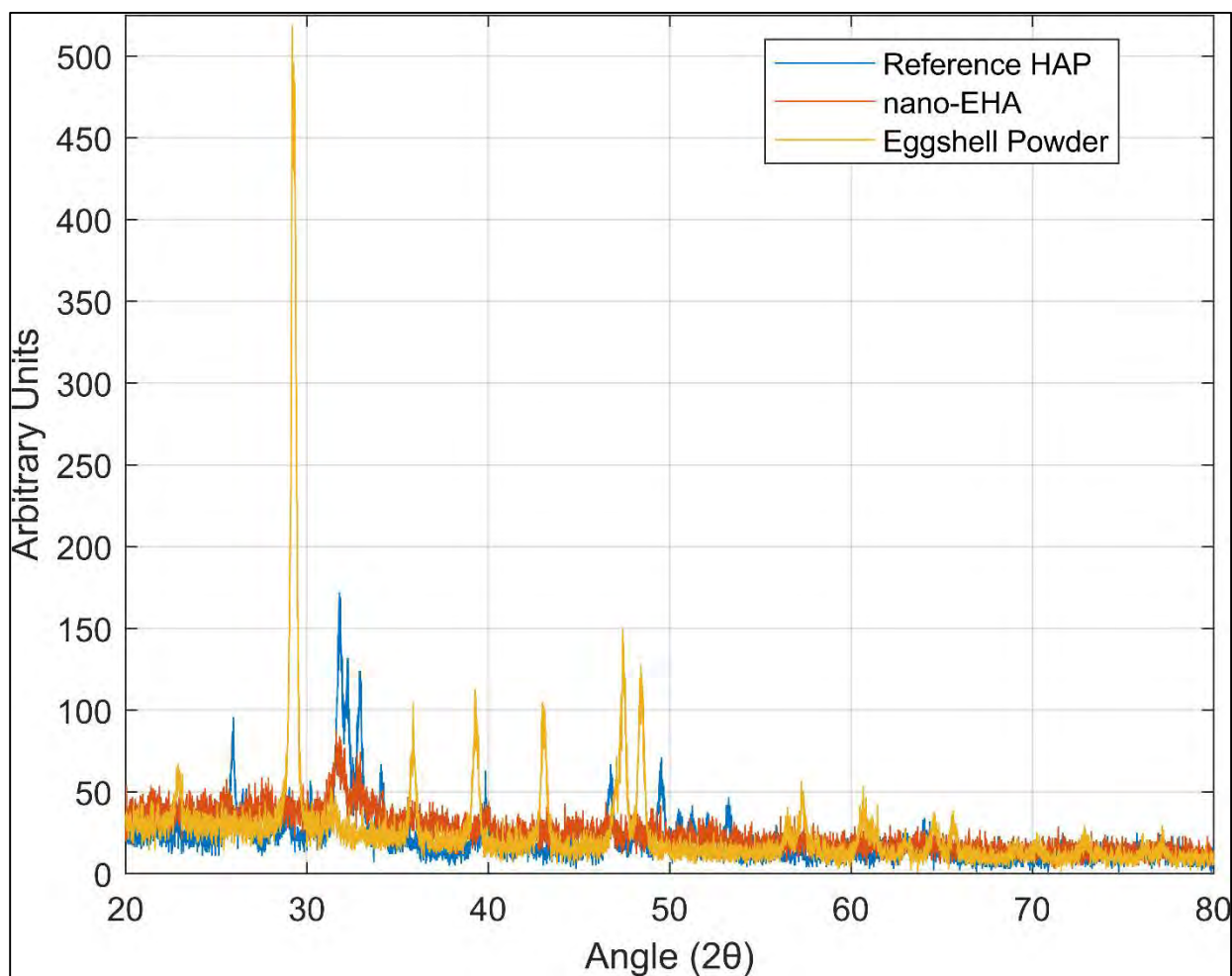
Figure-4.6: XRD Patterns of ESP and HAP.
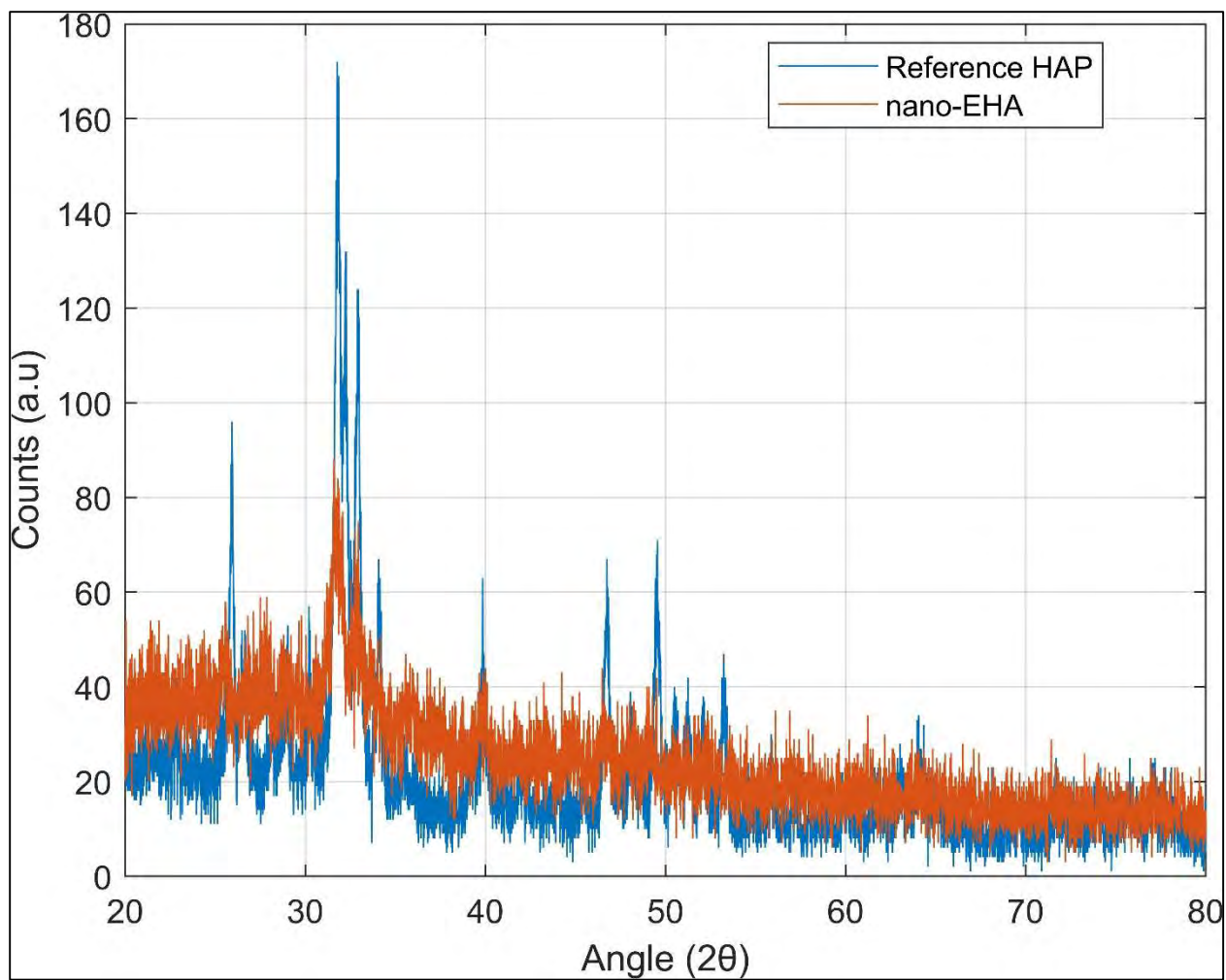
Figure-4.7: XRD patterns of reference HAP and nano-EHAP show similar peaks.
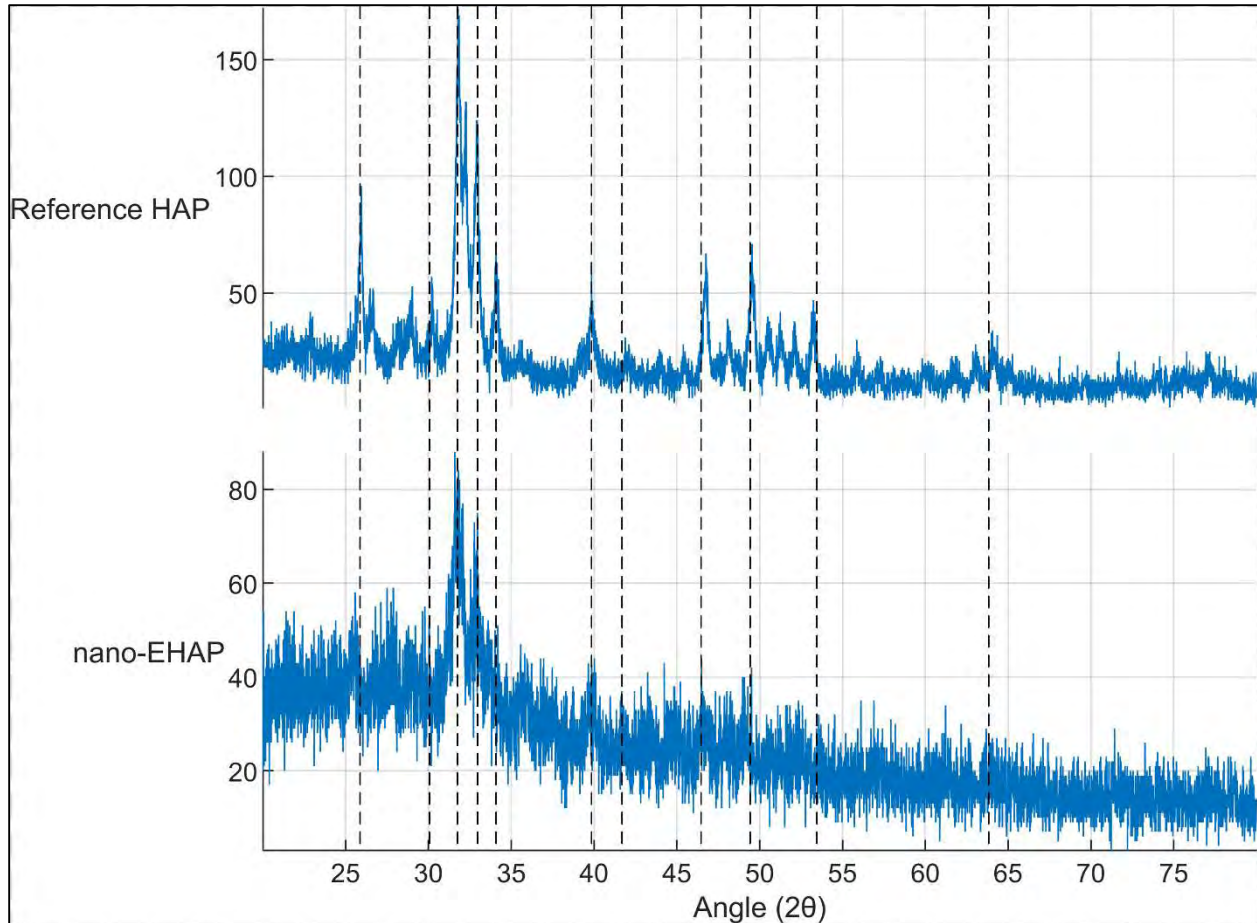
Figure-4.8: Matching peaks of reference HAP and nano-EHAP.

4.8. Water Vapor Transmission Rate (WVT)

The experiment of WVT of composites E1, E2 and E3 is underway. Preliminary results for E1 and E3 are available. The permeance of E2 is 1.62×10^{-5} g.Pa^{-1}.s^{-1}.m^{-2} and the permeance of E3 is 1.50×10^{-5} g.Pa^{-1}.s^{-1}.m^{-2}.

Apparently from this, the increasing nano-EHAP concentration decreased the permeance of the composite material. When the data are available, this section will be completed.

4.9. Moisture content of the composites

The experiment is underway. The details shall be written when the data are available.

4.10. Biodegradability of the composites

The experiment is underway. The details shall be written when the data are available.

4.11. Tensile Testing of compression molded composites

The tensile testing of compression molded samples C-10, C-20, and C-30 was performed according to ASTM D638-22. The stress at break/ ultimate stress (σ_{UT}) is called tensile strength of a material. The strain (ε) was calculated by the following formula:

$$\varepsilon = \int_{L_o}^{L} \frac{dL}{L} = \ln \frac{L}{L_o}$$

Where dL = increment of elongation at any length L,

L= distance between gauge marks at any given time, and

L_o= original length of sample. The ultimate tensile stress (σ_{UT}) was calculated from strain using this formula:

$$\sigma_{UT} = \sigma(1+\varepsilon) = \sigma \frac{L_u}{L_o}$$

Where σ= tensile stress at break (nominal)

L_u= length of sample at the time of rupture

L_o= original length of the sample.

The plot in Figure-4.9 shows the elongation in the test sample as a function of force. The point of break is marked by sudden drop in force to zero. The tensile strength of the composite C-10 was the highest, 234 kPa. The addition of more HAP in gluten resulted in increased pliability and lesser strength. The tensile strength of C-20 was only 7 kPa, and that of C-30 was 64 kPa. The mechanical parameters of the composites are given in the Table-4.1.
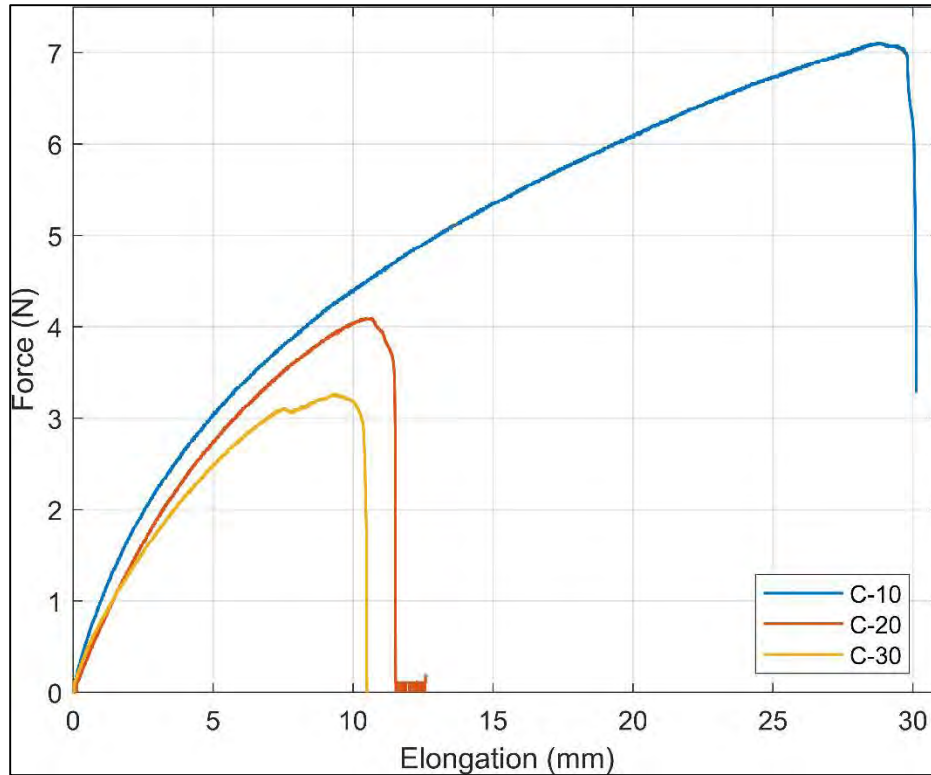
Figure-4.9: Tensile testing of compression molded composites.

Table-4.1: Mechanical Properties of compression molded composites.

Property	C-10	C-20	C-30
Sample Length (mm)	60.000	60.000	60.000
Sample Width (mm)	10.000	10.000	10.000
Sample Thickness (mm)	1.400	1.400	1.400
Area (mm^2) of test	14.000	14.000	14.000
Speed of test (mm/min)	2.000	2.000	2.000
Force (N) at break	3.280	0.100	-0.330*
Young's Modulus (N/mm^2)	2.331	2.509	2.159
Young's modulus in MPa	2.331	2.509	2.159
Stress at break (N/mm^2)	0.234	0.007	-0.024*
Strain at yield (%)	2.633	1.920	1.350
Tensile strength in kPa	234	7**	64
Energy to break (J)	0.149	0.031	0.023

*negative value because the ultimate yield was a second break.

**unusual value because the sample did not break in one step.

Together, these results show the ease of producing a high-quality and novel composite biomaterial sourced from waste by-products.

Conclusion

Eggshells and industrial wheat gluten are waste products that can be used to make high-quality, value-added products. In this study, waste eggshells were used to source calcium, to produce hydroxyapatite—the bone mineral. The hydroxyapatite was used to make different composites with wheat gluten and gelatin, with glycerol as plasticizer. The microwave irradiation method proved to be effective in producing HAP from eggshell, without the use of very high temperatures. The prepared HAP showed nano-sized crystals. The nano-EHAP was used to make composites with gluten and gelatin in different configurations via thermo-compression molding and single-screw extrusion. Uniform composites of nano-EHAP and WG were obtained with compression molding. Uniform composite of nano-EHAP with gelatin and WG were obtained with extrusion at 130 °C. The XRD of eggshell powder and nano-EHAP showed pure product. The crystallinity of nano-EHAP was lower to that of the synthetic, reference-HAP, which can be increased by sintering at high temperatures.

The FTIR analysis showed well bonded gluten and gelatin. The water vapor permeance of composites increased with increasing the HAP concentration. The compression molded composite C-10 showed the highest tensile strength of 234 kPa. The optimization performed for HAP synthesis using titrations provides a better way to create nano-HAP from eggshells. The optimization studies performed on the gluten and gelatin/ HAP composites provides a new class of novel biomaterials. These studies provide a first of its kind, novel biomaterial with interesting functional properties. Valorization of biowaste following this procedure shows good potential in circular economy and sustainable use of materials, reducing pollution problems and resource recycling.

Chapter-5

REFERENCES

1   Wegst, U. G., Bai, H., Saiz, E., Tomsia, A. P. & Ritchie, R. O. Bioinspired structural materials. *Nature materials* **14**, 23-36 (2015).

2   Wegst, U. G. & Ashby, M. The mechanical efficiency of natural materials. *Philosophical Magazine* **84**, 2167-2186 (2004).

3   Barthelat, F., Yin, Z. & Buehler, M. J. Structure and mechanics of interfaces in biological materials. *Nature Reviews Materials* **1**, 1-16 (2016).

4   Ling, S., Kaplan, D. L. & Buehler, M. J. Nanofibrils in nature and materials engineering. *Nature Reviews Materials* **3**, 1-15 (2018).

5   Legeros, R. Z. & Legeros, J. P. in *Bioceramics and their Clinical Applications*   (ed Tadashi Kokubo) 367-394 (Woodhead Publishing, 2008).

6   Nepal, D. *et al.* Hierarchically structured bioinspired nanocomposites. *Nature materials* **22**, 18-35 (2023).

7   Hunter, G. K., Kyle, C. L. & Goldberg, H. A. Modulation of crystal formation by bone phosphoproteins: structural specificity of the osteopontin-mediated inhibition of hydroxyapatite formation. *Biochemical Journal* **300**, 723-728 (1994).

8   Talal, A., Hamid, S. K., Khan, M. & Khan, A. S. in *Handbook of Ionic Substituted Hydroxyapatites* 1-19 (Elsevier, 2020).

9   Campbell, A. K. Calcium as an intracellular regulator. *Proceedings of the Nutrition Society* **49**, 51-56 (1990).

10   Elliott, J. Hydroxyapatite and nonstoichiometric apatites. *Structure and chemistry of the apatites and other calcium orthophosphates* **18**, 111-189 (1994).

11   Magalhaes, M., Marques, P. & Correia, R.   (John Wiley & Sons, Ltd, 2006).

12   Penido, M. G. M. & Alon, U. S. Phosphate homeostasis and its role in bone health. *Pediatric nephrology* **27**, 2039-2048 (2012).

13   Jahnen-Dechent, W., Heiss, A., Schäfer, C. & Ketteler, M. Fetuin-A regulation of calcified matrix metabolism. *Circulation research* **108**, 1494-1509 (2011).

14   Millán, J. L. Alkaline phosphatases: structure, substrate specificity and functional relatedness to other members of a large superfamily of enzymes. *Purinergic signalling* **2**, 335-341 (2006).

15   Omelon, S., Ariganello, M., Bonucci, E., Grynpas, M. & Nanci, A. A review of phosphate mineral nucleation in biology and geobiology. *Calcified Tissue International* **93**, 382-396 (2013).

16   He, K. *et al.* Revealing nanoscale mineralization pathways of hydroxyapatite using in situ liquid cell transmission electron microscopy. *Science Advances* **6**, eaaz7524 (2020).

17   He, G., Dahl, T., Veis, A. & George, A. Nucleation of apatite crystals in vitro by self-assembled dentin matrix protein 1. *Nature materials* **2**, 552-558 (2003).

18   George, A. & Veis, A. Phosphorylated proteins and control over apatite nucleation, crystal growth, and inhibition. *Chemical reviews* **108**, 4670-4693 (2008).

19   Luo, G. *et al.* Spontaneous calcification of arteries and cartilage in mice lacking matrix GLA protein. *Nature* **386**, 78-81 (1997).

20   Rasheed, F., Plivelic, T. s. S., Kuktaite, R., Hedenqvist, M. S. & Johansson, E. Unraveling the structural puzzle of the giant glutenin polymer—An interplay between protein polymerization, nanomorphology, and functional properties in bioplastic films. *ACS omega* **3**, 5584-5592 (2018).

21   Paux, E. *et al.* A physical map of the 1-gigabase bread wheat chromosome 3B. *science* **322**, 101-104 (2008).

22   Consortium, I. W. G. S. *et al.* A chromosome-based draft sequence of the hexaploid bread wheat (Triticum aestivum) genome. *Science* **345**, 1251788 (2014).

23   Bromilow, S. *et al.* A curated gluten protein sequence database to support development of proteomics methods for determination of gluten in gluten-free foods. *Journal of proteomics* **163**, 67-75 (2017).

24   Shewry, P. R., Tatham, A. S., Barro, F., Barcelo, P. & Lazzeri, P. Biotechnology of breadmaking: unraveling and manipulating the multi-protein gluten complex. *Bio/technology* **13**, 1185-1190 (1995).

25   Day, L. in *Handbook of food proteins*   267-288 (Elsevier, 2011).

26   Juhász, A. *et al.* Genome mapping of seed-borne allergens and immunoresponsive proteins in wheat. *Science advances* **4**, eaar8602 (2018).

27   Wieser, H. Chemistry of gluten proteins. *Food microbiology* **24**, 115-119 (2007).

28   Schofield, J. D. *Wheat Structure: biochemistry and functionality*. (Elsevier, 1996).

29   Bruyninckx, K., Jansens, K. J., Delcour, J. A. & Smet, M. The effect of cross-linking additives on the structure and properties of glassy wheat gluten material. *Industrial Crops and Products* **81**, 38-48 (2016).

30   Shan, L. & Khosla, C. Chemistry and biology of gluten proteins. *Immunology, Endocrine & Metabolic Agents in Medicinal Chemistry (Formerly Current Medicinal Chemistry-Immunology, Endocrine and Metabolic Agents)* **7**, 187-193 (2007).

31   Gobbetti, M. Will Europe toast GM wheat for gluten sufferers. *Nat Biotechnol* **34**, 369 (2016).

32   Koning, F., Thomas, R., Rossjohn, J. & Toes, R. E. Coeliac disease and rheumatoid arthritis: similar mechanisms, different antigens. *Nature Reviews Rheumatology* **11**, 450-461 (2015).

33   Lindfors, K. *et al.* Coeliac disease. *Nature Reviews Disease Primers* **5**, 3 (2019).

34   Jabri, B., Chen, X. & Sollid, L. M. How T cells taste gluten in celiac disease. *Nature Structural & Molecular Biology* **21**, 429-431 (2014).

35   Pham Minh, D. *et al.* Hydroxyapatite starting from calcium carbonate and orthophosphoric acid: synthesis, characterization, and applications. *Journal of Materials Science* **49**, 4261-4269 (2014).

36   Verwilghen, C. *et al.* Preparation of high specific surface area hydroxyapatite for environmental applications. *Journal of materials science* **42**, 6062-6066 (2007).

37   Clark, J. & Turner, R. Reactions between solid calcium carbonate and orthophosphate solutions. *Canadian Journal of Chemistry* **33**, 665-671 (1955).

38   Pokhrel, S. Hydroxyapatite: preparation, properties and its biomedical applications. *Advances in Chemical Engineering and Science* **8**, 225 (2018).

39   Oliveira, D., Benelli, P. & Amante, E. A literature review on adding value to solid residues: egg shells. *Journal of Cleaner Production* **46**, 42-47 (2013).

40   Saha, S. K., Banerjee, A., Banerjee, S. & Bose, S. Synthesis of nanocrystalline hydroxyapatite using surfactant template systems: role of templates in controlling morphology. *Materials Science and Engineering: C* **29**, 2294-2301 (2009).

41   Lim, G., Wang, J., Ng, S. & Gan, L. Formation of nanocrystalline hydroxyapatite in nonionic surfactant emulsions. *Langmuir* **15**, 7472-7477 (1999).

42   Gopi, D., Indira, J., Kavitha, L., Sekar, M. & Mudali, U. K. Synthesis of hydroxyapatite nanoparticles by a novel ultrasonic assisted with mixed hollow sphere template method. *Spectrochimica Acta Part A: Molecular and Biomolecular Spectroscopy* **93**, 131-134 (2012).

43   Jillavenkatesa, A. & Condrate Sr, R. Sol–gel processing of hydroxyapatite. *Journal of materials science* **33**, 4111-4119 (1998).

44   Parhi, P., Ramanan, A. & Ray, A. R. A convenient route for the synthesis of hydroxyapatite through a novel microwave-mediated metathesis reaction. *Materials letters* **58**, 3610-3612 (2004).

45   Siva Rama Krishna, D., Siddharthan, A., Seshadri, S. & Sampath Kumar, T. A novel route for synthesis of nanocrystalline hydroxyapatite from eggshell waste. *Journal of Materials Science: Materials in Medicine* **18**, 1735-1743 (2007).

46   Kumar, G. S., Thamizhavel, A. & Girija, E. Microwave conversion of eggshells into flower-like hydroxyapatite nanostructure for biomedical applications. *Materials Letters* **76**, 198-200 (2012).

47   Kumar, G. S. & Girija, E. Flower-like hydroxyapatite nanostructure obtained from eggshell: A candidate for biomedical applications. *Ceramics International* **39**, 8293-8299 (2013).

48   Türk, S. *et al.* Microwave–assisted biomimetic synthesis of hydroxyapatite using different sources of calcium. *Materials Science and Engineering: C* **76**, 528-535 (2017).

49   Ibrahim, A.-R., Wei, W., Zhang, D., Wang, H. & Li, J. Conversion of waste eggshells to mesoporous hydroxyapatite nanoparticles with high surface area. *Materials Letters* **110**, 195-197 (2013).

50   Kattimani, V., Lingamaneni, K. P., Chakravarthi, P. S., Kumar, T. S. & Siddharthan, A. Eggshell-derived hydroxyapatite: a new era in bone regeneration. *Journal of Craniofacial Surgery* **27**, 112-117 (2016).

51   Umesh, M. *et al.* Eggshells biowaste for hydroxyapatite green synthesis using extract piper betel leaf-Evaluation of antibacterial and antibiofilm activity. *Environmental Research* **200**, 111493 (2021).

52   Rhee, S.-H. Synthesis of hydroxyapatite via mechanochemical treatment. *Biomaterials* **23**, 1147-1152 (2002).

53   Silva, C., Pinheiro, A., Miranda, M., Góes, J. & Sombra, A. Structural properties of hydroxyapatite obtained by mechanosynthesis. *Solid state sciences* **5**, 553-558 (2003).

54   Goloshchapov, D. *et al.* Synthesis of nanocrystalline hydroxyapatite by precipitation using hen's eggshell. *ceramics International* **39**, 4539-4549 (2013).

55   Wu, S.-C., Hsu, H.-C., Hsu, S.-K., Chang, Y.-C. & Ho, W.-F. Synthesis of hydroxyapatite from eggshell powders through ball milling and heat treatment. *Journal of Asian Ceramic Societies* **4**, 85-90 (2016).

56   Kamalanathan, P. *et al.* Synthesis and sintering of hydroxyapatite derived from eggshells as a calcium precursor. *Ceramics International* **40**, 16349-16359 (2014).

57   Kokubo, T. *Bioceramics and their clinical applications*. (Elsevier, 2008).

58   Reichert, J. C. *et al.* A tissue engineering solution for segmental defect regeneration in load-bearing long bones. *Science translational medicine* **4**, 141ra193-141ra193 (2012).

59   Ebrahimi, Z., Irani, S., Ardeshirylajimi, A. & Seyedjafari, E. Enhanced osteogenic differentiation of stem cells by 3D printed PCL scaffolds coated with collagen and hydroxyapatite. *Scientific Reports* **12**, 1-15 (2022).

60   Wada, S. *et al.* Hydroxyapatite-coated double network hydrogel directly bondable to the bone: biological and biomechanical evaluations of the bonding property in an osteochondral defect. *Acta Biomaterialia* **44**, 125-134 (2016).

61   Pepla, E., Besharat, L. K., Palaia, G., Tenore, G. & Migliau, G. Nano-hydroxyapatite and its applications in preventive, restorative and regenerative dentistry: a review of literature. *Annali di stomatologia* **5**, 108 (2014).

62   Koons, G. L., Diba, M. & Mikos, A. G. Materials design for bone-tissue engineering. *Nature Reviews Materials* **5**, 584-603 (2020).

63   Venkatesan, J. & Kim, S.-K. Nano-hydroxyapatite composite biomaterials for bone tissue engineering—a review. *Journal of biomedical nanotechnology* **10**, 3124-3140 (2014).

64   Athinarayanan, J., Periasamy, V. S. & Alshatwi, A. A. Fabrication of cellulose nanocrystal-decorated hydroxyapatite nanostructures using ultrasonication for biomedical applications. *Biomass Conversion and Biorefinery*, 1-14 (2021).

65   Qi, Y., Cheng, Z., Ye, Z., Zhu, H. & Aparicio, C. Bioinspired mineralization with hydroxyapatite and hierarchical naturally aligned nanofibrillar cellulose. *ACS applied materials & interfaces* **11**, 27598-27604 (2019).

66   Sayed, M., El-Maghraby, H., Bondioli, F. & Naga, S. 3D carboxymethyl cellulose/hydroxyapatite (CMC/HA) scaffold composites based on recycled eggshell. *Journal of Applied Pharmaceutical Science* **8**, 023-030 (2018).

67   Ho, W.-F., Hsu, H.-C., Hsu, S.-K., Hung, C.-W. & Wu, S.-C. Calcium phosphate bioceramics synthesized from eggshell powders through a solid state reaction. *Ceramics international* **39**, 6467-6473 (2013).

68   El Boujaady, H. *et al.* Adsorption of a textile dye on synthesized calcium deficient hydroxyapatite (CDHAp): Kinetic and thermodynamic studies. *J. Mater. Environ. Sci* **7**, 4049-4063 (2016).

69   Fatimah, S., Ragadhita, R., Al Husaeni, D. F. & Nandiyanto, A. B. D. How to calculate crystallite size from x-ray diffraction (XRD) using Scherrer method. *ASEAN Journal of Science and Engineering* **2**, 65-76 (2022).

70   Aroyo, M. I. *International Tables for Crystallography*. (Wiley Online Library, 2013).

Appendix-A: Supplementary Data

Supplementary Table-1. Materials Properties List; source <u>MATWEB</u> database (www.matweb.com).

Material	Density (g/cc)	Strength (MPa)	Modulus (GPa)
Human Enamel (Molars)	3	384	100
Human Dentin (Molars)	2.15	250	42
Collagen	1.3	100	1
Femur	1.3		20
Human Compact Bone (Haversian System)	1.38	205	27.4
Human Skin	1.02	7.6	0.00128
Oak Wood	0.6	5.5	12.3
Maple Wood	0.52	4.96	9.17
Birch Wood	0.48	2.62	8.07
Tricalcium Phosphate (TCP)	3.14	120	162
Calcium Hydroxyapatite	3.15	450	130
Silicon Carbide (Reaction bonded)	3.1	2500	400
Steel	7.87	250	200
Timet Timetal® 21S Ti+SiC Composite Fiber	4.24	1720	186
Glass Fiber	2.44		68.9
DuPont Kevlar® 12 μm Fiber	1.47	3450	179
Lytex® 4149 55% Carbon Fiber Epoxy Composite	1.45	289	55.1

Supplementary Table-2.: List of Gluten Proteins of *Triticum aestivum*; source <u>UniProt</u> database.

Gluten Fraction	Protein Group	Name of Protein	Chromosome	Number of Proteins	Total Proteins in Group
Polymerics Glutenins	**High-molecular weight glutenin**	HMW-GS-1Ax	1A	1	6
		HMW-GS-1Ay	1A	1	
		HMW-GS-1Bx	1B	1	

subunit (HMW-GS)		HMW-GS-1By	1B	1	
		HMW-GS-1Dx	1D	1	
		HMW-GS-1Dy	1D	1	
	Low-molecular weight glutenin subunit (LMW-GS)	LMW-GS-i1-1A	1A	1	17
		LMW-GS-i2-1A	1A	1	
		LMW-GS-m1-1D	1D	1	
		LMW-GS-m3-1A	1A	1	
		LMW-GS-m3-1D	1D	1	
		LMW-GS-m4-1A	1A	1	
		LMW-GS-m4-1B	1B	1	
		LMW-GS-m4-1D	1D	1	
		LMW-GS-m5-1B	1B	1	
		LMW-GS-m5-1D	1D	1	
		LMW-GS-m6-1D	1D	1	
		LMW-GS-m7-1D	1D	1	
		LMW-GS-m8-1D	1D	1	
		LMW-GS-s1-1B	1B	1	
		LMW-GS-s2-1B	1B	1	
		LMW-GS-s2-1D	1D	1	
		LMW-GS-s3-1B	1B	1	
Monomeric Gliadins	**α/β-Gliadins**	α/β-Gli-a-6B	6B	1	57
		α/β-Gli-a-6D	6D	1	
		α/β-Gli-1-6A	6A	1	
		α/β-Gli-1-6B	6B	1	
		α/β-Gli-1-6D	6D	1	
		α/β-Gli-2-6A	6A	1	
		α/β-Gli-2-6B	6B	1	
		α/β-Gli-2-6D	6D	1	
		α/β-Gli-3-6A	6A	1	
		α/β-Gli-3-6B	6B	1	
		α/β-Gli-3-6D	6D	1	
		α/β-Gli-4-6A	6A	1	
		α/β-Gli-4-6B	6B	1	

		α/β-Gli-4-6D	6D	1	
		α/β-Gli-5-6A	6A	1	
		α/β-Gli-5-6B	6B	1	
		α/β-Gli-5-6D	6D	1	
		α/β-Gli-6-6A	6A	1	
		α/β-Gli-6-6B	6B	1	
		α/β-Gli-6-Un-6D	Un-6D	1	
		α/β-Gli-7-6A	6A	1	
		α/β-Gli-7-6B	6B	1	
		α/β-Gli-7-6D	6D	1	
		α/β-Gli-8-6A	6A	1	
		α/β-Gli-8-6B	6B	1	
		α/β-Gli-8-6D	6D	1	
		α/β-Gli-9-6A	6A	1	
		α/β-Gli-9-6B	6B	1	
		α/β-Gli-9-6D	6D	1	
		α/β-Gli-10-6B	6B	1	
		α/β-Gli-10-6D	6D	1	
		α/β-Gli-11-6B	6B	1	
		α/β-Gli-11-6D	6D	1	
		α/β-Gli-12-6B	6B	1	
		α/β-Gli-12-6BS	6B	1	
		α/β-Gli-13-6B	6B	1	
		α/β-Gli-13-Un-6BS	Un-6B	1	
		α/β-Gli-14-6B	6B	1	
		α/β-Gli-14-Un-6BS	Un-6B	1	
		α/β-Gli-15-6B	6B	1	
		α/β-Gli-15-Un-6BS	Un-6B	1	
		α/β-Gli-16-6B	6B	1	
		α/β-Gli-16-Un-6AS	Un-6A	1	
		α/β-Gli-17-6B	6B	1	
		α/β-Gli-17-Un-6AS	Un-6A	1	
		α/β-Gli-18-6B	6B	1	

		α/β-Gli-18-Un-6AS	Un-6A	1	
		α/β-Gli-19-6B	6B	1	
		α/β-Gli-19-Un-6BS	Un-6B	1	
		α/β-Gli-20-Un-6AS	Un-6A	1	
		α/β-Gli-21-Un-6AS	Un-6A	1	
		α/β-Gli-22-Un-6AS	Un-6A	1	
		α/β-Gli-23-Un-6AS	Un-6A	1	
		α/β-Gli-24-Un-6BS	Un-6B	1	
		α/β-Gli-25-Un-6BS	Un-6B	1	
		α/β-Gli-26-Un-6AS	Un-6A	1	
		α/β-Gli-27-Un-6BS	Un-6B	1	
	δ-Gliadins	δ-Gli-a-1D	1D	1	2
		δ-Gli-b-1D	1D	1	
	γ-Gliadins	γ-Gli-1-1A	1A	1	18
		γ-Gli-1-1B	1B	1	
		γ-Gli-1-1D	1D	1	
		γ-Gli-2-1A	1A	1	
		γ-Gli-2-1B	1B	1	
		γ-Gli-2-1D	1D	1	
		γ-Gli-3-1A	1A	1	
		γ-Gli-3-1B	1B	1	
		γ-Gli-3-1D	1D	1	
		γ-Gli-4-1A	1A	1	
		γ-Gli-4-1B	1B	1	
		γ-Gli-4-1D	1D	1	
		γ-Gli-5-1A	1A	1	
		γ-Gli-5-1B	1B	1	
		γ-Gli-6-1A	1A	1	
		γ-Gli-6-1B	1B	1	
		γ-Gli-7-1B	1B	1	
		γ-Gli-8-1B	1B	1	
	Gliadin-Like Proteins	Gli-like-3B	3B	1	2
		Gli-like-3D	3D	1	

	ω-Gliadins	ω-Gli-1-1B	1B	1	38
		ω-Gli-1-1D	1D	1	
		ω-Gli-1-Un-1BS	Un-1B	1	
		ω-Gli-2-1AS	1A	1	
		ω-Gli-2-1BS	1B	1	
		ω-Gli-2-Un-1BS	Un-1B	1	
		ω-Gli-2-1D	1D	1	
		ω-Gli-3-1A	1A	1	
		ω-Gli-3-1B	1B	1	
		ω-Gli-3-Un-1B	Un-1B	1	
		ω-Gli-3-1D	1D	1	
		ω-Gli-4-1A	1A	1	
		ω-Gli-4-1B	1B	1	
		ω-Gli-4-Un-1BS	Un-1B	1	
		ω-Gli-4-1D	1D	1	
		ω-Gli-5-1A	1A	1	
		ω-Gli-5-1B	1B	1	
		ω-Gli-5-1D	1D	1	
		ω-Gli-5-Un-1AS	Un-1A	1	
		ω-Gli-6-1B	1B	1	
		ω-Gli-6-Un-1BS	Un-1B	1	
		ω-Gli-7-1B	1B	1	
		ω-Gli-8-1B	1B	1	
		ω-Gli-9-1B	1B	1	
		ω-Gli-28-Un-1DS	Un-1D	1	
		ω-Gli-1AS	1A	3	
		ω-Gli-1BS	1B	6	
		ω-Gli-1DS	1D	4	
TOTAL Proteins					**140**

Supplementary Table-3: Gluten proteins with known allergenicity

IWGSC_ RefSeqv1.1ID	Protein type	Chromosome	Reference allergen in wheat	Allergen source	Celiac disease	WDEIA	Bakers' asthma	Atopic dermatitis	Urticaria	Wheat allergy	Reference PubMed ID
TraesCS6A02G048900	Alpha gliadin	6A	Tri a 21	inhalation/ ingestion	celiac disease	WDEIA	Bakers' asthma	Atopic dermatitis	Urticaria	Wheat allergy	21557753; 19170508; 18036646; 10782525; 8581843; 9061215
TraesCS6B02G066001	Alpha gliadin	6B	Tri a 21	inhalation/ ingestion	celiac disease	WDEIA	Bakers' asthma	Atopic dermatitis	Urticaria	Wheat allergy	21557753; 19170508; 18036646; 10782525; 8581843; 9061215
TraesCSU02G108000	Alpha gliadin	Un_6D	Tri a 21	inhalation/ ingestion	celiac disease	WDEIA	Bakers' asthma	Atopic dermatitis	Urticaria	Wheat allergy	21557753; 19170508; 18036646; 10782525; 8581843; 9061215
TraesCS6B02G065749	Alpha gliadin	6B	Tri a 21	inhalation/ ingestion	celiac disease	WDEIA	Bakers' asthma	Atopic dermatitis	Urticaria	Wheat allergy	21557753; 19170508; 18036646; 10782525; 8581843; 9061215

				inhalation/ ingestion	celiac disease	WDEIA	Bakers' asthma	Atopic dermatitis	Urticaria	Wheat allergy	
TraesCSU02G108600	Alpha gliadin	Un_6D	Tri a 21								21557753; 19170508; 18036646; 10782525; 8581843; 9061215
TraesCS6B02G066100	Alpha gliadin	6B	Tri a 21								21557753; 19170508; 18036646; 10782525; 8581843; 9061215
TraesCSU02G108700	Alpha gliadin	Un_6D	Tri a 21								21557753; 19170508; 18036646; 10782525; 8581843; 9061215
Ta_Alphagli_12_6B_chr6B	Alpha gliadin	6B	Tri a 21								21557753; 19170508; 18036646; 10782525; 8581843; 9061215
TraesCSU02G149933	Alpha gliadin	6B	Tri a 21								21557753; 19170508; 18036646; 10782525; 8581843; 9061215

				inhalation/ ingestion	celiac disease	WDEIA	Bakers' asthma	Atopic dermatitis	Urticaria	Wheat allergy	
Ta_Alphagli_13_6B_chr6B	Alpha gliadin	6B	Tri a 21	inhalation/ ingestion	celiac disease	WDEIA	Bakers' asthma	Atopic dermatitis	Urticaria	Wheat allergy	21557753; 19170508; 18036646; 10782525; 8581843; 9061215
TraesCSU02G149938	Alpha gliadin	6B	Tri a 21	inhalation/ ingestion	celiac disease	WDEIA	Bakers' asthma	Atopic dermatitis	Urticaria	Wheat allergy	21557753; 19170508; 18036646; 10782525; 8581843; 9061215
Ta_Alphagli_14_6B_chr6B	Alpha gliadin	6B	Tri a 21	inhalation/ ingestion	celiac disease	WDEIA	Bakers' asthma	Atopic dermatitis	Urticaria	Wheat allergy	21557753; 19170508; 18036646; 10782525; 8581843; 9061215
TraesCSU02G149946	Alpha gliadin	6B	Tri a 21	inhalation/ ingestion	celiac disease	WDEIA	Bakers' asthma	Atopic dermatitis	Urticaria	Wheat allergy	21557753; 19170508; 18036646; 10782525; 8581843; 9061215
Ta_Alphagli_15_6B_chr6B	Alpha gliadin	6B	Tri a 21	inhalation/ ingestion	celiac disease	WDEIA	Bakers' asthma	Atopic dermatitis	Urticaria	Wheat allergy	21557753; 19170508; 18036646; 10782525; 8581843; 9061215

				inhalation/ingestion	celiac disease	WDEIA	Bakers' asthma	Atopic dermatitis	Urticaria	Wheat allergy	
TraesCSU02G149951	Alpha gliadin	6B	Tri a 21	inhalation/ingestion	celiac disease	WDEIA	Bakers' asthma	Atopic dermatitis	Urticaria	Wheat allergy	21557753; 19170508; 18036646; 10782525; 8581843; 9061215
TraesCS6B02G066000	Alpha gliadin	6B	Tri a 21	inhalation/ingestion	celiac disease	WDEIA	Bakers' asthma	Atopic dermatitis	Urticaria	Wheat allergy	21557753; 19170508; 18036646; 10782525; 8581843; 9061215
TraesCSU02G153800	Alpha gliadin	6A	Tri a 21	inhalation/ingestion	celiac disease	WDEIA	Bakers' asthma	Atopic dermatitis	Urticaria	Wheat allergy	21557753; 19170508; 18036646; 10782525; 8581843; 9061215
Ta_Alphagli_17_6B_chr6B	Alpha gliadin	6B	Tri a 21	inhalation/ingestion	celiac disease	WDEIA	Bakers' asthma	Atopic dermatitis	Urticaria	Wheat allergy	21557753; 19170508; 18036646; 10782525; 8581843; 9061215
TraesCSU02G160200	Alpha gliadin	6A	Tri a 21	inhalation/ingestion	celiac disease	WDEIA	Bakers' asthma	Atopic dermatitis	Urticaria	Wheat allergy	21557753; 19170508; 18036646; 10782525; 8581843; 9061215

				inhalation/ ingestion	celiac disease	WDEIA	Bakers' asthma	Atopic dermatitis	Urticaria	Wheat allergy	
TraesCS6B02G086500	Alpha gliadin	6B	Tri a 21	inhalation/ ingestion	celiac disease	WDEIA	Bakers' asthma	Atopic dermatitis	Urticaria	Wheat allergy	21557753; 19170508; 18036646; 10782525; 8581843; 9061215
TraesCSU02G188800	Alpha gliadin	Un _6 D	Tri a 21	inhalation/ ingestion	celiac disease	WDEIA	Bakers' asthma	Atopic dermatitis	Urticaria	Wheat allergy	21557753; 19170508; 18036646; 10782525; 8581843; 9061215
TraesCS6B02G086522	Alpha gliadin	6B	Tri a 21	inhalation/ ingestion	celiac disease	WDEIA	Bakers' asthma	Atopic dermatitis	Urticaria	Wheat allergy	21557753; 19170508; 18036646; 10782525; 8581843; 9061215
TraesCSU02G202177	Alpha gliadin	Un _6 B	Tri a 21	inhalation/ ingestion	celiac disease	WDEIA	Bakers' asthma	Atopic dermatitis	Urticaria	Wheat allergy	21557753; 19170508; 18036646; 10782525; 8581843; 9061215
TraesCS6A02G049066	Alpha gliadin	6A	Tri a 21	inhalation/ ingestion	celiac disease	WDEIA	Bakers' asthma	Atopic dermatitis	Urticaria	Wheat allergy	21557753; 19170508; 18036646; 10782525; 8581843; 9061215

				inhalation/ ingestion	celiac disease	WDEIA	Bakers' asthma	Atopic dermatitis	Urticaria	Wheat allergy	
TraesCS6B02G065993	Alpha gliadin	6B	Tri a 21	inhalation/ ingestion	celiac disease	WDEIA	Bakers' asthma	Atopic dermatitis	Urticaria	Wheat allergy	21557753; 19170508; 18036646; 10782525; 8581843; 9061215
TraesCSU02G108098	Alpha gliadin	Un _6 D	Tri a 21	inhalation/ ingestion	celiac disease	WDEIA	Bakers' asthma	Atopic dermatitis	Urticaria	Wheat allergy	21557753; 19170508; 18036646; 10782525; 8581843; 9061215
TraesCSU02G220200	Alpha gliadin	6A	Tri a 21	inhalation/ ingestion	celiac disease	WDEIA	Bakers' asthma	Atopic dermatitis	Urticaria	Wheat allergy	21557753; 19170508; 18036646; 10782525; 8581843; 9061215
TraesCSU02G220600	Alpha gliadin	Un _6 A	Tri a 21	inhalation/ ingestion	celiac disease	WDEIA	Bakers' asthma	Atopic dermatitis	Urticaria	Wheat allergy	21557753; 19170508; 18036646; 10782525; 8581843; 9061215
TraesCSU02G239000	Alpha gliadin	Un _6 D	Tri a 21	inhalation/ ingestion	celiac disease	WDEIA	Bakers' asthma	Atopic dermatitis	Urticaria	Wheat allergy	21557753; 19170508; 18036646; 10782525; 8581843; 9061215

				inhalation/ ingestion	celiac disease	WDEIA	Bakers' asthma	Atopic dermatitis	Urticaria	Wheat allergy	
TraesCSU02G251939	Alpha gliadi n	Un _6 A	Tri a 21	inhalation/ ingestion	celiac disease	WDEIA	Bakers' asthma	Atopic dermatitis	Urticaria	Wheat allergy	21557753; 19170508; 18036646; 10782525; 8581843; 9061215
TraesCSU02G255529	Alpha gliadi n	Un _6 B	Tri a 21	inhalation/ ingestion	celiac disease	WDEIA	Bakers' asthma	Atopic dermatitis	Urticaria	Wheat allergy	21557753; 19170508; 18036646; 10782525; 8581843; 9061215
TraesCSU02G257591	Alpha gliadi n	Un _6 B	Tri a 21	inhalation/ ingestion	celiac disease	WDEIA	Bakers' asthma	Atopic dermatitis	Urticaria	Wheat allergy	21557753; 19170508; 18036646; 10782525; 8581843; 9061215
TraesCSU02G265913	Alpha gliadi n	Un _6 A	Tri a 21	inhalation/ ingestion	celiac disease	WDEIA	Bakers' asthma	Atopic dermatitis	Urticaria	Wheat allergy	21557753; 19170508; 18036646; 10782525; 8581843; 9061215
TraesCSU02G267761	Alpha gliadi n	Un _6 B	Tri a 21	inhalation/ ingestion	celiac disease	WDEIA	Bakers' asthma	Atopic dermatitis	Urticaria	Wheat allergy	21557753; 19170508; 18036646; 10782525; 8581843; 9061215

				inhalation/ ingestion	celiac disease	WDEIA	Bakers' asthma	Atopic dermatitis	Urticaria	Wheat allergy	
TraesCS6A02G049100	Alpha gliadin	6A	Tri a 21	inhalation/ ingestion	celiac disease	WDEIA	Bakers' asthma	Atopic dermatitis	Urticaria	Wheat allergy	21557753; 19170508; 18036646; 10782525; 8581843; 9061215
TraesCS6B02G065900	Alpha gliadin	6B	Tri a 21	inhalation/ ingestion	celiac disease	WDEIA	Bakers' asthma	Atopic dermatitis	Urticaria	Wheat allergy	21557753; 19170508; 18036646; 10782525; 8581843; 9061215
TraesCSU02G108100	Alpha gliadin	Un_6D	Tri a 21	inhalation/ ingestion	celiac disease	WDEIA	Bakers' asthma	Atopic dermatitis	Urticaria	Wheat allergy	21557753; 19170508; 18036646; 10782525; 8581843; 9061215
TraesCS6A02G049200	Alpha gliadin	6A	Tri a 21	inhalation/ ingestion	celiac disease	WDEIA	Bakers' asthma	Atopic dermatitis	Urticaria	Wheat allergy	21557753; 19170508; 18036646; 10782525; 8581843; 9061215
TraesCS6B02G065856	Alpha gliadin	6B	Tri a 21	inhalation/ ingestion	celiac disease	WDEIA	Bakers' asthma	Atopic dermatitis	Urticaria	Wheat allergy	21557753; 19170508; 18036646; 10782525; 8581843; 9061215

				inhalation/ ingestion	celiac disease	WDEIA	Bakers' asthma	Atopic dermatitis	Urticaria	Wheat allergy	
TraesCSU02G108200	Alpha gliadin	Un_6 D	Tri a 21	inhalation/ ingestion	celiac disease	WDEIA	Bakers' asthma	Atopic dermatitis	Urticaria	Wheat allergy	21557753; 19170508; 18036646; 10782525; 8581843; 9061215
TraesCS6A02G049400	Alpha gliadin	6A	Tri a 21	inhalation/ ingestion	celiac disease	WDEIA	Bakers' asthma	Atopic dermatitis	Urticaria	Wheat allergy	21557753; 19170508; 18036646; 10782525; 8581843; 9061215
TraesCS6B02G065800	Alpha gliadin	6B	Tri a 21	inhalation/ ingestion	celiac disease	WDEIA	Bakers' asthma	Atopic dermatitis	Urticaria	Wheat allergy	21557753; 19170508; 18036646; 10782525; 8581843; 9061215
TraesCSU02G108205	Alpha gliadin	Un_6 D	Tri a 21	inhalation/ ingestion	celiac disease	WDEIA	Bakers' asthma	Atopic dermatitis	Urticaria	Wheat allergy	21557753; 19170508; 18036646; 10782525; 8581843; 9061215
TraesCS6A02G049500	Alpha gliadin	6A	Tri a 21	inhalation/ ingestion	celiac disease	WDEIA	Bakers' asthma	Atopic dermatitis	Urticaria	Wheat allergy	21557753; 19170508; 18036646; 10782525; 8581843; 9061215

				inhalation/ ingestion	celiac disease	WDEIA	Bakers' asthma	Atopic dermatitis	Urticaria	Wheat allergy	
TraesCS6B02G065536	Alpha gliadin	6B	Tri a 21	inhalation/ ingestion	celiac disease	WDEIA	Bakers' asthma	Atopic dermatitis	Urticaria	Wheat allergy	21557753; 19170508; 18036646; 10782525; 8581843; 9061215
TraesCSU02G108300	Alpha gliadin	Un _6 D	Tri a 21	inhalation/ ingestion	celiac disease	WDEIA	Bakers' asthma	Atopic dermatitis	Urticaria	Wheat allergy	21557753; 19170508; 18036646; 10782525; 8581843; 9061215
TraesCS6A02G049600	Alpha gliadin	6A	Tri a 21	inhalation/ ingestion	celiac disease	WDEIA	Bakers' asthma	Atopic dermatitis	Urticaria	Wheat allergy	21557753; 19170508; 18036646; 10782525; 8581843; 9061215
TraesCS6B02G065578	Alpha gliadin	6B	Tri a 21	inhalation/ ingestion	celiac disease	WDEIA	Bakers' asthma	Atopic dermatitis	Urticaria	Wheat allergy	21557753; 19170508; 18036646; 10782525; 8581843; 9061215
TraesCSU02G108363	Alpha gliadin	Un _6 D	Tri a 21	inhalation/ ingestion	celiac disease	WDEIA	Bakers' asthma	Atopic dermatitis	Urticaria	Wheat allergy	21557753; 19170508; 18036646; 10782525; 8581843; 9061215

				inhalation/ ingestion	celiac disease	WDEIA	Bakers' asthma	Atopic dermatitis	Urticaria	Wheat allergy	
TraesCS6A02G049700	Alpha gliadin	6A	Tri a 21								21557753; 19170508; 18036646; 10782525; 8581843; 9061215
TraesCS6B02G065600	Alpha gliadin	6B	Tri a 21								21557753; 19170508; 18036646; 10782525; 8581843; 9061215
TraesCSU02G108400	Alpha gliadin	Un_6D	Tri a 21								21557753; 19170508; 18036646; 10782525; 8581843; 9061215
TraesCS6A02G049800	Alpha gliadin	6A	Tri a 21								21557753; 19170508; 18036646; 10782525; 8581843; 9061215
Ta_Alphagli_9_6B_chr6B	Alpha gliadin	6B	Tri a 21								21557753; 19170508; 18036646; 10782525; 8581843; 9061215

Gene	Type	Chr	Tri a	inhalation/ingestion	celiac disease	WDEIA	Bakers' asthma	Atopic dermatitis	Urticaria	Wheat allergy	PubMed IDs
TraesCSU02G108500	Alpha gliadin	Un_6D	Tri a 21	inhalation/ ingestion	celiac disease	WDEIA	Bakers' asthma	Atopic dermatitis	Urticaria	Wheat allergy	21557753; 19170508; 18036646; 10782525; 8581843; 9061215
Ta_Alphagli_a_6B_chr6B	Alpha gliadin	6B	Tri a 21	inhalation/ ingestion	celiac disease	WDEIA	Bakers' asthma	Atopic dermatitis	Urticaria	Wheat allergy	21557753; 19170508; 18036646; 10782525; 8581843; 9061215
Ta_Alphagli_a_Un_6DS_chrUn	Alpha gliadin	Un_6D	Tri a 21	inhalation/ ingestion	celiac disease	WDEIA	Bakers' asthma	Atopic dermatitis	Urticaria	Wheat allergy	21557753; 19170508; 18036646; 10782525; 8581843; 9061215
Ta_Deltagli_a_1DS_chr1D_1.0	Gamma gliadin	1D	Tri a 20	inhalation/ing estion	celiac disease	WDEIA					
TraesCS1D02G001300	Gamma gliadin	1D	Tri a 20	inhalation/ing estion	celiac disease	WDEIA					
TraesCS1A02G007200	Gamma gliadin	1A	Tri a 20	inhalation/ ingestion	celiac disease	WDEIA		Atopic dermatitis		Wheat allergy	9738916; 8604979; 9383251; 14581135; 17655322; 22737987; 23963475

				inhalation/ ingestion	celiac disease	WDEIA	Atopic dermatitis		Wheat allergy	
TraesCS1B02G009877	Gamma gliadin	1B	Tri a 20	inhalation/ ingestion	celiac disease	WDEIA	Atopic dermatitis		Wheat allergy	9738916; 8604979; 9383251; 14581135; 17655322; 22737987
TraesCS1D02G001000	Gamma gliadin	1D	Tri a 20	inhalation/ ingestion	celiac disease	WDEIA	Atopic dermatitis		Wheat allergy	9738916; 8604979; 9383251; 14581135; 17655322; 22737987
TraesCS1A02G007236	Gamma gliadin	1A	Tri a 20	inhalation/ ingestion	celiac disease	WDEIA	Atopic dermatitis		Wheat allergy	9738916; 8604979; 9383251; 14581135; 17655322; 22737987
TraesCS1B02G010400	Gamma gliadin	1B	Tri a 20	inhalation/ ingestion	celiac disease	WDEIA	Atopic dermatitis		Wheat allergy	9738916; 8604979; 9383251; 14581135; 17655322; 22737987
TraesCS1D02G001100	Gamma gliadin	1D	Tri a 20	inhalation/ ingestion	celiac disease	WDEIA	Atopic dermatitis		Wheat allergy	9738916; 8604979; 9383251; 14581135; 17655322; 22737987

				inhalation/ ingestion	celiac disease	WDEIA	Atopic dermatitis		Wheat allergy	
TraesCS1A02G007300	Gam ma gliadi n	1A	Tri a 20	inhalation/ ingestion	celiac disease	WDEIA	Atopic dermatitis		Wheat allergy	9738916; 8604979; 9383251; 14581135; 17655322; 22737987
TraesCS1B02G010500	Gam ma gliadi n	1B	Tri a 20	inhalation/ ingestion	celiac disease	WDEIA	Atopic dermatitis		Wheat allergy	9738916; 8604979; 9383251; 14581135; 17655322; 22737987
TraesCS1D02G001200	Gam ma gliadi n	1D	Tri a 20	inhalation/ ingestion	celiac disease	WDEIA	Atopic dermatitis		Wheat allergy	9738916; 8604979; 9383251; 14581135; 17655322; 22737987
TraesCS1A02G007344	Gam ma gliadi n	1A	Tri a 20	inhalation/ ingestion	celiac disease	WDEIA	Atopic dermatitis		Wheat allergy	9738916; 8604979; 9383251; 14581135; 17655322; 22737987
TraesCS1B02G010600	Gam ma gliadi n	1B	Tri a 20	inhalation/ ingestion	celiac disease	WDEIA	Atopic dermatitis		Wheat allergy	9738916; 8604979; 9383251; 14581135; 17655322; 22737987

				inhalation/ ingestion	celiac disease	WDEIA	Atopic dermatitis		Wheat allergy	
TraesCS1D02G001400	Gam ma gliadi n	1D	Tri a 20	inhalation/ ingestion	celiac disease	WDEIA	Atopic dermatitis		Wheat allergy	9738916; 8604979; 9383251; 14581135; 17655322; 22737987
TraesCS1A02G007400	Gam ma gliadi n	1A	Tri a 20	inhalation/ ingestion	celiac disease	WDEIA	Atopic dermatitis		Wheat allergy	9738916; 8604979; 9383251; 14581135; 17655322; 22737987
TraesCS1B02G010700	Gam ma gliadi n	1B	Tri a 20	inhalation/ ingestion	celiac disease	WDEIA	Atopic dermatitis		Wheat allergy	9738916; 8604979; 9383251; 14581135; 17655322; 22737987
TraesCS1A02G007405	Gam ma gliadi n	1A	Tri a 20	inhalation/ ingestion	celiac disease	WDEIA	Atopic dermatitis		Wheat allergy	9738916; 8604979; 9383251; 14581135; 17655322; 22737987
TraesCS1B02G010800	Gam ma gliadi n	1B	Tri a 20	inhalation/ ingestion	celiac disease	WDEIA	Atopic dermatitis		Wheat allergy	9738916; 8604979; 9383251; 14581135; 17655322; 22737987

				inhalation/ingestion	celiac disease	WDEIA	Atopic dermatitis	Urticaria	Wheat allergy	
TraesCS1B02G010900	Gamma gliadin	1B	Tri a 20	inhalation/ingestion	celiac disease	WDEIA	Atopic dermatitis		Wheat allergy	9738916; 8604979; 9383251; 14581135; 17655322; 22737987
TraesCS1B02G011000	Gamma gliadin	1B	Tri a 20	inhalation/ingestion	celiac disease	WDEIA	Atopic dermatitis		Wheat allergy	9738916; 8604979; 9383251; 14581135; 17655322; 22737987
TraesCS3B02G475019	Gliadin-like protein	3B	Tri a 20	inhalation/ingestion	celiac disease		Atopic dermatitis		Wheat allergy	9738916; 8604979; 9383251; 14581135; 17655322; 22737987
TraesCS3D02G433755	Gliadin-like protein	3D	Tri a 20	inhalation/ingestion	celiac disease		Atopic dermatitis		Wheat allergy	9738916; 8604979; 9383251; 14581135; 17655322; 22737987
TraesCS1A02G007934	LMW glutenin	1A	Tri a 36	inhalation/ingestion	celiac disease	WDEIA	Atopic dermatitis	Urticaria		17655322; 10782525; 8753845; 9061215; 8581843; 22904302; 17960887; 17496422;

101

				inhalation/ ingestion	celiac disease	WDEIA	Atopic dermatitis	Urticaria		
TraesCS1A02G008000	LMW glutenin	1A	Tri a 36	inhalation/ ingestion	celiac disease	WDEIA	Atopic dermatitis	Urticaria		17655322; 10782525; 8753845; 9061215; 8581843; 22904302; 17960887; 17496422;
TraesCS1D02G000200	LMW glutenin	1D	Tri a 36	inhalation/ ingestion	celiac disease	WDEIA	Atopic dermatitis	Urticaria		17655322; 10782525; 8753845; 9061215; 8581843; 22904302; 17960887; 17496422;
TraesCS1A02G010900	LMW glutenin	1A	Tri a 36	inhalation/ ingestion	celiac disease	WDEIA	Atopic dermatitis	Urticaria		17655322; 10782525; 8753845; 9061215; 8581843; 22904302; 17960887; 17496422;
TraesCS1D02G007400	LMW glutenin	1D	Tri a 36	inhalation/ ingestion	celiac disease	WDEIA	Atopic dermatitis	Urticaria		17655322; 10782525; 8753845; 9061215; 8581843; 22904302; 17960887; 17496422;

TraesCS1A02G010905	LMW glutenin	1A	Tri a 36	inhalation/ ingestion	celiac disease	WDEIA	Atopic dermatitis	Urticaria	17655322; 10782525; 8753845; 9061215; 8581843; 22904302; 17960887; 17496422;
TraesCS1B02G013500	LMW glutenin	1B	Tri a 36	inhalation/ ingestion	celiac disease	WDEIA	Atopic dermatitis	Urticaria	17655322; 10782525; 8753845; 9061215; 8581843; 22904302; 17960887; 17496422;
TraesCS1D02G007626	LMW glutenin	1D	Tri a 36	inhalation/ ingestion	celiac disease	WDEIA	Atopic dermatitis	Urticaria	17655322; 10782525; 8753845; 9061215; 8581843; 22904302; 17960887; 17496422;
TraesCS1B02G042700	LMW glutenin	1B	Tri a 36	inhalation/ ingestion	celiac disease	WDEIA	Atopic dermatitis	Urticaria	17655322; 10782525; 8753845; 9061215; 8581843; 22904302; 17960887; 17496422;

				inhalation/ ingestion	celiac disease	WDEIA	Atopic dermatitis	Urticaria		
TraesCS1D02G008600	LMW glutenin	1D	Tri a 36	inhalation/ ingestion	celiac disease	WDEIA	Atopic dermatitis	Urticaria		17655322; 10782525; 8753845; 9061215; 8581843; 22904302; 17960887; 17496422;
TraesCS1D02G009400	LMW glutenin	1D	Tri a 36	inhalation/ ingestion	celiac disease	WDEIA	Atopic dermatitis	Urticaria		17655322; 10782525; 8753845; 9061215; 8581843; 22904302; 17960887; 17496422;
TraesCS1D02G009900	LMW glutenin	1D	Tri a 36	inhalation/ ingestion	celiac disease	WDEIA	Atopic dermatitis	Urticaria		17655322; 10782525; 8753845; 9061215; 8581843; 22904302; 17960887; 17496422;
TraesCS1D02G015100	LMW glutenin	1D	Tri a 36	inhalation/ ingestion	celiac disease	WDEIA	Atopic dermatitis	Urticaria		17655322; 10782525; 8753845; 9061215; 8581843; 22904302; 17960887; 17496422;

				inhalation/ ingestion	celiac disease	WDEIA	Atopic dermatitis	Urticaria		
TraesCS1B02G011523	LMW gluten in	1B	Tri a 36	inhalation/ ingestion	celiac disease	WDEIA	Atopic dermatitis	Urticaria		17655322; 10782525; 8753845; 9061215; 8581843; 22904302; 17960887; 17496422;
TraesCS1B02G011600	LMW gluten in	1B	Tri a 36	inhalation/ ingestion	celiac disease	WDEIA	Atopic dermatitis	Urticaria		17655322; 10782525; 8753845; 9061215; 8581843; 22904302; 17960887; 17496422;
TraesCS1D02G000300	LMW gluten in	1D	Tri a 36	inhalation/ ingestion	celiac disease	WDEIA	Atopic dermatitis	Urticaria		17655322; 10782525; 8753845; 9061215; 8581843; 22904302; 17960887; 17496422;
TraesCS1B02G011700	LMW gluten in	1B	Tri a 36	inhalation/ingestion	celiac disease	WDEIA	Atopic dermatitis	Urticaria		17655322; 10782525; 8753845; 9061215; 8581843; 22904302; 17960887; 17496422;

				inhalation/ ingestion	celiac disease	WDEIA, Anaphylaxis	Atopic dermatitis	Urticaria	Wheat allergy	
TraesCS1B02G011439	Omega gliadin	1B	Tri a 19	inhalation/ ingestion	celiac disease	WDEIA, Anaphylaxis	Atopic dermatitis	Urticaria	Wheat allergy	14699123; 16339549; 28054973; 26109797; 11590393; 12534555; 25576081
TraesCS1D02G000524	Omega gliadin	1D	Tri a 19	inhalation/ ingestion	celiac disease	WDEIA, Anaphylaxis	Atopic dermatitis	Urticaria	Wheat allergy	14699123; 16339549; 28054973; 26109797; 11590393; 12534555; 25576081
TraesCSU02G002414	Omega gliadin	Un_1B	Tri a 19	inhalation/ ingestion	celiac disease	WDEIA, Anaphylaxis	Atopic dermatitis	Urticaria	Wheat allergy	14699123; 16339549; 28054973; 26109797; 11590393; 12534555; 25576081
Ta_Omegagli_1AS_NMPL02092730.1_149875..150924	Omega gliadin	1A	Tri a 19	inhalation/ ingestion	celiac disease	WDEIA, Anaphylaxis	Atopic dermatitis	Urticaria	Wheat allergy	14699123; 16339549; 28054973; 26109797; 11590393; 12534555; 25576081

				inhalation/ ingestion	celiac disease	WDEIA, Anaphylaxis	Atopic dermatitis	Urticaria	Wheat allergy	
Ta_Omegagli_1AS_N MPL02092730.1_169 343..170422	Omeg a gliadi n	1A	Tri a 19	inhalation/ ingestion	celiac disease	WDEIA, Anaphylaxis	Atopic dermatitis	Urticaria	Wheat allergy	14699123; 16339549; 28054973; 26109797; 11590393; 12534555; 25576081
Ta_Omegagli_1AS_N MPL02092730.1_223 939..224925	Omeg a gliadi n	1A	Tri a 19	inhalation/ ingestion	celiac disease	WDEIA, Anaphylaxis	Atopic dermatitis	Urticaria	Wheat allergy	14699123; 16339549; 28054973; 26109797; 11590393; 12534555; 25576081
Ta_Omegagli_1BS_N MPL02099594.1_221 03..23560	Omeg a gliadi n	1B	Tri a 19	inhalation/ ingestion	celiac disease	WDEIA, Anaphylaxis	Atopic dermatitis	Urticaria	Wheat allergy	14699123; 16339549; 28054973; 26109797; 11590393; 12534555; 25576081
Ta_Omegagli_1BS_N MPL02126093.1_com plement(13350..13532)	Omeg a gliadi n	1B	Tri a 19	inhalation/ ingestion	celiac disease	WDEIA, Anaphylaxis	Atopic dermatitis	Urticaria	Wheat allergy	14699123; 16339549; 28054973; 26109797; 11590393; 12534555; 25576081

Ta_Omegagli_1BS_NMPL02126093.1_complement(25591..26892)	Omega gliadin	1B	Tri a 19	inhalation/ ingestion	celiac disease	WDEIA, Anaphylaxis	Atopic dermatitis	Urticaria	Wheat allergy	14699123; 16339549; 28054973; 26109797; 11590393; 12534555; 25576081
Ta_Omegagli_1BS_NMPL02126093.1_complement(6321..7739)	Omega gliadin	1B	Tri a 19	inhalation/ ingestion	celiac disease	WDEIA, Anaphylaxis	Atopic dermatitis	Urticaria	Wheat allergy	14699123; 16339549; 28054973; 26109797; 11590393; 12534555; 25576081
Ta_Omegagli_1BS_NMPL02255630.1_complement(34875..36121)	Omega gliadin	1B	Tri a 19	inhalation/ ingestion	celiac disease	WDEIA, Anaphylaxis	Atopic dermatitis	Urticaria	Wheat allergy	14699123; 16339549; 28054973; 26109797; 11590393; 12534555; 25576081
Ta_Omegagli_1BS_NMPL02255630.1_complement(62321..63622)	Omega gliadin	1B	Tri a 19	inhalation/ ingestion	celiac disease	WDEIA, Anaphylaxis	Atopic dermatitis	Urticaria	Wheat allergy	14699123; 16339549; 28054973; 26109797; 11590393; 12534555; 25576081

				inhalation/ ingestion	celiac disease	WDEIA, Anaphylaxis	Atopic dermatitis	Urticaria	Wheat allergy	
Ta_Omegagli_1DS_N MPL02250468.1_431 275..432432	Omeg a gliadi n	1D	Tri a 19	inhalation/ ingestion	celiac disease	WDEIA, Anaphylaxis	Atopic dermatitis	Urticaria	Wheat allergy	14699123; 16339549; 28054973; 26109797; 11590393; 12534555; 25576081
Ta_Omegagli_1DS_N MPL02250468.1_445 195..446352	Omeg a gliadi n	1D	Tri a 19	inhalation/ ingestion	celiac disease	WDEIA, Anaphylaxis	Atopic dermatitis	Urticaria	Wheat allergy	14699123; 16339549; 28054973; 26109797; 11590393; 12534555; 25576081
Ta_Omegagli_1DS_N MPL02250468.1_459 100..460257	Omeg a gliadi n	1D	Tri a 19	inhalation/ ingestion	celiac disease	WDEIA, Anaphylaxis	Atopic dermatitis	Urticaria	Wheat allergy	14699123; 16339549; 28054973; 26109797; 11590393; 12534555; 25576081
Ta_Omegagli_1DS_N MPL02250468.1_com plement(746935..7480 96)	Omeg a gliadi n	1D	Tri a 19	inhalation/ ingestion	celiac disease	WDEIA, Anaphylaxis	Atopic dermatitis	Urticaria	Wheat allergy	14699123; 16339549; 28054973; 26109797; 11590393; 12534555; 25576081

				inhalation/ ingestion	celiac disease	WDEIA, Anaphylaxis	Atopic dermatitis	Urticaria	Wheat allergy	
TraesCS1A02G005368	Omega gliadin	1A	Tri a 19	inhalation/ ingestion	celiac disease	WDEIA, Anaphylaxis	Atopic dermatitis	Urticaria	Wheat allergy	14699123; 16339549; 28054973; 26109797; 11590393; 12534555; 25576081
Ta_Omegagli_2_1BS_ NMPL02255630.1_co mplement(98412..997 46)	Omega gliadin	1B	Tri a 19	inhalation/ ingestion	celiac disease	WDEIA, Anaphylaxis	Atopic dermatitis	Urticaria	Wheat allergy	14699123; 16339549; 28054973; 26109797; 11590393; 12534555; 25576081
TraesCS1D02G000531	Omega gliadin	1D	Tri a 19	inhalation/ ingestion	celiac disease	WDEIA, Anaphylaxis	Atopic dermatitis	Urticaria	Wheat allergy	14699123; 16339549; 28054973; 26109797; 11590393; 12534555; 25576081
Ta_Omegagli_2_Un_1 BS_NMPL02255630.1 _complement(117528.. 118824)	Omega gliadin	Un _1 B	Tri a 19	inhalation/ ingestion	celiac disease	WDEIA, Anaphylaxis	Atopic dermatitis	Urticaria	Wheat allergy	14699123; 16339549; 28054973; 26109797; 11590393; 12534555; 25576081

				inhalation/ ingestion	celiac disease	WDEIA, Anaphylaxis	Atopic dermatitis	Urticaria	Wheat allergy	
TraesCSU02G272393	Omega gliadin	Un_1 DS	Tri a 19	inhalation/ ingestion	celiac disease	WDEIA, Anaphylaxis	Atopic dermatitis	Urticaria	Wheat allergy	14699123; 16339549; 28054973; 26109797; 11590393; 12534555; 25576081
TraesCS1A02G005387	Omega gliadin	1A	Tri a 19	inhalation/ ingestion	celiac disease	WDEIA, Anaphylaxis	Atopic dermatitis	Urticaria	Wheat allergy	14699123; 16339549; 28054973; 26109797; 11590393; 12534555; 25576081
Ta_Omegagli_3_1BS NMPL02255630.1 complement(74668..75968)	Omega gliadin	1B	Tri a 19	inhalation/ ingestion	celiac disease	WDEIA, Anaphylaxis	Atopic dermatitis	Urticaria	Wheat allergy	14699123; 16339549; 28054973; 26109797; 11590393; 12534555; 25576081
Ta_Omegagli_3_1DS_ _NMPL02250468.1_c omplement(759437..760585)	Omega gliadin	1D	Tri a 19	inhalation/ ingestion	celiac disease	WDEIA, Anaphylaxis	Atopic dermatitis	Urticaria	Wheat allergy	14699123; 16339549; 28054973; 26109797; 11590393; 12534555; 25576081

				inhalation/ ingestion	celiac disease	WDEIA, Anaphylaxis	Atopic dermatitis	Urticaria	Wheat allergy	
TraesCSU02G165233	Omega gliadin	Un_1B	Tri a 19	inhalation/ ingestion	celiac disease	WDEIA, Anaphylaxis	Atopic dermatitis	Urticaria	Wheat allergy	14699123; 16339549; 28054973; 26109797; 11590393; 12534555; 25576081
TraesCS1A02G033288	Omega gliadin	1A	Tri a 19	inhalation/ ingestion	celiac disease	WDEIA, Anaphylaxis	Atopic dermatitis	Urticaria	Wheat allergy	14699123; 16339549; 28054973; 26109797; 11590393; 12534555; 25576081
TraesCS1B02G011467	Omega gliadin	1B	Tri a 19	inhalation/ ingestion	celiac disease	WDEIA, Anaphylaxis	Atopic dermatitis	Urticaria	Wheat allergy	14699123; 16339549; 28054973; 26109797; 11590393; 12534555; 25576081
TraesCS1D02G000582	Omega gliadin	1D	Tri a 19	inhalation/ ingestion	celiac disease	WDEIA, Anaphylaxis	Atopic dermatitis	Urticaria	Wheat allergy	14699123; 16339549; 28054973; 26109797; 11590393; 12534555; 25576081

				inhalation/ ingestion	celiac disease	WDEIA, Anaphylaxis	Atopic dermatitis	Urticaria	Wheat allergy	
TraesCSU02G165363	Omega gliadin	1B	Tri a 19	inhalation/ ingestion	celiac disease	WDEIA, Anaphylaxis	Atopic dermatitis	Urticaria	Wheat allergy	14699123; 16339549; 28054973; 26109797; 11590393; 12534555; 25576081
TraesCS1A02G033501	Omega gliadin	1A	Tri a 19	inhalation/ ingestion	celiac disease	WDEIA, Anaphylaxis	Atopic dermatitis	Urticaria	Wheat allergy	14699123; 16339549; 28054973; 26109797; 11590393; 12534555; 25576081
Ta_Omegagli_5_1BS_NMPL02232860.1_3223..4541	Omega gliadin	1B	Tri a 19	inhalation/ ingestion	celiac disease	WDEIA, Anaphylaxis	Atopic dermatitis	Urticaria	Wheat allergy	14699123; 16339549; 28054973; 26109797; 11590393; 12534555; 25576081
Ta_Omegagli_5_1DS_NMPL02250468.1_410561..411695	Omega gliadin	1D	Tri a 19	inhalation/ ingestion	celiac disease	WDEIA, Anaphylaxis	Atopic dermatitis	Urticaria	Wheat allergy	14699123; 16339549; 28054973; 26109797; 11590393; 12534555; 25576081

				inhalation/ ingestion	celiac disease	WDEIA, Anaphylaxis	Atopic dermatitis	Urticaria	Wheat allergy	
TraesCSU02G182638	Omega gliadin	Un_1A	Tri a 19	inhalation/ ingestion	celiac disease	WDEIA, Anaphylaxis	Atopic dermatitis	Urticaria	Wheat allergy	14699123; 16339549; 28054973; 26109797; 11590393; 12534555; 25576081
TraesCS1B02G011474	Omega gliadin	1B	Tri a 19	inhalation/ ingestion	celiac disease	WDEIA, Anaphylaxis	Atopic dermatitis	Urticaria	Wheat allergy	14699123; 16339549; 28054973; 26109797; 11590393; 12534555; 25576081
Ta_Omegagli_6_Un_1BS_NMPL02055150.1_44613..45980	Omega gliadin	Un_1B	Tri a 19	inhalation/ ingestion	celiac disease	WDEIA, Anaphylaxis	Atopic dermatitis	Urticaria	Wheat allergy	14699123; 16339549; 28054973; 26109797; 11590393; 12534555; 25576081
Ta_Omegagli_7_1BS_NMPL02099594.1_32257..33634	Omega gliadin	1B	Tri a 19	inhalation/ ingestion	celiac disease	WDEIA, Anaphylaxis	Atopic dermatitis	Urticaria	Wheat allergy	14699123; 16339549; 28054973; 26109797; 11590393; 12534555; 25576081

TraesCS1B02G011487	Omega gliadin	1B	Tri a 19	inhalation/ ingestion	celiac disease	WDEIA, Anaphylaxis	Atopic dermatitis	Urticaria	Wheat allergy	14699123; 16339549; 28054973; 26109797; 11590393; 12534555; 25576081
TraesCS1B02G041928	Omega gliadin	1B	Tri a 19	inhalation/ ingestion	celiac disease	WDEIA, Anaphylaxis	Atopic dermatitis	Urticaria	Wheat allergy	14699123; 16339549; 28054973; 26109797; 11590393; 12534555; 25576081
TraesCS1A02G317311	HMW glutenin	1A	Tri a 26	inhalation/ ingestion	celiac disease	WDEIA, Anaphylaxis	Atopic dermatitis		Wheat allergy	16339549; 23612492; 24007624; http://dx.doi.org/10.1016/j.jaci.2011.12.215; 22805477
TraesCS1B02G329711	HMW glutenin	1B	Tri a 26	inhalation/ ingestion	celiac disease	WDEIA, Anaphylaxis	Atopic dermatitis		Wheat allergy	16339549; 23612492; 24007624; http://dx.doi.org/10.1016/j.jaci.2011.12.215; 22805477

				inhalation/ ingestion	celiac disease	WDEIA, Anaphylaxis	Atopic dermatitis		Wheat allergy	
TraesCS1D02G317211	HMW glutenin	1D	Tri a 26	inhalation/ ingestion	celiac disease	WDEIA, Anaphylaxis	Atopic dermatitis		Wheat allergy	16339549; 23612492; 24007624; http://dx.doi.org/10.1016/j.jaci.2011.12.215; 22805477
TRIAE_Ta_HMWglu_y_1AL	HMW glutenin	1A	Tri a 26	inhalation/ ingestion	celiac disease	WDEIA, Anaphylaxis	Atopic dermatitis		Wheat allergy	16339549; 23612492; 24007624; http://dx.doi.org/10.1016/j.jaci.2011.12.215; 22805477
TraesCS1B02G329992	HMW glutenin	1B	Tri a 26	inhalation/ ingestion	celiac disease	WDEIA, Anaphylaxis	Atopic dermatitis		Wheat allergy	16339549; 23612492; 24007624; http://dx.doi.org/10.1016/j.jaci.2011.12.215; 22805477
TraesCS1D02G317301	HMW glutenin	1D	Tri a 26	inhalation/ ingestion	celiac disease	WDEIA, Anaphylaxis	Atopic dermatitis		Wheat allergy	16339549; 23612492; 24007624; http://dx.doi.org/10.1016/j.jaci.2011.12.215; 22805477

Supplementary Table-4: Instruments/equipment used in this study.

Instrument Type	Make	Model
Water Bath	VWR	
Optical Microscope	Olympus	CX41
pH Meter	Hanna Instruments	HI2111 pH/ORP Meter
pH Meter	Eutech Instruments	PC 700
Grinder	Silver Crest	SC-150
Drying Oven	Leidal Medical England	60 L model
Hot Plate w/ magnetic stirrer	Heidolph	MR 3001 K
Hot Plate w/ magnetic stirrer	IKA	RCT basic
Shaking Incubator	Eppendorf New Brunswick	Innova 40 Inc
Microwave Oven	Dawlance	DW-MD10
Weigh Balance	VWR	164AC
Vortex Mixer	VWR	Heavy-Duty Vortex Mixer
Centrifuge	Local/ Chinese	80-3
Extruder	Local make	
Compression Mold	Manual/ Local make	
Extensometer	Testometric	x350
XRD	Malvern Panalytical	EMPYREAN

Supplementary Table-5A: XRD peak list of ESP.

No.	Pos. [°2Th.]	FWHM [°2Th.]	Area [cts*°2Th.]	Derivation	Backgr.[cts]	d-spacing [Å]	Height [cts]
1	22.9697	0.3149	7.59	Mixed K-Alpha1 / K-Alpha2	30	3.87194	24.42
2	29.1927	0.096	60.25	Pure K-Alpha1	26	3.05665	470.73

3	29.34	0.0787	33.4	Mixed K-Alpha1 / K-Alpha2	26	3.04415	430.12
4	31.3657	0.6298	7.92	Mixed K-Alpha1 / K-Alpha2	24	2.85202	12.75
5	35.9058	0.2755	14.71	Mixed K-Alpha1 / K-Alpha2	21	2.50113	54.13
6	39.2846	0.2362	18.94	Mixed K-Alpha1 / K-Alpha2	18	2.29345	81.3
7	43.1338	0.2755	19.87	Mixed K-Alpha1 / K-Alpha2	16	2.09729	73.12
8	47.4735	0.1968	21.89	Mixed K-Alpha1 / K-Alpha2	16	1.91521	112.78
9	48.4268	0.3149	29.43	Mixed K-Alpha1 / K-Alpha2	15	1.87971	94.75
10	56.4801	0.3149	5.41	Mixed K-Alpha1 / K-Alpha2	12	1.62931	17.41
11	57.3204	0.2362	7.98	Mixed K-Alpha1 / K-Alpha2	12	1.60741	34.27
12	60.6047	0.3936	9.32	Mixed K-Alpha1 / K-Alpha2	11	1.52793	24.01
13	63.0352	0.2362	1.99	Mixed K-Alpha1 / K-Alpha2	10	1.47474	8.53
14	64.6333	0.3936	7.82	Mixed K-Alpha1 / K-Alpha2	10	1.44209	20.13
15	65.6693	0.3149	5.91	Mixed K-Alpha1 / K-Alpha2	10	1.42183	19.01
16	70.2709	0.4723	3.34	Mixed K-Alpha1 / K-Alpha2	10	1.33957	7.16
17	72.8544	0.3936	4.18	Mixed K-Alpha1 / K-Alpha2	9	1.29831	10.76
18	77.1846	0.576	6.98	Pure K-Alpha1	9	1.2349	9.09

FWHM= full width at half maximum intensity; cts: counts; Th.: theta.

Supplementary table-5B: XRD peak list of reference HAP.

No.	Pos. [°2Th.]	FWHM [°2Th.]	Area [cts*°2Th.]	Derivation	Backgr.[cts]	d-spacing [Å]	Height [cts]
1	25.92674	0.15744	10.13343	Mixed K-Alpha1 / K-Alpha2	20	3.43665	65.25
2	26.5755	0.31488	6.22948	Mixed K-Alpha1 / K-Alpha2	20	3.35421	20.06
3	28.91511	0.23616	4.80839	Mixed K-Alpha1 / K-Alpha2	19	3.08791	20.62
4	30.22905	0.11808	2.94095	Mixed K-Alpha1 / K-Alpha2	19	2.95662	25.25
5	31.81369	0.17712	25.22593	Mixed K-Alpha1 / K-Alpha2	19	2.81288	144.38
6	32.26244	0.15744	14.88649	Mixed K-Alpha1 / K-Alpha2	19	2.77477	95.85
7	32.96738	0.13776	12.88347	Mixed K-Alpha1 / K-Alpha2	19	2.71703	94.81
8	34.08849	0.1968	7.50993	Mixed K-Alpha1 / K-Alpha2	18	2.6302	38.68
9	39.87173	0.31488	9.62389	Mixed K-Alpha1 / K-Alpha2	13	2.26102	30.98
10	42.03802	0.47232	3.32874	Mixed K-Alpha1 / K-Alpha2	13	2.14939	7.14
11	46.75797	0.31488	13.65101	Mixed K-Alpha1 / K-Alpha2	12	1.94283	43.95
12	48.13945	0.23616	4.22154	Mixed K-Alpha1 / K-Alpha2	12	1.89026	18.12
13	49.51461	0.23616	11.68449	Mixed K-Alpha1 / K-Alpha2	11	1.84093	50.16
14	50.51998	0.23616	5.03297	Mixed K-Alpha1 / K-Alpha2	11	1.80663	21.6
15	51.28096	0.31488	5.85301	Mixed K-Alpha1 / K-Alpha2	11	1.7816	18.84

16	52.14005	0.23616	4.01921	Mixed K-Alpha1 / K-Alpha2	11	1.75425	17.25
17	53.26257	0.31488	7.35766	Mixed K-Alpha1 / K-Alpha2	10	1.71989	23.69
18	55.86568	0.31488	2.69338	Mixed K-Alpha1 / K-Alpha2	10	1.64577	8.67
19	57.33911	0.47232	2.1893	Mixed K-Alpha1 / K-Alpha2	10	1.60693	4.7
20	60.07007	0.47232	2.7066	Mixed K-Alpha1 / K-Alpha2	10	1.54024	5.81
21	61.7465	0.62976	4.06182	Mixed K-Alpha1 / K-Alpha2	10	1.50239	6.54
22	64.09306	0.3936	5.72888	Mixed K-Alpha1 / K-Alpha2	11	1.45293	14.76
23	77.0903	0.576	5.7405	Pure K-Alpha1	10	1.23617	7.47

Supplementary table-5C: XRD peak lists of nano-EHAP.

No.	Pos. [°2Th.]	FWHM [°2Th.]	Area [cts*°2Th.]	Derivation	Backgr.[cts]	d-spacing [Å]	Height [cts]
1	25.4471	0.4723	3.33	Mixed K-Alpha1 / K-Alpha2	36	3.50032	7.16
2	27.7603	0.4723	3	Mixed K-Alpha1 / K-Alpha2	36	3.21369	6.43
3	31.6741	0.3149	11.12	Mixed K-Alpha1 / K-Alpha2	35	2.82495	35.8
4	32.8984	0.3149	5.31	Mixed K-Alpha1 / K-Alpha2	34	2.72257	17.11
5	40.0058	0.551	5.15	Mixed K-Alpha1 / K-Alpha2	25	2.25375	9.47
6	45.1143	0.9446	4.83	Mixed K-Alpha1 / K-Alpha2	22	2.00971	5.18

| 7 | 46.6031 | 0.4723 | 3.7 | Mixed K-Alpha1 / K-Alpha2 | 21 | 1.94893 | 7.94 |
| 8 | 49.2037 | 0.768 | 6.41 | Pure K-Alpha1 | 21 | 1.8503 | 6.26 |
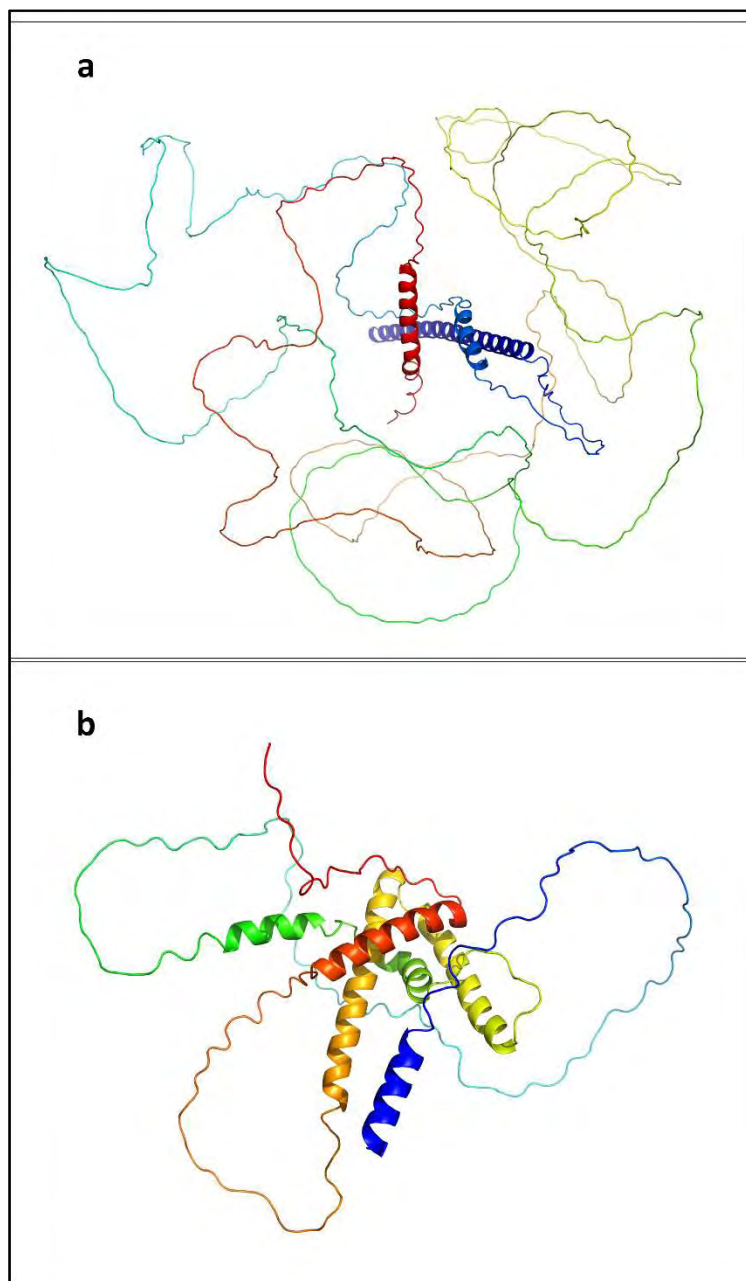
Supplementary figure-S1: Structures of glutenin proteins; predicted structures of gluten proteins by AlphaFold F1 model v2.0. N-terminus is blue and C-terminus is red; notice huge lengths of unstructured polypeptide chains. (a) HMW-GS DX5, (b) LMW-GS 1D1. These

unstructured stretches of polypeptide chain randomly arrange and intertwine when gluten is melted and new interactions intra-chain and inter-chain give rise to the plastic gluten.
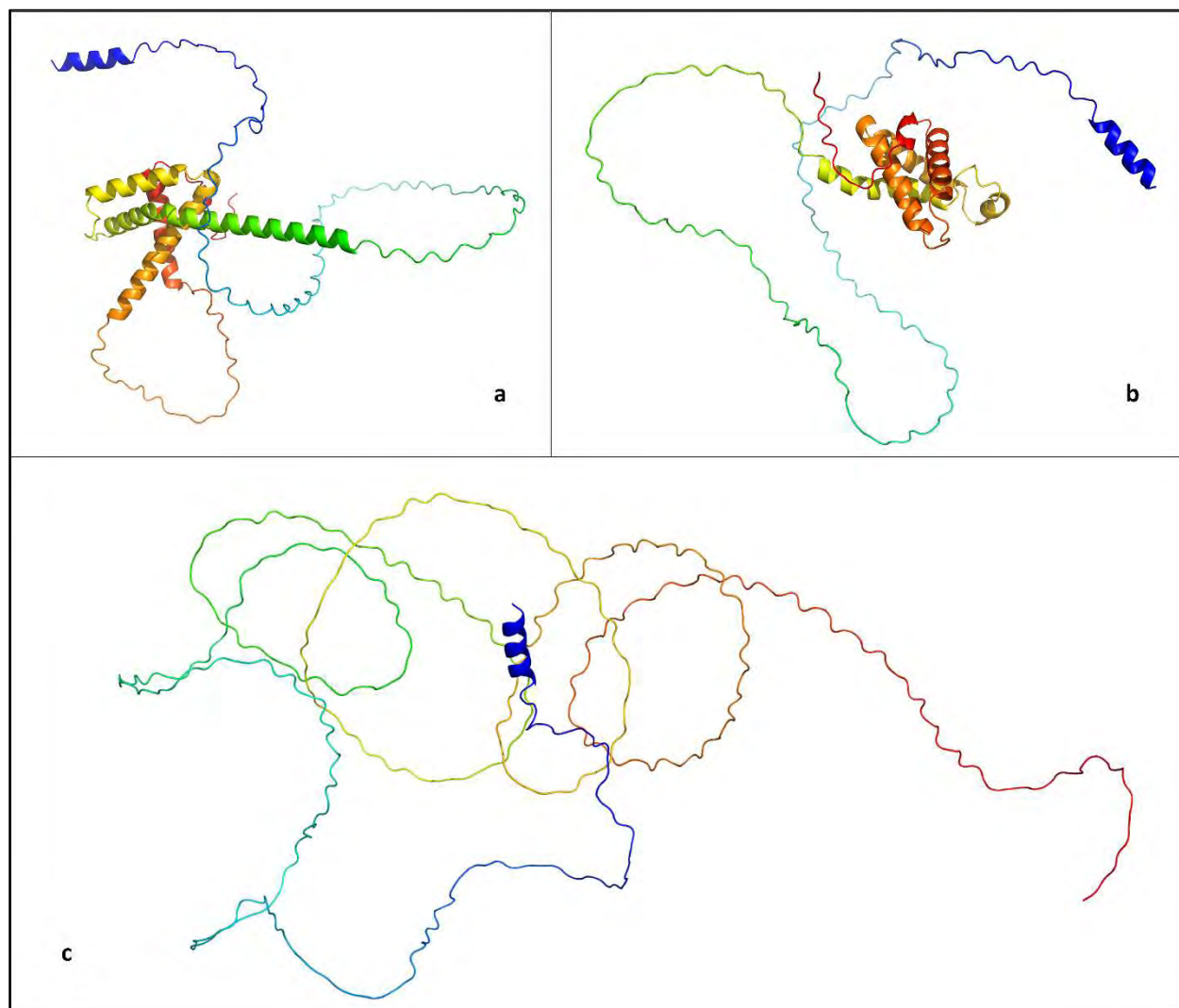
Supplementary figure-S2: Structures of gliadins, as predicted by AlphaFold F1 model v2.0; (a) α/β-Gli MM1, (b) γ-Gli L7R4Z9, and (c) ω-5-Gli. N- and C- termini are shown in blue and red, respectively.

Appendix-B: List of software/ tools/ databases used in this study

Use	Software/ tool/ database	Version
Molecular Visualization	PyMOL	Incentive PyMOL v2.5.2
	UCSF ChimeraX	v1.6.1
	AlphaFold	F1 model v4
Design	Biorender	www.biorender.com
	Adobe Illustrator	2022
	Draw.io	v20.8.16
	Microsoft Visio Professional	v2304
Graphing and Data Analysis	Microsoft Excel	v2304
	MATLAB	R2020a
	ImageJ	v1.8
FTIR	MestReLab Mnova (ElViS)	v14.2.1
	MATLAB	R2020a
XRD	X'Pert Highscore Plus	v2.1
	Match!	v3.15
	ICDD PDF	v2
	COD	inorganic database
	MATLAB	R2020a
Wheat proteins	IWGSC RefSeq	v2.1
	NCBI Genome	Taxonomy ID: 4565
	UniProt	Taxon ID: 4565

Appendix-C: MATLAB Code

The MATLAB code used for graphing/ analysis in this study is given here.

XRD Data of Eggshell and Hydroxyapatite

R1: Analytical Grade Hydroxyapatite [Sigma]

R2: Eggshell Powder

R3: Synthesized Hydroxyapatite [from eggshell]

1. Plot Charts

```
plot(R1_x,R1_y)
hold on
plot(R3_x,R3_y)
hold off
grid on
%xlim([20,60])
%ylim([0,180])
ylabel("Counts (a.u)")
xlabel("Angle (2θ)")
legend("Reference HAP","nano-EHA","Location","best")
%exportgraphics(gca,"C:\Users\rzn\Desktop\MPhil Biotech QAU\Research\M.Phil Thesis\XRD\XRD
HAPs.png","Resolution",900)
```

2. Stacked plots

```
columnnanmes=["Reference HAP","nano-EHAP"];
stackedplot(R1_x,HAPs,"DisplayLabels",columnnanmes)
xlabel("Angle (2θ)")
grid on
%exportgraphics(gca,"HAP_XRD_stacked.png","Resolution",900)
```

Tensile Testing Data of compression molded composites

The tensile testing data are available in the terms of elongation (mm) as a function of applied force (N). The variable (var) names for composites are as follows:

(Composite name) | (force var) | (elongation var)

C-10 Force1 Elongation1

C-20 Force2 Elongation2

C-30 Force3 Elongation3

```
plot(Elongation1,Force1,"LineWidth",1)
hold on
grid on
x=["C-10","C-20","C-30"];
plot(Elongation2,Force2,"LineWidth",1)
plot(Elongation3,Force3,"LineWidth",1)
xlim([0,31])
ylim([0,7.5])
hold off
legend(x,"Location","best")
xlabel("Elongation (mm)")
ylabel("Force (N)")
f=gca;
%exportgraphics(f,"C:\Users\rzn\Desktop\MPhil Biotech QAU\Research\M.Phil Thesis\Fwd_ Tensile testing data (samples_ BIO 1 to 5)\Tensile Test.png","Resolution",900)
```

Materials Properties Plot of Natural & Composite Materials

This is for Figure 1.2 of thesis main text, and additional supplementary images if need be. I am going to plot max values of moduli, strength (tensile/compressive) and densities of materials.

```
yyaxis("left")
scatter(Density,StrengthMPa,'filled')
grid on
xlabel("Density (g/cc)")
ylabel("Strength (MPa)")
yyaxis("right")
scatter(Density,ModulusGPa,'filled')
ylabel("Modulus (GPa)")
%exportgraphics(gca,"materials_propertiesFull.png","Resolution",900)
```

FTIR of nHap and EHap-(old) WG Composites

These are the FTIR plots for nHAP and EHAP prepared in the first attempt, and their WG composites.

nHap: prepared by direct reaction (sol-gel synthesis) from Ca(OH)2 and H3PO4 [no titration; variable name **nHap**].

EHap: prepared by microwave method, from eggshells [no titration; variable name **EHap**].

The composites are:

Control: Hap:WG:GLY----->00: 70:30 [variable name **A**]

C-10:   EHap:WG:GLY---> 10:60:30 [variable name **C10**]

C-20:   EHap:WG:GLY---> 20:50:30 [variable name **C20**]

C-30:   EHap:WG:GLY---> 30:40:30 [variable name **C30**]

The comments or the code excluded from compiling/execution is what follows after % sign.

1. HAP Plots

```
scatter(nHap_x,nHap_y,'.')
hold on
scatter(EHap_x,EHap_y,'.')
set(gca,'xdir','reverse')
hold off
grid on
xlim([400,4000])
xlabel("Wavenumber (1/cm)")
ylabel("Transmittance (a.u.)")
legend ("nHap","EHap","Location","best")
%exportgraphics(gca,"C:\Users\rzn\Desktop\MPhil Biotech QAU\Research\M.Phil Thesis\old-FTIR\Hap-FTIR.png","Resolution",600)
%xlim([400,2000])
%exportgraphics(gca,"C:\Users\rzn\Desktop\MPhil Biotech QAU\Research\M.Phil Thesis\old-FTIR\Hap-FTIRzoom.png","Resolution",600)
```

2. Composite Plots

```
composite=["Control-A","C-10","C-20","C-30"];
```

```matlab
plot(A_x,A_y,"LineWidth",1.25)
hold on
plot(C10_x,C10_y,"LineWidth",1.25)
plot(C20_x,C20_y,"LineWidth",1.25)
plot(C30_x,C30_y,"LineWidth",1.25)
hold off
grid on
set(gca,'xdir','reverse')
xlabel("Wavenumber (1/cm)")
ylabel("Transmittance (a.u.)")
legend(composite,"Location","best")
xlim([400,4000])
%exportgraphics(gca,"C:\Users\rzn\Desktop\MPhil Biotech QAU\Research\M.Phil Thesis\old-FTIR\compositeFTIR.png","Resolution",600)
%xlim([2500,3700])
%ylim([40,95])
%exportgraphics(gca,"C:\Users\rzn\Desktop\MPhil Biotech QAU\Research\M.Phil Thesis\old-FTIR\compositeFTIR2500-3500.png","Resolution",600)
%xlim([800,1800])
%ylim([30,80])
%exportgraphics(gca,"C:\Users\rzn\Desktop\MPhil Biotech QAU\Research\M.Phil Thesis\old-FTIR\compositeFTIR800-1800.png","Resolution",600)
%xlim([1480,1720])
%exportgraphics(gca,"C:\Users\rzn\Desktop\MPhil Biotech QAU\Research\M.Phil Thesis\old-FTIR\compositeFTIR-amide.png","Resolution",600)
```

MPhil thesis

8% SIMILARITY INDEX

7% INTERNET SOURCES

5% PUBLICATIONS

3% STUDENT PAPERS

PRIMARY SOURCES

1	**Submitted to University of Warwick** Student Paper	**1**%
2	**docksci.com** Internet Source	**<1**%
3	**ds.inflibnet.ac.in** Internet Source	**<1**%
4	**N. S. Al-Qasas, S. Rohani. "Synthesis of Pure Hydroxyapatite and the Effect of Synthesis Conditions on its Yield, Crystallinity, Morphology and Mean Particle Size", Separation Science and Technology, 2005** Publication	**<1**%
5	**link.springer.com** Internet Source	**<1**%
6	**epdf.tips** Internet Source	**<1**%
7	**www.nbfira.org.bw** Internet Source	**<1**%
8	**www.mdpi.com** Internet Source	

<1 %

9   Aasma Saeed, Muhammad Asif Hanif, Haq
    Nawaz, Rashad Waseem Khan Qadri. "The
    production of biodiesel from plum waste oil
    using nano-structured catalyst loaded into
    supports", Scientific Reports, 2021
    Publication   <1 %

10 N.A.M. Rasid, N.N.M. Nazmi, M.I.N. Isa, N.M.
    Sarbon. "Rheological, functional and
    antioxidant properties of films forming
    solution and active gelatin films incorporated
    with Centella asiatica (L.) urban extract", Food
    Packaging and Shelf Life, 2018
    Publication   <1 %

11 Submitted to Shorewood High School
    Student Paper   <1 %

12 www.registrar.ucla.edu
    Internet Source   <1 %

13 Submitted to Pennsylvania State System of
    Higher Education
    Student Paper   <1 %

14 en.wikipedia.org
    Internet Source   <1 %

15 "Biomineralization", Wiley, 2008
    Publication   <1 %

16 digitalcommons.usf.edu
Internet Source
<1 %

17 V. Madhusudhan Rao, Sreedevi Nimishakavi, Ashok Kumar Singh, T.N. Aishwarya. "Effect of Plant Leaf Mediated Natural Extracts as Natural Stabilizers on Synthesis and Characterization of Nano-Hydroxyapatite Powders", Key Engineering Materials, 2023
Publication
<1 %

18 journals.plos.org
Internet Source
<1 %

19 orca.cardiff.ac.uk
Internet Source
<1 %

20 pgsdspace.ictp.it
Internet Source
<1 %

21 Submitted to Brunel University
Student Paper
<1 %

22 N.I. Agbeboh, I.O. Oladele, O.O. Daramola, A.A. Adediran, O.O. Olasukanmi, M.O. Tanimola. "Environmentally sustainable processes for the synthesis of hydroxyapatite", Heliyon, 2020
Publication
<1 %

23 Amit Kumar Sharma, Ankita Dhiman, Amit Kumar Nayak, Rishabh Mishra, Garima Agrawal. "Environmentally benign approach
<1 %

for the efficient sequestration of methylene blue and coomassie brilliant blue using graphene oxide emended gelatin/κ-carrageenan hydrogels", International Journal of Biological Macromolecules, 2022
Publication

24   Submitted to University of Pretoria
      Student Paper   <1 %

25   escholarship.mcgill.ca
      Internet Source   <1 %

26   Choudhury, P., and D. C. Agrawal.
      "Hydroxyapatite (HA) coatings for
      biomaterials", Nanomedicine, 2012.   <1 %
      Publication

27   Seed Proteins, 1999.
      Publication   <1 %

28   kipdf.com
      Internet Source   <1 %

29   www.frontiersin.org
      Internet Source   <1 %

30   Anabelle Rodrigues, Albert Lebugle.
      "Influence of ethanol in the precipitation
      medium on the composition, structure and
      reactivity of tricalcium phosphate", Colloids   <1 %
      and Surfaces A: Physicochemical and
      Engineering Aspects, 1998
      Publication

31 Submitted to University of Edinburgh
Student Paper   <1%

32 dspace.plymouth.ac.uk
Internet Source   <1%

33 kogi.udea.edu.co
Internet Source   <1%

34 prism.ucalgary.ca
Internet Source   <1%

35 prr.hec.gov.pk
Internet Source   <1%

36 Submitted to Imperial College of Science,
Technology and Medicine
Student Paper   <1%

37 Submitted to Indian Institute of Science,
Bangalore
Student Paper   <1%

38 Fred Brouns, Gonny Rooy, Peter Shewry,
Sachin Rustgi, Daisy Jonkers. "Adverse
Reactions to Wheat or Wheat Components",
Comprehensive Reviews in Food Science and
Food Safety, 2019
Publication   <1%

39 Submitted to National Institute of Technology,
Rourkela
Student Paper   <1%

Submitted to University of Huddersfield

| 40 | Student Paper | <1 % |

| 41 | aab.com.pk
Internet Source | <1 % |

| 42 | ebin.pub
Internet Source | <1 % |

| 43 | 123dok.net
Internet Source | <1 % |

| 44 | Submitted to Higher Education Commission Pakistan
Student Paper | <1 % |

| 45 | Submitted to University of Sheffield
Student Paper | <1 % |

| 46 | shareok.org
Internet Source | <1 % |

| 47 | Chang, Q.. "Toughening mechanisms in iron-containing hydroxyapatite/titanium composites", Biomaterials, 201003
Publication | <1 % |

| 48 | Dutta, K.. "Inter-annual variation in atmospheric @D^1^4C over the Northern Indian Ocean", Atmospheric Environment, 200608
Publication | <1 % |

49 R. Yamamoto, S. Oida, Y. Yamakoshi. "Dentin Sialophosphoprotein–derived Proteins in the Dental Pulp", Journal of Dental Research, 2015
Publication

<1%

50 bmccancer.biomedcentral.com
Internet Source

<1%

51 repository.up.ac.za
Internet Source

<1%

52 theses.hal.science
Internet Source

<1%

53 C. Du, L. Xie. "Stability analysis and stabilization of uncertain two-dimensional discrete systems: an LMI approach", IEEE Transactions on Circuits and Systems I: Fundamental Theory and Applications, 1999
Publication

<1%

54 Hornez, J.C.. "Biological and physico-chemical assessment of hydroxyapatite (HA) with different porosity", Biomolecular Engineering, 200711
Publication

<1%

55 researchrepository.wvu.edu
Internet Source

<1%

56 www.100md.com
Internet Source

<1%

57 www.biorxiv.org
Internet Source

<1%

58 www.spandidos-publications.com
Internet Source

<1%

59 "Biopolymer Nanocomposites", Wiley, 2013
Publication

<1%

60 "Development of bioplastics based on agricultural side-stream products: Film extrusion of Crambe abyssinica /wheat gluten blends for packaging purposes", Journal of Applied Polymer Science, 2016.
Publication

<1%

61 9dok.org
Internet Source

<1%

62 Mao, D.. "Influence of calcination temperature and preparation method of TiO"2-ZrO"2 on conversion of cyclohexanone oxime to @e-caprolactam over B"2O"3/TiO"2-ZrO"2 catalyst", Applied Catalysis A, General, 20040528
Publication

<1%

63 Mostafa, N.Y.. "Characterization, thermal stability and sintering of hydroxyapatite powders prepared by different routes", Materials Chemistry & Physics, 20051215
Publication

<1%

64 Satumarja M. Stenman, Jarkko I. Venäläinen, Katri Lindfors, Seppo Auriola et al. "Enzymatic detoxification of gluten by germinating wheat proteases: Implications for new treatment of celiac disease", Annals of Medicine, 2009
Publication

<1%

65 Submitted to The Hong Kong Polytechnic University
Student Paper

<1%

66 aast.edu
Internet Source

<1%

67 discovery.ucl.ac.uk
Internet Source

<1%

68 es.scribd.com
Internet Source

<1%

69 healthdocbox.com
Internet Source

<1%

70 joam.inoe.ro
Internet Source

<1%

71 pure.manchester.ac.uk
Internet Source

<1%

72 researchbank.swinburne.edu.au
Internet Source

<1%

73 scienze-como.uninsubria.it
Internet Source

<1%

74 tel.archives-ouvertes.fr
Internet Source
<1%

75 upcommons.upc.edu
Internet Source
<1%

76 "Modern Synthetic Methods in Carbohydrate Chemistry", Wiley, 2013
Publication
<1%

77 Alexander Mezhov, Simon Ulka, Youri Gendel, Charles E. Diesendruck, Konstantin Kovler. "The working mechanisms of low molecular weight polynaphthalene sulfonate superplasticizers", Construction and Building Materials, 2020
Publication
<1%

78 Jérôme Dumur. "Proteomic analysis of aneuploid lines in the homeologous group 1 of the hexaploid wheat cultivar Courtot", PROTEOMICS, 09/2004
Publication
<1%

79 Liu, C.. "Template synthesis and characterization of highly ordered lamellar hydroxyapatite", Applied Surface Science, 20070615
Publication
<1%

80 Onwu Francis Kalu. "Biosorption of Cd(ll), Cu(ll) and Ni(ll) Ions from Aqueous Solution
<1%

Using Jatropha Curcas Seed Pod", Advances in Materials, 2017
Publication

81 Ramaswamy, Janani, Hwa Kyung Nam, Harsha Ramaraju, Nan E. Hatch, and David H. Kohn. "Inhibition of osteoblast mineralization by phosphorylated phage-derived apatite-specific peptide", Biomaterials, 2015.
Publication
<1%

82 Zhao, X.. "Aedes aegypti peroxidase gene characterization and developmental expression", Insect Biochemistry and Molecular Biology, 20010315
Publication
<1%

83 apps.itd.idaho.gov
Internet Source
<1%

84 docplayer.net
Internet Source
<1%

85 edoc.unibas.ch
Internet Source
<1%

86 eprints.nottingham.ac.uk
Internet Source
<1%

87 hdl.handle.net
Internet Source
<1%

88 kupdf.net
Internet Source
<1%

89 libweb.kpfu.ru
Internet Source

<1%

90 mdpi-res.com
Internet Source

<1%

91 researchcommons.waikato.ac.nz
Internet Source

<1%

92 www.freepatentsonline.com
Internet Source

<1%

93 www.nihe.gov.uk
Internet Source

<1%

94 www.riff-o-matic.com
Internet Source

<1%

95 www.science.gov
Internet Source

<1%

96 Giampaolo Ricci, Laura Andreozzi, Francesca Cipriani, Arianna Giannetti, Marcella Gallucci, Carlo Caffarelli. "Wheat Allergy in Children: A Comprehensive Update", Medicina, 2019
Publication

<1%

97 Humayun Nadeem, Mahdi Naseri, Kirubanandan Shanmugam, Mostafa Dehghani et al. "An Energy Efficient Production of High Moisture Barrier Nanocellulose/Carboxymethyl cellulose Films

<1%

via Spray-deposition Technique", Carbohydrate Polymers, 2020
Publication

98 Julia Guedes, Wagner Martins Florentino, Daniella Regina Mulinari. "Thermoplastics Polymers Reinforced with Natural Fibers", Elsevier BV, 2016
Publication
<1 %

99 digital.library.unt.edu
Internet Source
<1 %

100 Koning, Frits, Ranjeny Thomas, Jamie Rossjohn, and Rene E. Toes. "Coeliac disease and rheumatoid arthritis: similar mechanisms, different antigens", Nature Reviews Rheumatology, 2015.
Publication
<1 %

101 Reza Rizvi. "Synthesis and characterization of novel low density polyethylene–multiwall carbon nanotube porous composites", Smart Materials and Structures, 10/01/2009
Publication
<1 %

102 Wim S. Veraverbeke, Jan A. Delcour. "Wheat Protein Composition and Properties of Wheat Glutenin in Relation to Breadmaking Functionality", Critical Reviews in Food Science and Nutrition, 2002
Publication
<1 %